STM/STS STUDIES OF 2D MATERIALS

J-Y Veuillen

Institut Néel, Grenoble *(www.neel.cnrs.fr)*

jean-yves.veuillen@neel.cnrs.fr

GRAPHENE FLAGSHIP

New Frontiers in 2D materials: Approaches & Applications, Villard de Lans, January 2017

NÉEL institut

Introduction:

Scanning Tunneling Microscopy (STM) and Spectroscopy (STS)

WSXMsoftware, Nanotec, Spain

Heinrich Rohrer & Gerd Binnig, IBM Zürich (1982)

Introduction to Scanning Tunneling Microscopy (STM)

- **Principle of constant current imaging.**

In a simple 1D model ($V \ll \Phi$):

$$I \propto V \times \exp(-2.\kappa.d) \quad \kappa \approx 1\ Å^{-1}$$

Topographic image:
- Scanning the tip at constant V and constant I (feedback).

$\Rightarrow$ **Constant tip-sample distance**

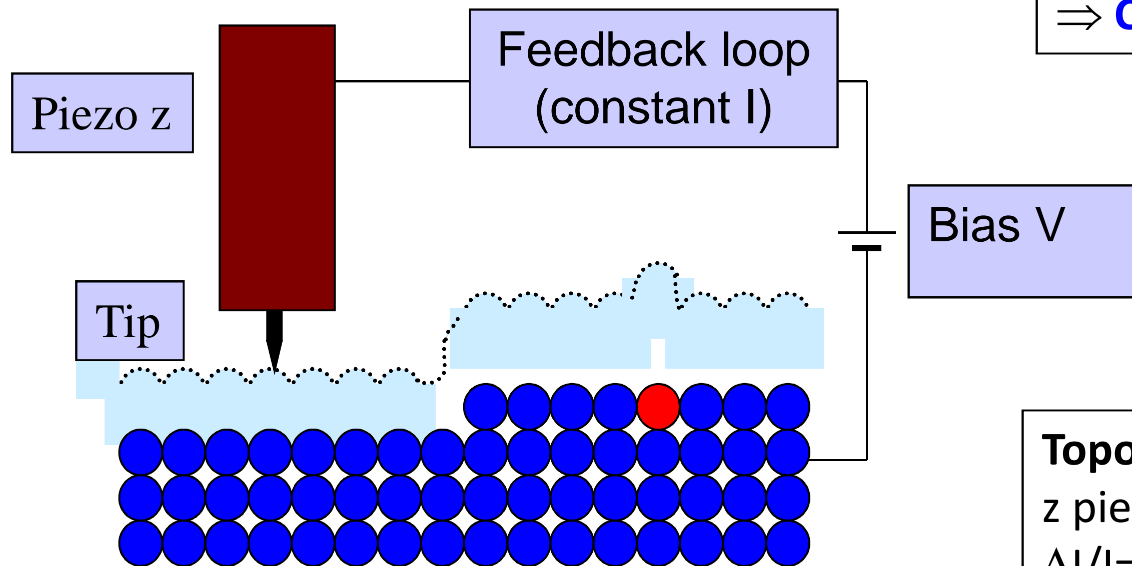

Topography: displacement of the z piezo to keep I constant.
$\Delta I/I = 10\% \Rightarrow \Delta d = 0.05$ Å

Introduction to Scanning Tunneling Microscopy (STM)

- **Role of the electronic structure.**

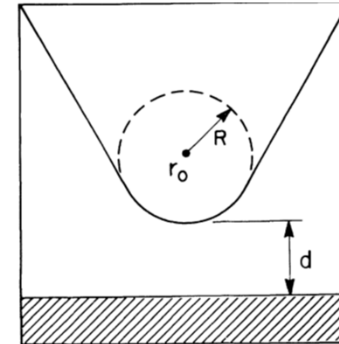

Tersoff-Hamann theory (PRL 50, 1988 (1983)).

Full 3D theory: spherical tip (radius R) .

At **low bias** (V) and **low temperature**, the tunneling current is given by:

$$I \approx \frac{e^2 V}{\hbar} \beta \, e^{2kR} \rho_s(\vec{r}, E_f) \rho_t(E_f)$$

$$\beta = \frac{2\pi^3 \hbar^4 R^2}{m^2}$$

$\rho_s(\vec{r}, E_f)$: LDOS of the sample at E_f, evaluated at the **center** of the tip.

$\rho_t(E_f)$: DOS of the tip at E_f.

Both the topography and the spatial variations of the LDOS of the sample contribute to the current.

Introduction to Scanning Tunneling Microscopy (STM)

- **Voltage dependent imaging: electronic effects.**

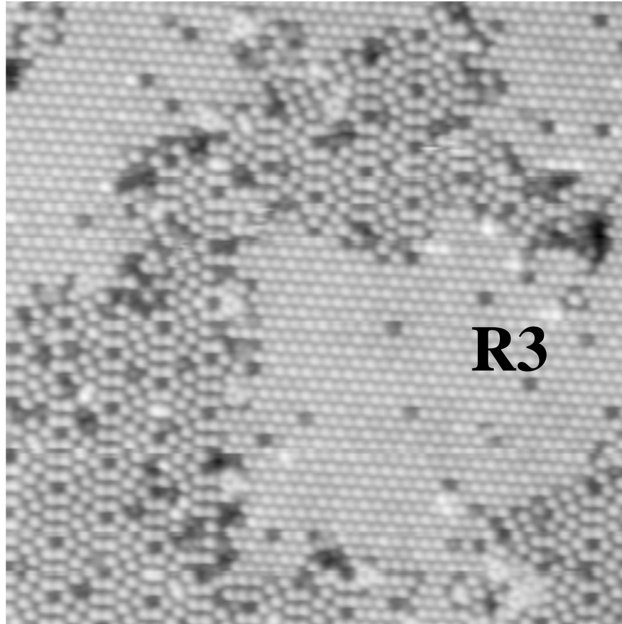

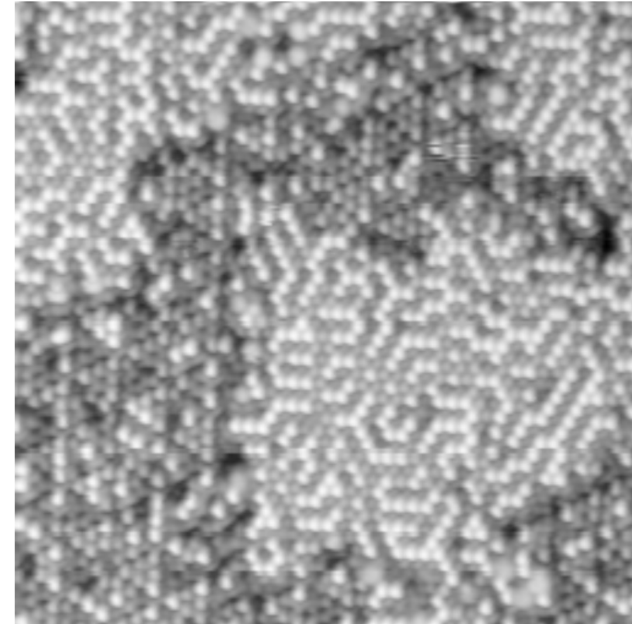

Empty states : **V=1V**

Occupied states : **V=-1 V**

γ (mixed) phase of Pb/Si(111) (R3 type) **Same area**.
Size : 30x30 nm²

Gòmez-Rodrìguez et al, Surf. Sci. 377, 45 (1997)

Tunneling current between a metallic tip and a conductive surface

Model of **Tersoff & Hamann (PRL 1983)**, extended by Lang (PRB 1986)

Sample bias: *V* tip-surface distance: *s* *T=0K*, $N_T(E)$*=Cste…*

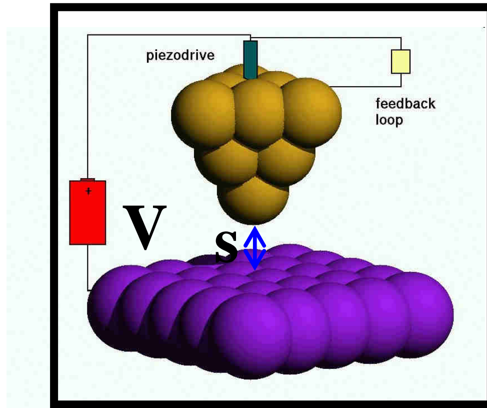

$$I(\vec{r},V)=\frac{e\beta}{\hbar}N_T(E_F)e^{-2\kappa s}\int_{E_F}^{E_F+eV}\rho_S(\vec{r}_{//},E)dE$$

Tunneling current between a metallic tip and a conductive surface

Model of **Tersoff & Hamann (PRL 1983)**, extended by Lang (PRB 1986)

Sample bias: *V* tip-surface distance: *s* *T=0K*, $N_T(E)=Cste$…

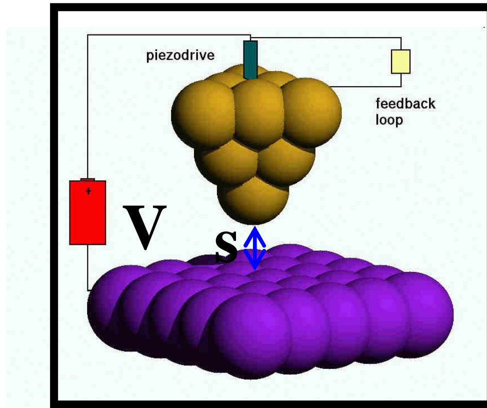

$$I(\vec{r},V) = \frac{e\beta}{\hbar} N_T(E_F) e^{-2\kappa s} \int_{E_F}^{E_F+eV} \rho_S(\vec{r}_{//},E)\,dE$$

Surface Local Density of States (LDOS)

Surface Topography

Surface electronic properties

Tunneling current between a metallic tip and a conductive surface

Model of Tersoff & Hamann (PRL 1983) extended by Lang (PRB86)

Sample bias: *V* tip-surface distance: *s* *T=0K,* $N_T(E)$*=Cste…*

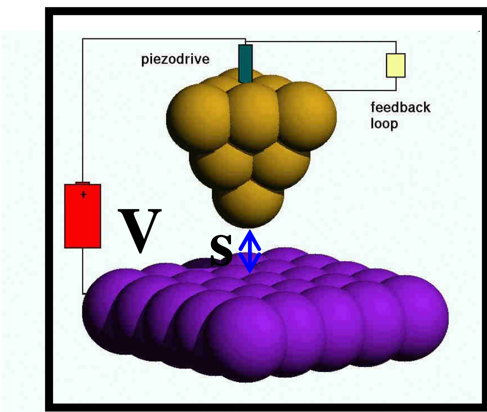

$$I(\vec{r},V) = \frac{e\beta}{\hbar} N_T(E_F) e^{-2\kappa s} \int_{E_F}^{E_F+eV} \rho_S(\vec{r}_{//},E)\,dE$$

Surface Local Density of States (LDOS)

Surface Topography

Surface electronic properties

Constant current STM mode:

map of **Δz_{tip}(x,y)** with a **current feedbackloop activated**

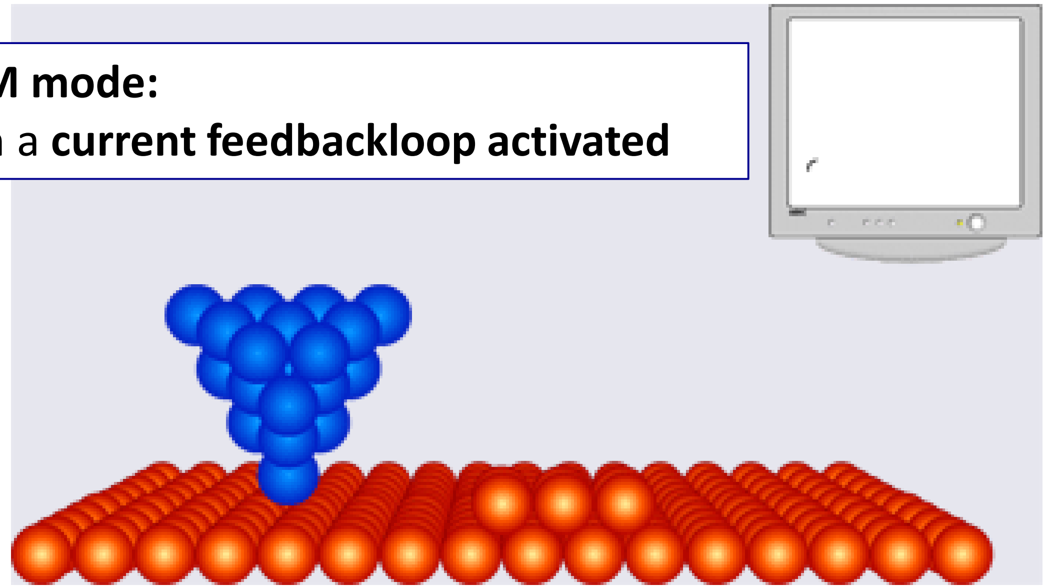

Tunneling current between a metallic tip and a conductive surface

Model of Tersoff & Hamann (PRL 1983) extended by Lang (PRB86)

Sample bias: *V* tip-surface distance: *s* $T=0K$, $N_T(E)=Cste$…

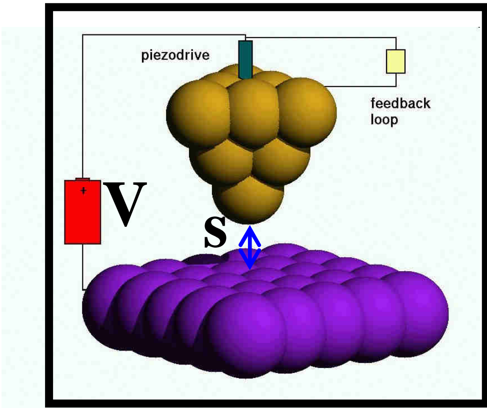

$$I(\vec{r},V) = \frac{e\beta}{\hbar} N_T(E_F) e^{-2\kappa s} \int_{E_F}^{E_F+eV} \rho_S(\vec{r}_{//},E)\,dE$$

Surface Local Density of States (LDOS)

Surface Topography

Surface electronic properties

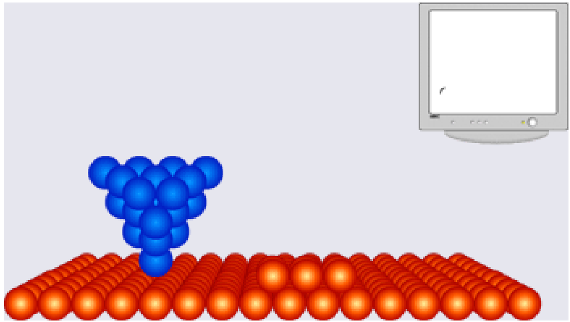

Constant current STM image:
map of **Δz(x,y)** with **current feedbackloop activated**

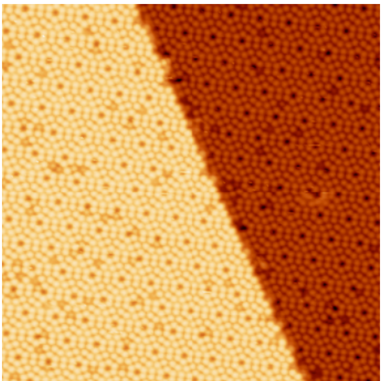

Si(111) 7x7, 35 x 35 nm^2
Sample Bias : +1,5 V

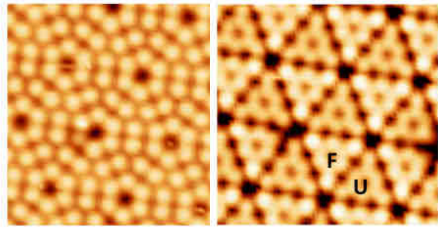

Sample Bias: 1,5V
Unoccupied states

Sample Bias: -1,5V
Occupied states

STM in UHV @ 300K
Mallet/Veuillen, LEPES-CNRS

Tunneling current between a metallic tip and a conductive surface

Model of Tersoff & Hamann (PRL 1983) extended by Lang (PRB86)
Sample bias: *V*   tip-surface distance: *s*   *T=0K, $N_T(E)$=Cste…*

$$I(\vec{r},V) = \frac{e\beta}{\hbar} N_T(E_F)\, e^{-2\kappa s} \int_{E_F}^{E_F+eV} \rho_S(\vec{r}_{//},E)\, dE$$

Surface Local Density of States (LDOS)

Accounts for the decay of the sample eigenstates into vacuum. E and k// dependence?

Wavefunction matching at the sample-vacuum interface: E and k// are conserved for a given state.

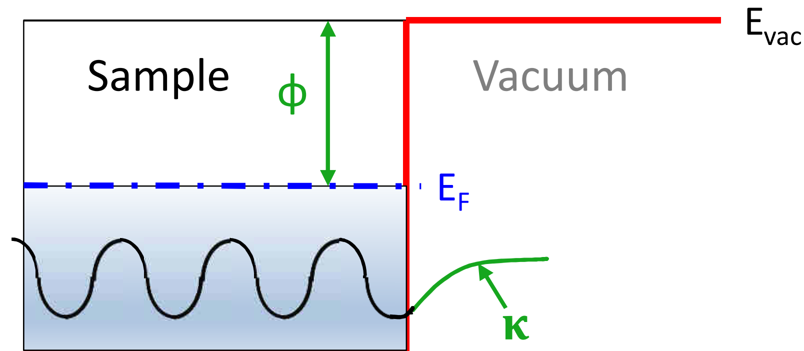

κ can be obtained from I(z) spectroscopy: open feedback loop, ramp « s » by tens of pm and measure I (at given V).

For the simple « **step potential** » **model** of the interface. Schrödinger equation in vacuum **for a state at E_F**:

$$\phi=\frac{\hbar^2}{2m}(\kappa^2-k_{//}^2) \text{ thus } \kappa=\sqrt{0.262\Phi + k_{//}^2}$$

κ and $k_{//}$ in Å^{-1}, ϕ in eV. Typically: ϕ≈4 eV.

- For $k_{//}$=0 Å^{-1} (Γ point): κ≈1 Å^{-1}
- For $k_{//}$=1.7 Å^{-1} (K point in Gr): κ≈2 Å^{-1}

Since s≈5Å, the tunneling current is more sensitive to the states with small wavevectors.

Introduction to Scanning Tunneling Spectroscopy (STS)

- **Principle: I(V) curves at constant tip-sample separation (feedback off).**

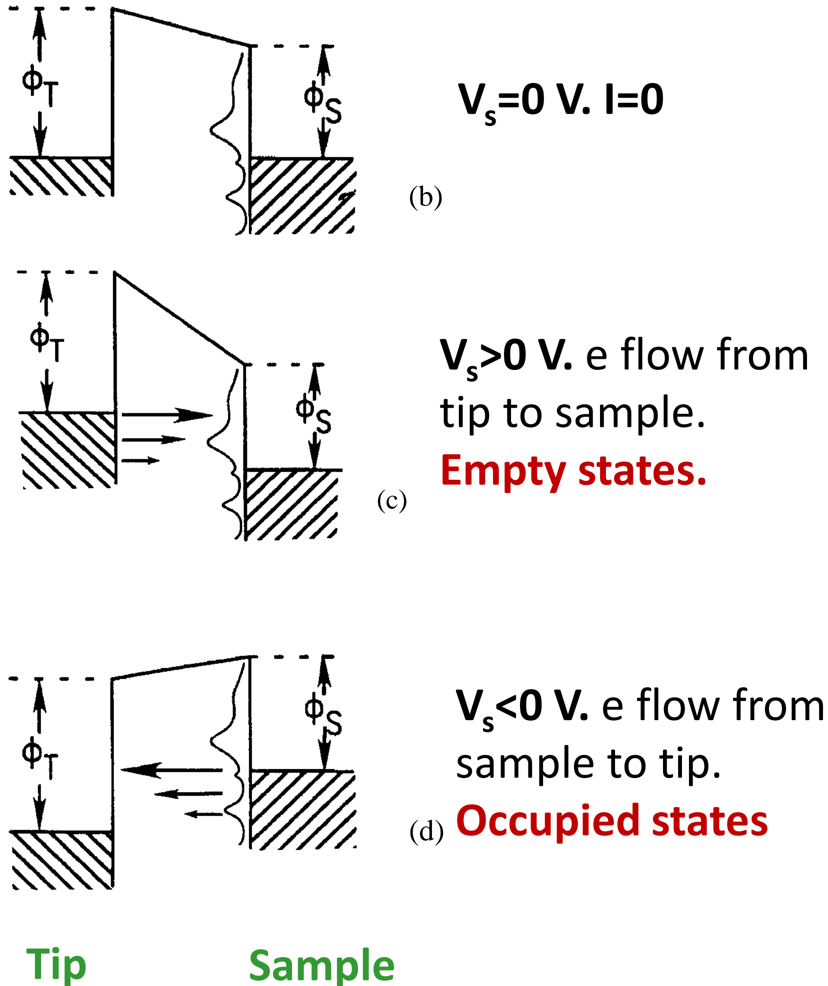

V_s=0 V. I=0

V_s>0 V. e flow from tip to sample. **Empty states.**

V_s<0 V. e flow from sample to tip. **Occupied states**

For a **structureless tip DOS**, at low bias and temperature:

$$\frac{dI}{dV} \propto \rho_s(\vec{r}, E_F + eV)$$

Spectroscopy ⇔ LDOS of the sample

N. D. Lang, PRB 34, 5947 (1986)

Asymmetry between occupied and empty states.

Other normalisation (high bias):

$$\rho_s(eV) \propto \frac{V}{I}\frac{dI}{dV}$$

R. M. Feenstra et al. Surf. Sci. 181, 295 (87).

Scanning Tunneling Spectroscopy (STS)

Dynamical Tunneling Conductance at Zero temperature:

$$dI/dV(\vec{r},V) \sim \rho_S(\vec{r},E_F + eV)$$

$$|V| < 1V$$

Scanning Tunneling Spectroscopy (STS)

Dynamical Tunneling Conductance at Zero temperature:

$$dI/dV(\vec{r},V) \sim \rho_S(\vec{r},E_F+eV)$$

$$|V| < 1V$$

At finite temperature:

$$dI/dV(\vec{r},V) \sim \int_{-\infty}^{\infty} dE \frac{df(E-eV,T)}{dE} \rho_S(\vec{r},E)$$

Quantity roughly proportional to $\rho_S(r, E_F+eV)$, with a thermal broadening of 3.52 $k_B T$

→ **Need for cryogenic STM/STS**

→ Spectroscopic resolution: ~ 1meV à 4,2K

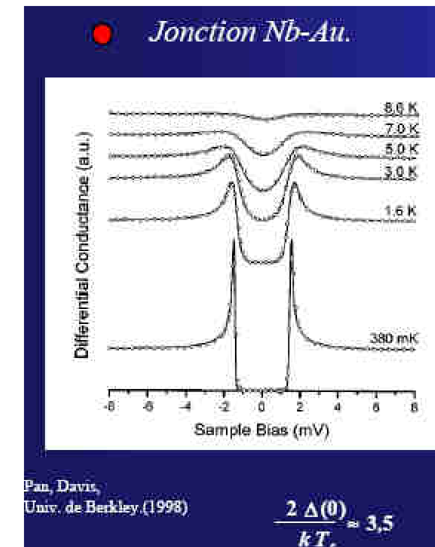

Scanning Tunneling Spectroscopy (STS)

Dynamical Tunneling Conductance at Zero temperature:

$$dI/dV(\vec{r},V) \sim \rho_S(\vec{r},E_F+eV)$$

$$|V| < 1V$$

2 modes of spectroscopic imaging:

« CITS » mode: spectra taken at each point of a constant current image @ (V_{set}, I_{set})

- Time consuming but complete set of data.
- Ultimately atomic resolution spectroscopy can be achieved.

Conductance image @ (V_{set}, I_{set}) with small ac (ω) bias added to dc bias.

- Closed loop image: faster, but only one sample bias/image…
- ω between the cut-off frequencies of feedback loop and current PA.
- Allows for fast identification of changes in electronic structure at large scale.

In both cases some **cross-talk with « topographic » features @ (V_{set}, I_{set})** may occur. Change V_{set}…

A few STM setups in several environments…

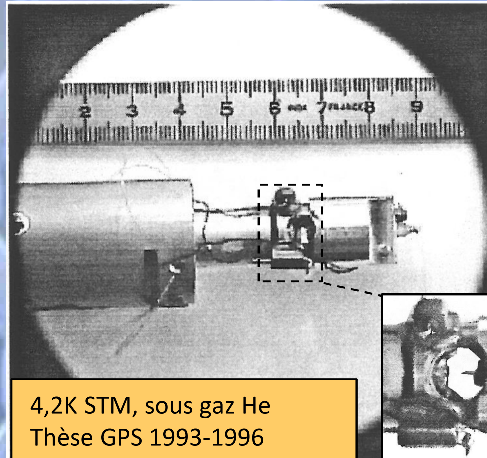

P. Mallet, D. Défourneau, D. Roditchev

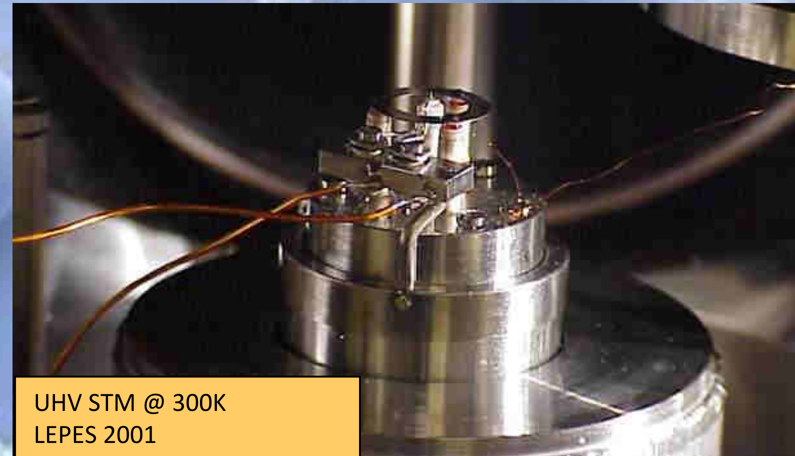

P. Mallet, J.Y. Veuillen, M. Pissard

R. Cinti, P. Mallet, P. Chevalier, J.Y. Veuillen

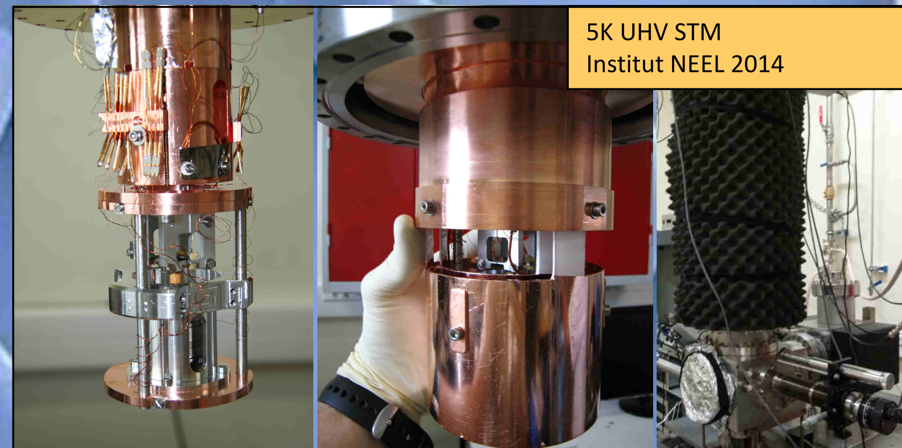

P. Mallet, J.Y. Veuillen, J.F. Motte

Implementation of our setups in the Nanoscience building @ NEEL Institute

VT-UHV-STM and LT-UHV-STM (march 2013 - …)

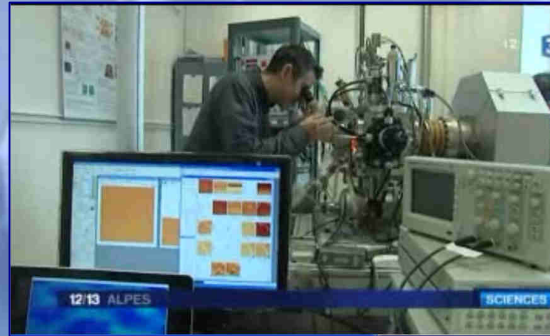

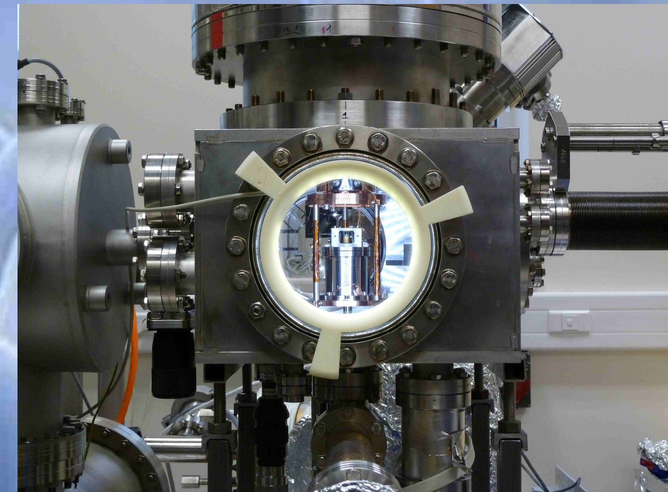

Experiments on concrete foundations (mass 500 tons)

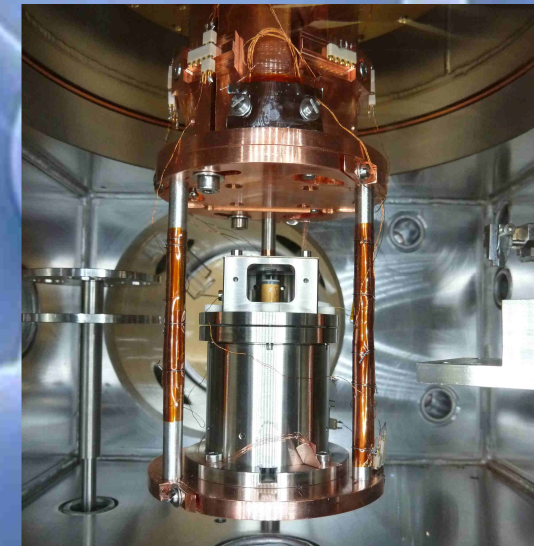

LT-STM head (here without thermal screens)

www.neel.cnrs.fr

STM on 2D conductive systems at surfaces

- ✓ STM is a nice tool to study their electronic structure at atomic scale
- ✓ **UHV environment is required** to preserve most of the 2D systems
- ✓ Complementary techniques are most of time necessary, for instance ARPES for the band structure of the occupied states, and ab initio calculation
- ✓ STM tells a lot regarding the morphology of the disorder existing in the system, and its direct impact on the 2D properties
- ✓ More importantly, disorder can be tuned exposing the 2D system to ionic bombardment, deposition of any metals, exposition to a gas…

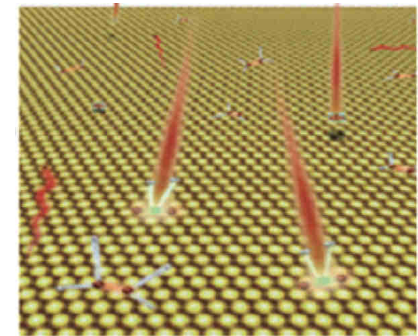

Courtesy I. Brihuega, UAM, Madrid

STM/STS of graphene and graphene-based nanostructures

Outline: graphene

I. Atomic resolution
II. Interface contribution to graphene STM images
III. Local spectroscopy and spatial variations of the Dirac point
IV. Dirac Quasiparticle Interferences
V. STM/STS under magnetic field
VI. Point defects
VII. Moiré ingeneering of graphene’s band structure

- Mostly on G/SiC, G/SiO2, G/BN (HOPG and G/HOPG)

Synthesis of graphene on SiC in UHV @ NEEL

(A technique introduced by van Bommel in… 1975!)

- We use commercial wafers of hexagonal 6H-SiC n-doped or semi-insulating
- **Either SiC (0001) or SiC(000-1) are studied** (resp. Si- and C- terminated)

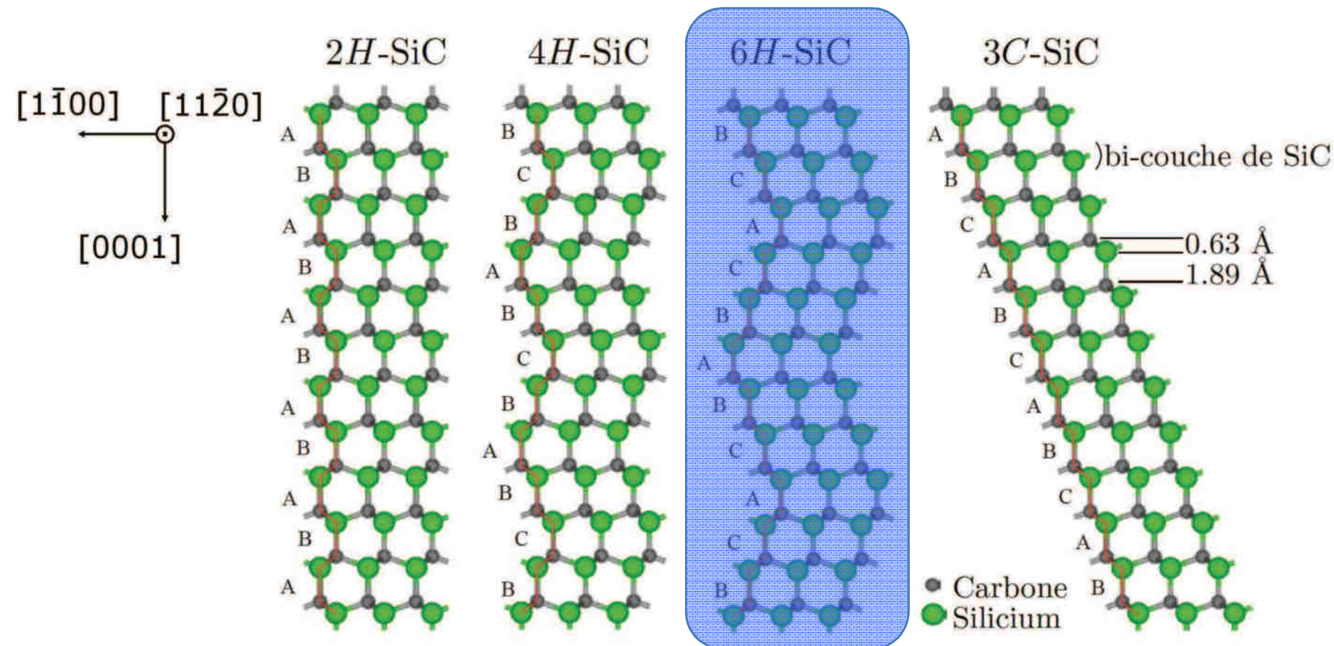

- Graphitization occurs **using thermal decomposition in UHV (some other groups use non UHV conditions, Ar pressure…)**

Synthesis of graphene on SiC in UHV (NEEL Institute)

- ✓ **UHV preparation chamber equiped for standard surface science (ebeam anneling, LEED and Auger electron spectroscopy)**
- ✓ **SiO_2 removal under Si flux @ 850° C**
- ✓ **Progressive annealing (900° C → 1200° C), graphitization process controlled by LEED and Auger spectroscopy**

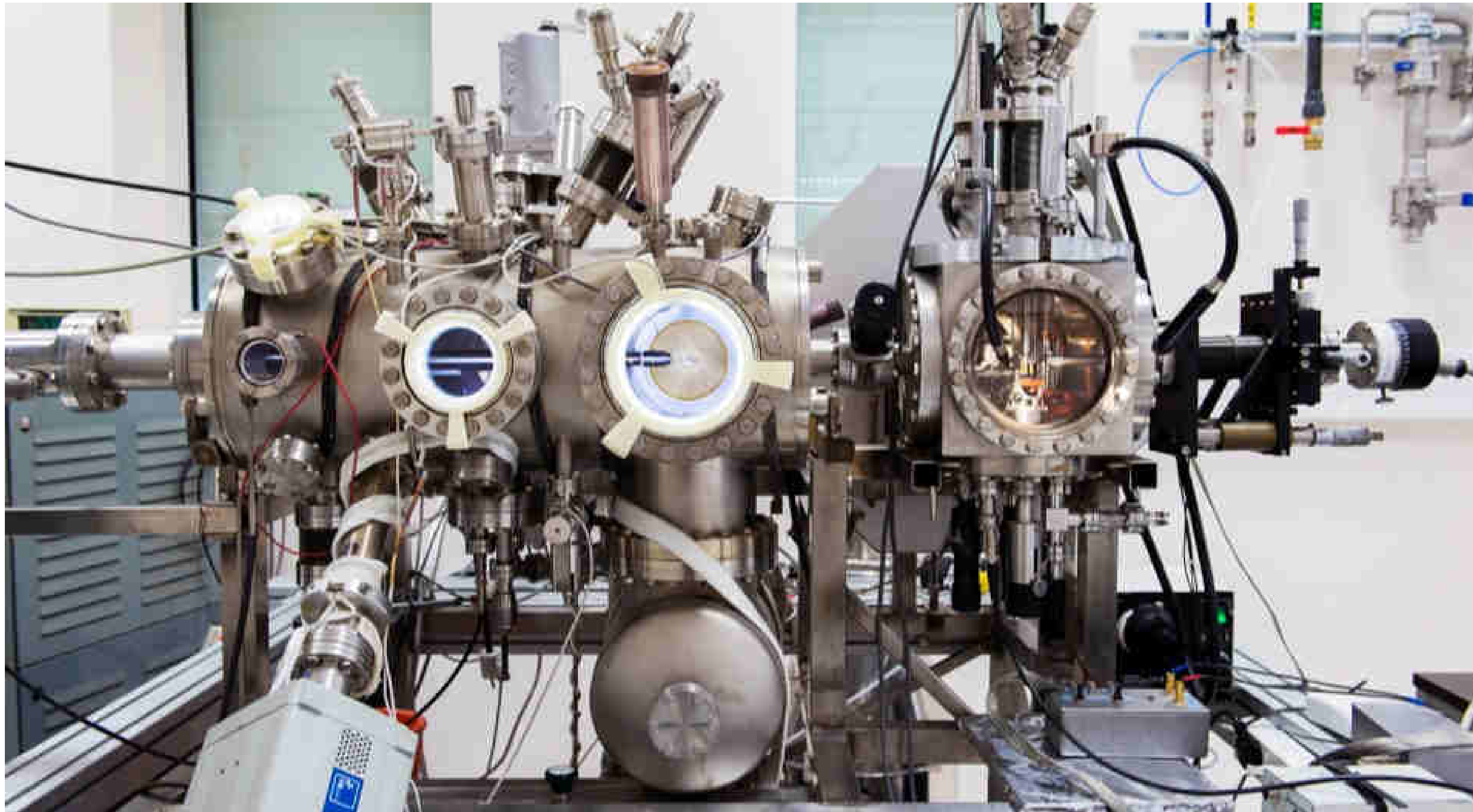

Low Energy Electron Diffraction patterns

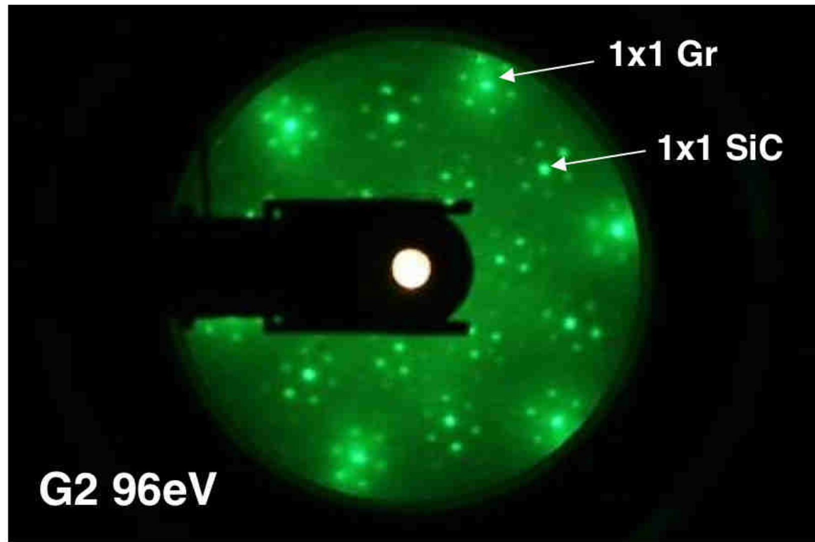

Si face: epitaxial layer.
6R3 interface reconstruction

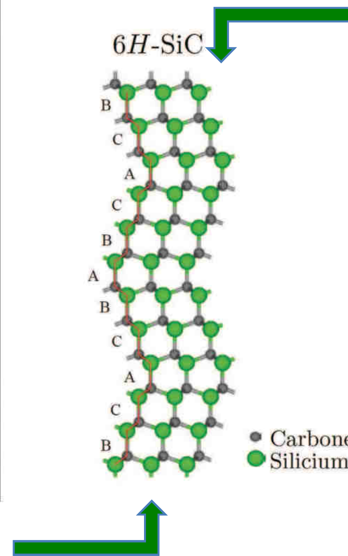

C face: rotational disorder

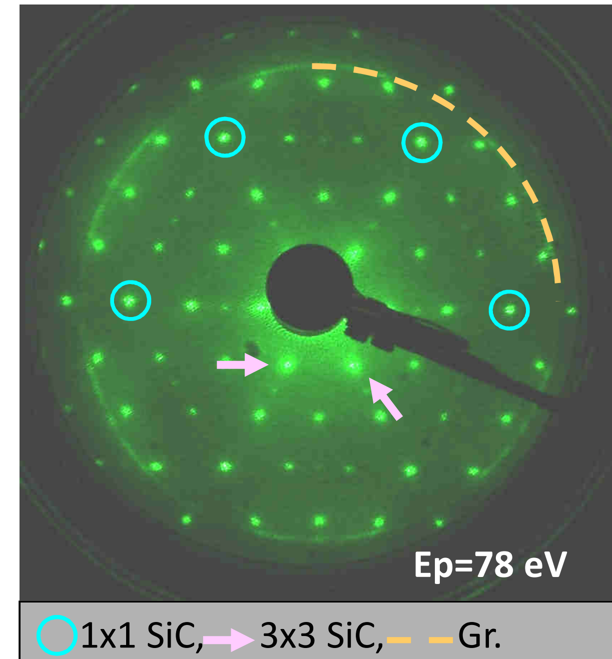

Difference in the structure of graphene layers grown on:

6H-SiC(0001) (Si face) **6H-SiC(000-1) (C face)**

Known from van Bommel et al., Surf. Sci. 1975

Part I. Atomic resolution on graphene STM images

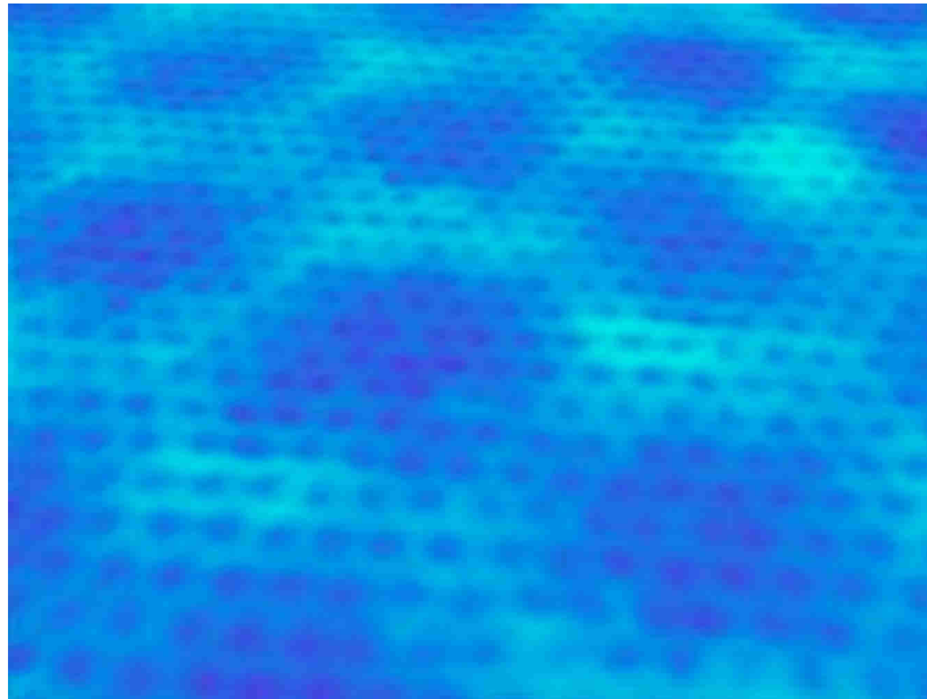

ML graphene on SiC(0001)
P. Mallet/J.Y. Veuillen, Institut NEEL CNRS/UJF, Grenoble

Electronic structure of pristine graphene

Cristal structure

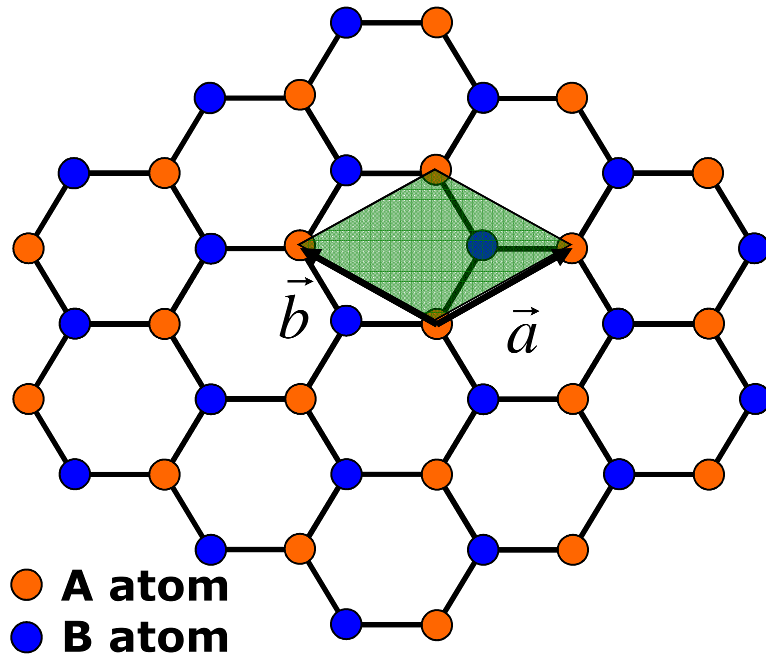

Electronic structure

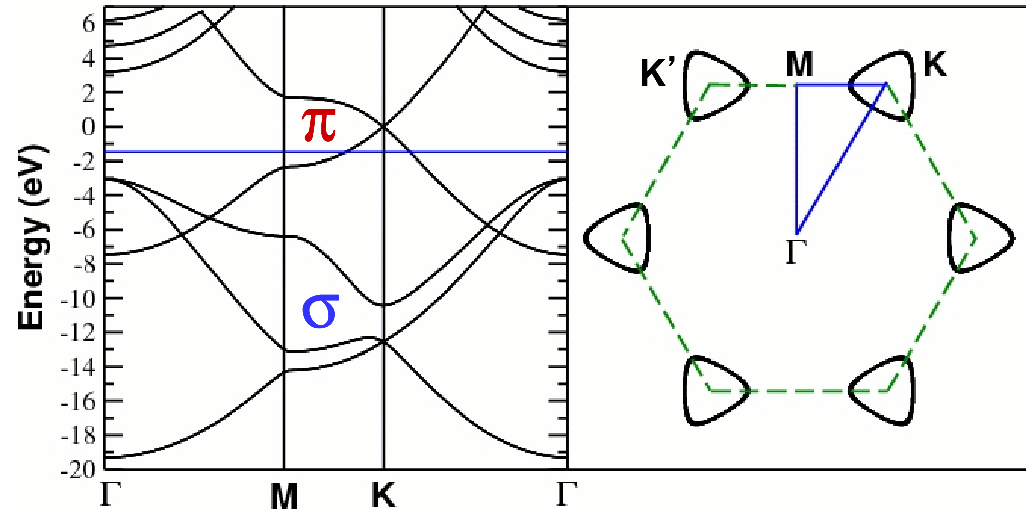

F. Varchon, DFT calculation (PHD thesis)

Graphene is a single carbon plane arranged on a honeycomb lattice

- **two sublattices** (A and B atoms)
- $d_{A\text{-}B}$=1,418 Å
- **a=b=2,456 Å**

Graphene is a gapless semiconductor:

- **Linear and isotropic band structure** around K and K' points
- **Trigonal warping** for $|E|$ >0.5eV

NÉEL institut

Electronic structure of pristine graphene

Honeycomb atomic structure:

- **Two equivalent C atoms per unit cell**
- **Low energy bands arise from p_z orbitals bonding**

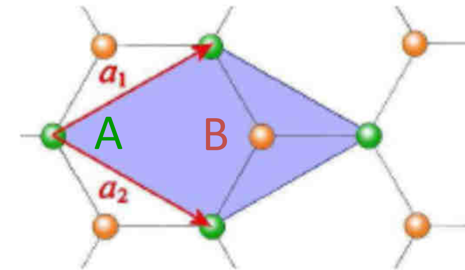

Tight binding calculation, Wallace 1947

$$\Psi^{\mathbf{k}}(\mathbf{r}) = c_A(\mathbf{k})\Phi_A^{\mathbf{k}}(\mathbf{r}) + c_B(\mathbf{k})\Phi_B^{\mathbf{k}}(\mathbf{r}) \qquad |c_A(\mathbf{k})| = |c_B(\mathbf{k})|$$

$$E_\pm(\mathbf{k}) = \pm t\sqrt{3 + f(\mathbf{k})} \qquad f(\mathbf{k}) = 2\cos\left(\sqrt{3}k_y a\right) + 4\cos\left(\frac{\sqrt{3}}{2}k_y a\right)\cos\left(\frac{3}{2}k_x a\right)$$

$$\vec{K} = \Gamma\vec{K} + q$$

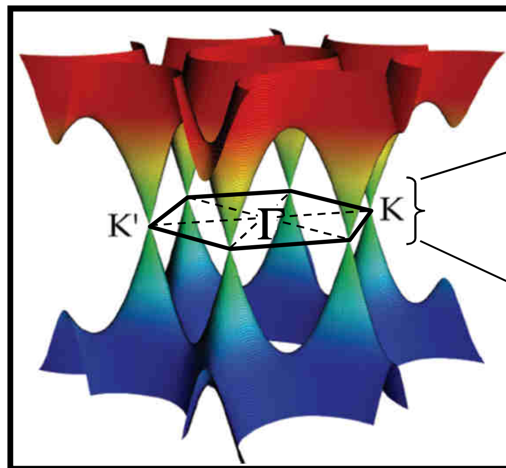

π and π* bands

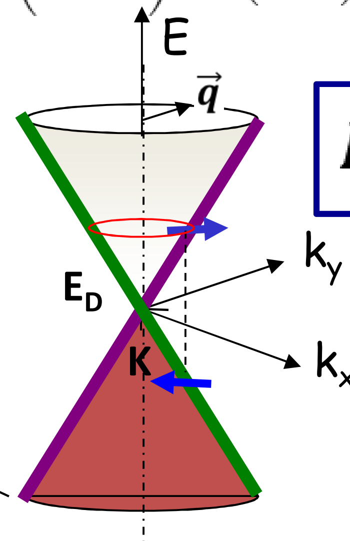

$$E_\pm = E_D \pm \hbar v_F|\vec{q}|$$

avec $v_F \approx 1.0 \times 10^6\ m.s^{-1}$

Linear and isotropic dispersion at K et K' valleys: **Dirac Cones**

Massless Dirac Quasiparticles

Band structure: ML versus BL

Monolayer

$$\Psi^{\mathbf{k}}(\mathbf{r}) = c_A(\mathbf{k})\Phi_A^{\mathbf{k}}(\mathbf{r}) + c_B(\mathbf{k})\Phi_B^{\mathbf{k}}(\mathbf{r})$$

$$|c_A(\mathbf{k})| = |c_B(\mathbf{k})|$$

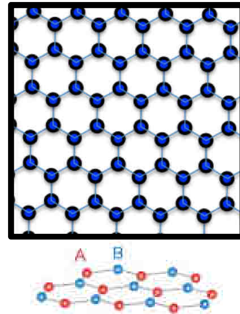

Bernal
Bilayer

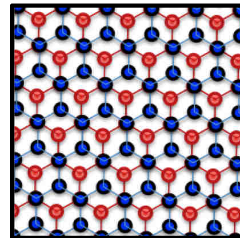

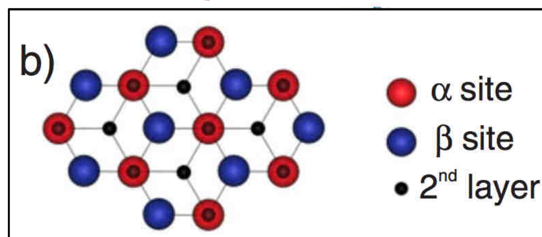

Band structure: ML versus BL

LDOS calculated on A and B sites
(from Real-space analytical expression of the Green's function)

Monolayer

$$\Psi^{\mathbf{k}}(\mathbf{r}) = c_A(\mathbf{k})\Phi_A^{\mathbf{k}}(\mathbf{r}) + c_B(\mathbf{k})\Phi_B^{\mathbf{k}}(\mathbf{r})$$

$$|c_A(\mathbf{k})| = |c_B(\mathbf{k})|$$

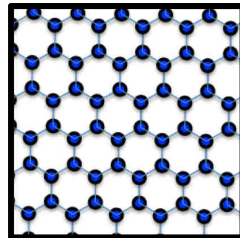

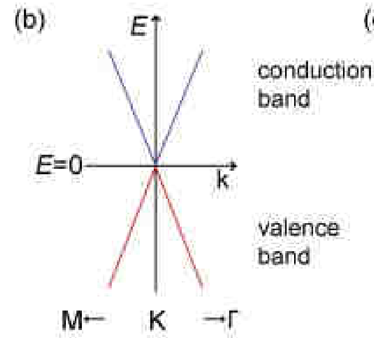

Bernal Bilayer

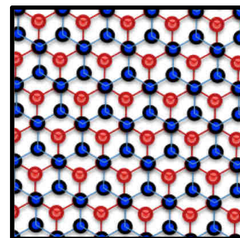

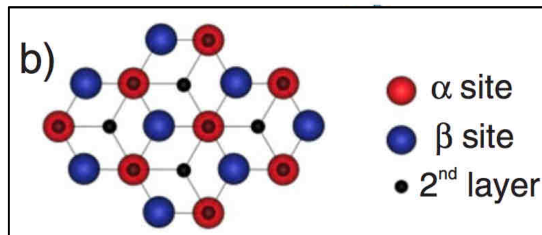

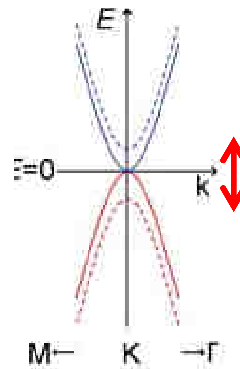

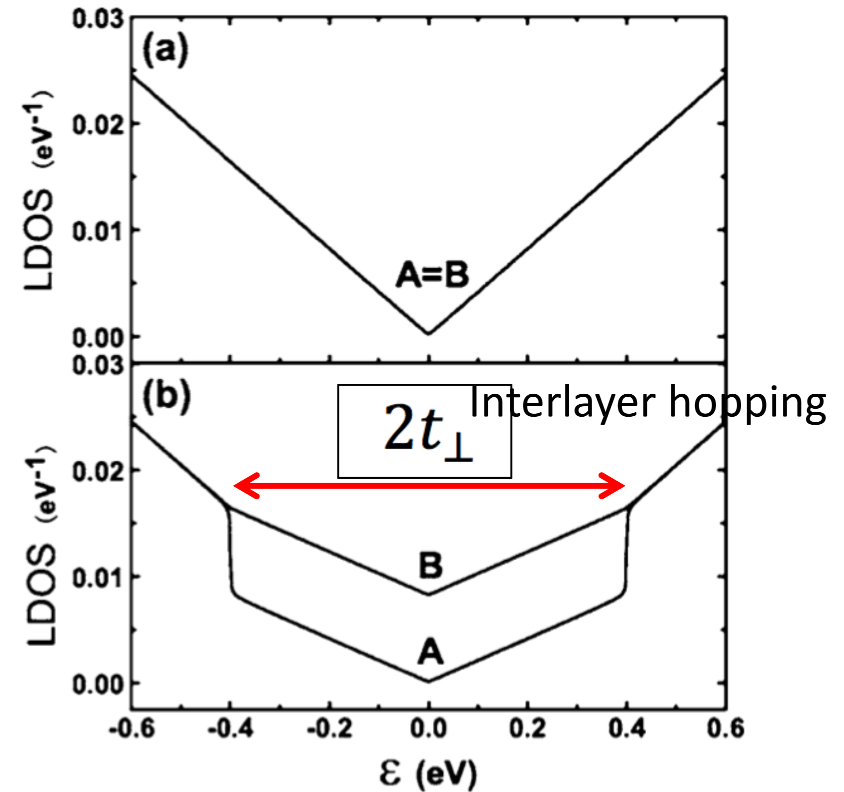

Wang et al. PRB 2007

RAPID COMMUNICATIONS

PHYSICAL REVIEW B 76, 041403(R) (2007)

Electron states of mono- and bilayer graphene on SiC probed by scanning-tunneling microscopy

P. Mallet,[1] F. Varchon,[1] C. Naud,[1] L. Magaud,[1] C. Berger,[1,2] and J.-Y. Veuillen[1]
[1]Institut Néel, CNRS—Université Joseph Fourier, Boîte Postale 166, F-38042 Grenoble Cedex 9, France
[2]Georgia Institute of Technology, Atlanta, Georgia 30332-0430, USA

ML and BL Graphene on SiC – Si face

STM in UHV @ 40K

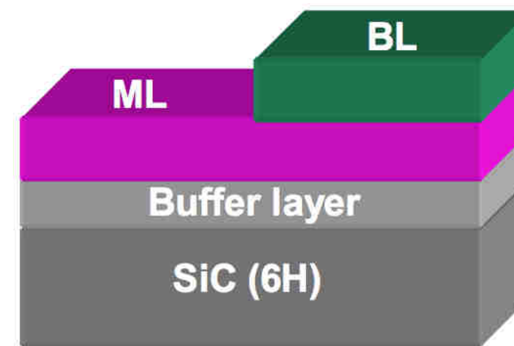

On the SiC - Si face, a carbon buffer layer exists at the interface, strongly bond to the SiC substrate

Buffer layer: Complex interface reconstruction: SiC-6√3x6√3 R30°

Apparent distorsion of period ≈ 1.9 nm

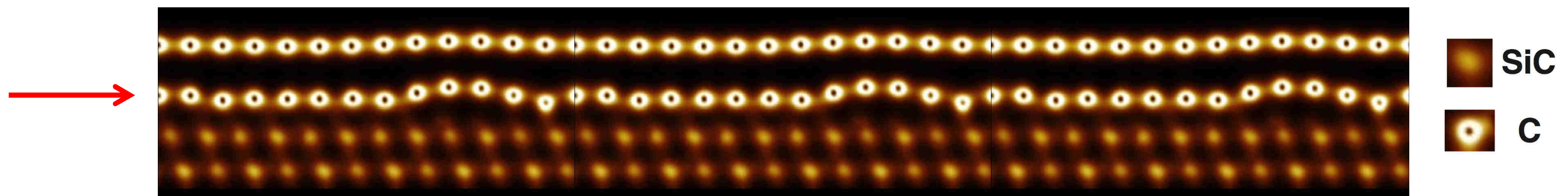

Total charge density map (DFT calculation)
F. Varchon, P. Mallet, J.Y. Veuillen and L. Magaud, PRB'08

RAPID COMMUNICATIONS

PHYSICAL REVIEW B 76, 041403(R) (2007)

Electron states of mono- and bilayer graphene on SiC probed by scanning-tunneling microscopy

P. Mallet,[1] F. Varchon,[1] C. Naud,[1] L. Magaud,[1] C. Berger,[1,2] and J.-Y. Veuillen[1]
[1]*Institut Néel, CNRS—Université Joseph Fourier, Boîte Postale 166, F-38042 Grenoble Cedex 9, France*
[2]*Georgia Institute of Technology, Atlanta, Georgia 30332-0430, USA*

ML and BL Graphene on SiC – Si face

STM in UHV @ 40K

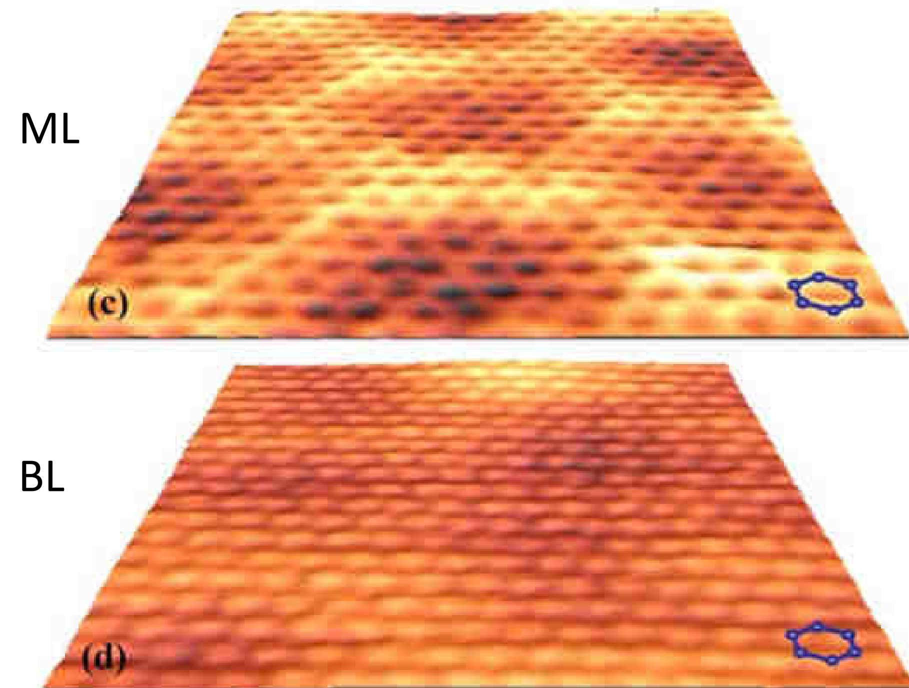

ML: Honeycomb atomic pattern
BK: Triangular atomic pattern

Sample Bias: 200 mV.
Size: 4 x 4 nm^2

See also Brar et al., APL 2007

Atomic contrast: STM versus theory

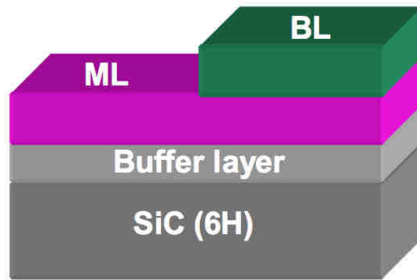

ML

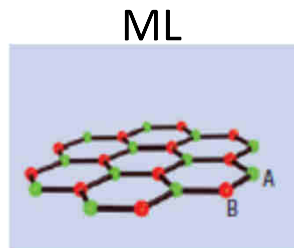

BL

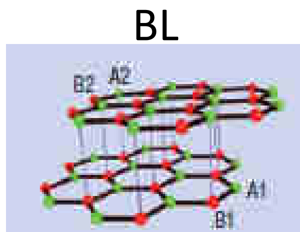

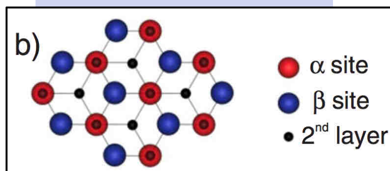

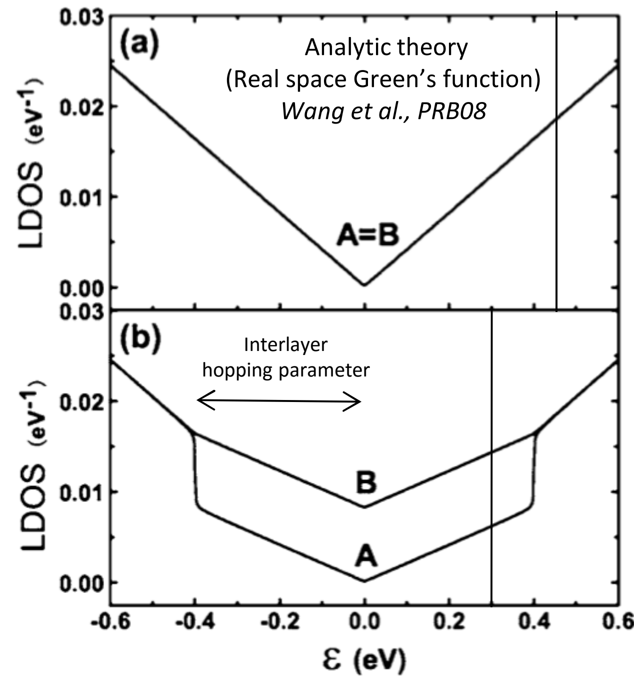

STM

Sample bias +2mV, T=5K

ML

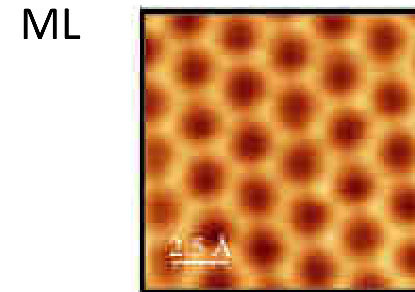

BL

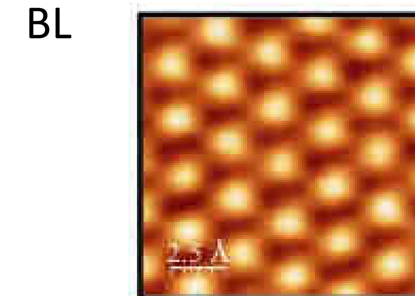

S. Bose et al., New Journ. of Phys. 2010
P. Mallet et al., PRB 2007

STM measurements at low bias:

ML: Same LDOS on A and B sublattices

BL: Strong LDOS asymmetry between A and B atoms

Structural and electronic properties of bilayer epitaxial graphene

G.M. Rutter, J.N. Crain, N.P. Guisinger, P.N. First and J.A. Stroscio, JVST 26, 938 (2008)

STM in UHV @ 5K

BL Graphene on 4H SiC – Si face

STM in UHV @ 5K

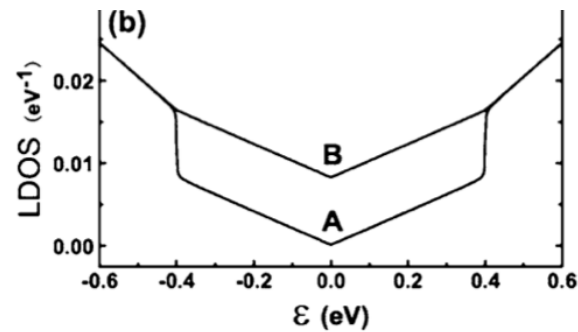

Wang et al. PRB 2007

Sample Bias

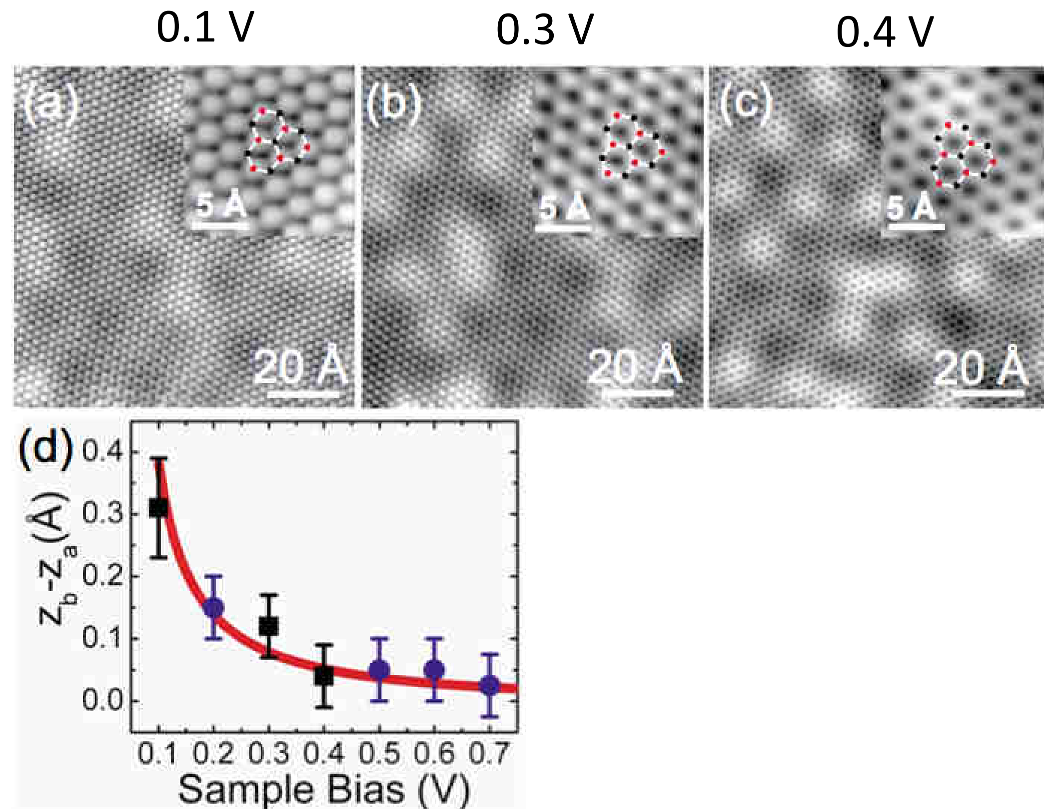

BL graphene:

At sample bias higher than 0.4 eV (interlayer hoping energy): **honeycomb-like atomic pattern**

same LDOS on A and B surface sublattices

Part II.
Interface contribution to the STM images

(non metallic substrates)

Scanning tunnelling microscopy and spectroscopy of ultra-flat graphene on hexagonal boron nitride

Jiamin Xue[1], Javier Sanchez-Yamagishi[2], Danny Bulmash[2], Philippe Jacquod[1,3], Aparna Deshpande[1†], K. Watanabe[4], T. Taniguchi[4], Pablo Jarillo-Herrero[2] and Brian J. LeRoy[1]*

NATURE MATERIALS | VOL 10 | APRIL 2011

Local Electronic Properties of Graphene on a BN Substrate via Scanning Tunneling Microscopy

Régis Decker,*,†,‡,§ Yang Wang,†,§ Victor W. Brar,†,‡ William Regan,† Hsin-Zon Tsai,† Qiong Wu,† William Gannett,†,‡ Alex Zettl,†,‡ and Michael F. Crommie†,‡

Nano Lett. 2011, 11, 2291–2295

Graphene on h-BN/SiO_2/Si++ ,
+ Au electrode
STM in UHV @ 5K

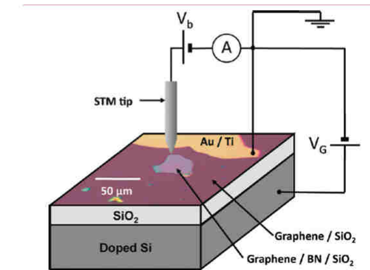

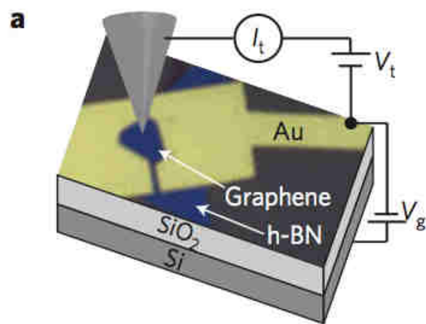

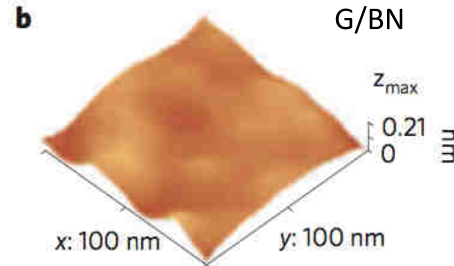

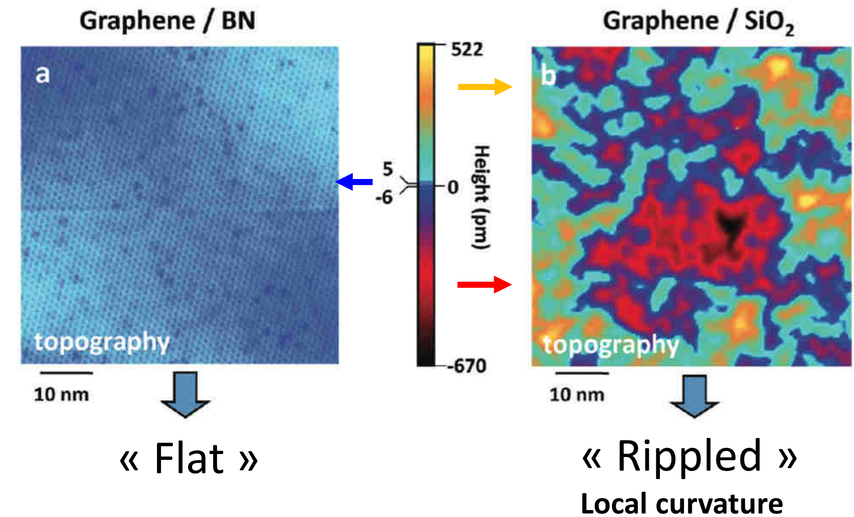

« Flat »

« Rippled »
Local curvature

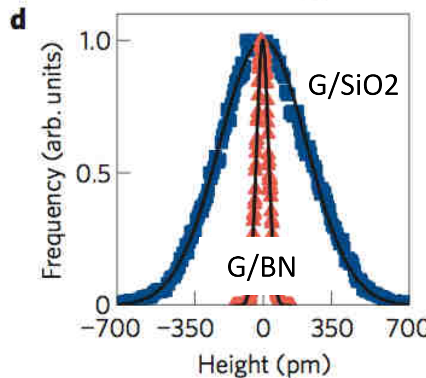

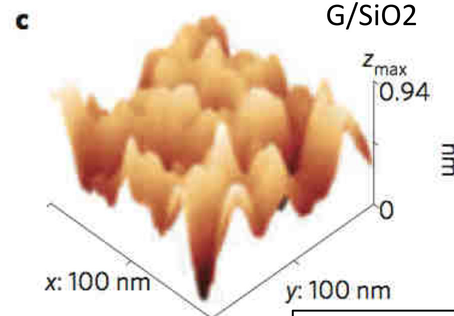

Large corrugation for G/SiO2: (≈1 nm)
Weak Z corrugation on G/h-BN: (10 to 100 pm)
NB same order of magnitude on G on SiC

Morphology of UHV-grown Graphene on SiC – Si face

STM @ 40K

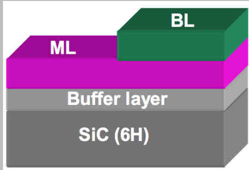

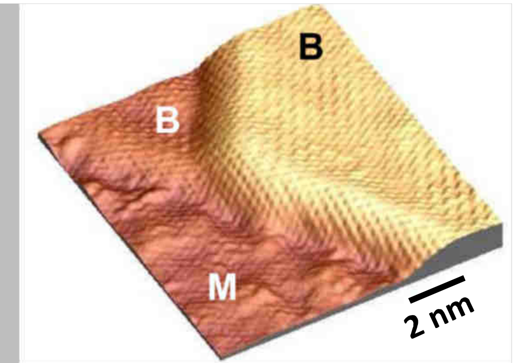

BL

ML

BL

ML

BL

BL

BL

Constant current image

200x126 nm², sample bias: -1V

■ Rough terraces **(ML)** → graphene ML

Apparent roughness related to the interface

■ Smooth terraces **(BL)** → mostly graphene BL

■ **No abrupt step edges: "carpet" like behaviour** (cf insert)

Mallet et al., *PRB **7**6, 041403(R) (07)*

Graphene ML and BL on SiC(0001)Interface states

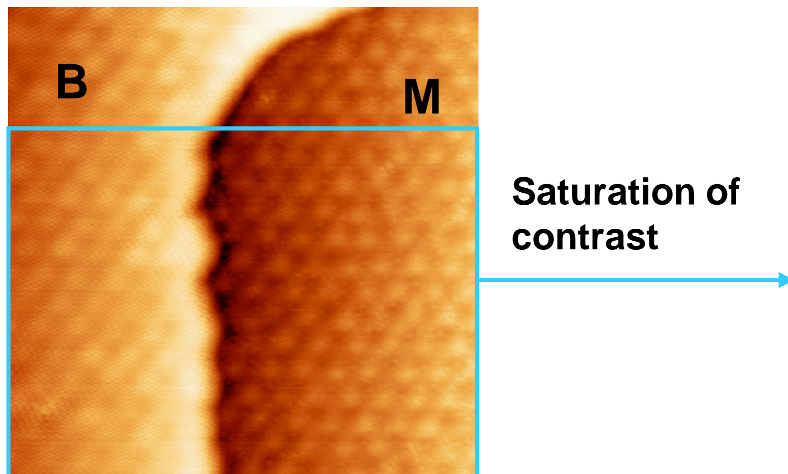

L58, 25x25 nm², -0.1V, 0.1nA.

Saturation of contrast

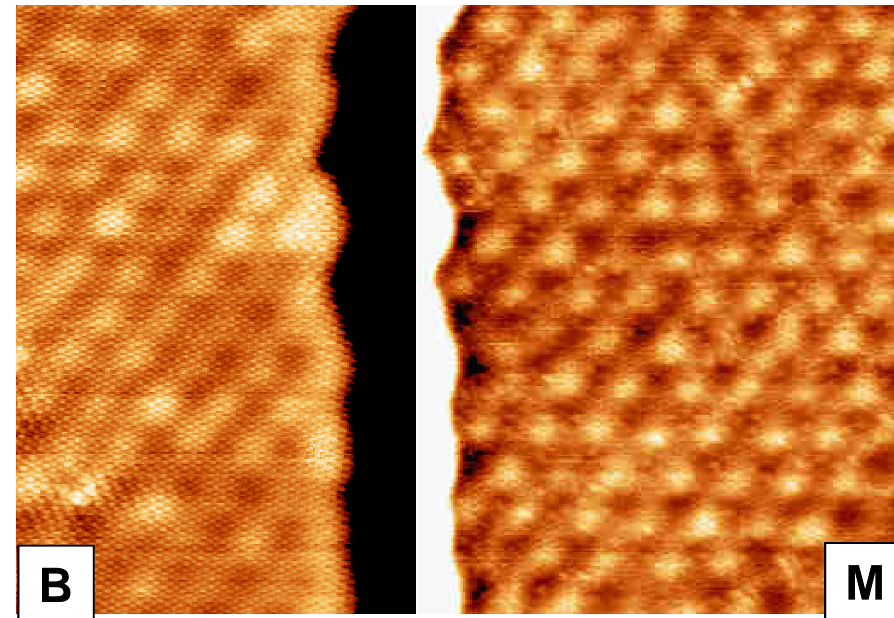

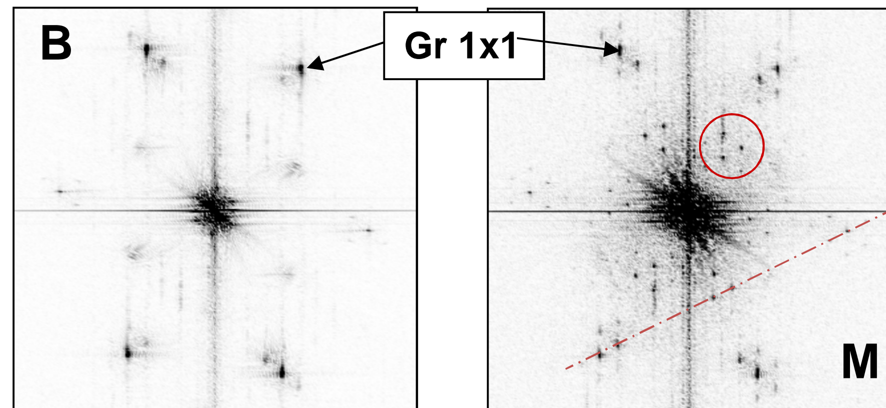

TF: 12.2x12.2 1/nm²

- Low bias image: **-100mV**.
- **M**: monolayer, **B**: bilayer.
- Same orientation for M and B.

- **"Interface" states probed below Monolayer.**
- **No such effect on Bilayer.**

(id. **Riedl et al.**, PRB **76**, 245406 (07)
Lauffer et al., **Rutter et al.**)

- **Spots in the red are related to the SiC-6√3x6√3 R30° interface reconstruction**

Varchon et al, PRB **77**, 235412 (08)

STM "Transparency" of ML graphene at high sample bias

Graphene on SiC – Si face

Iset=1.0nA, 8x8 nm².

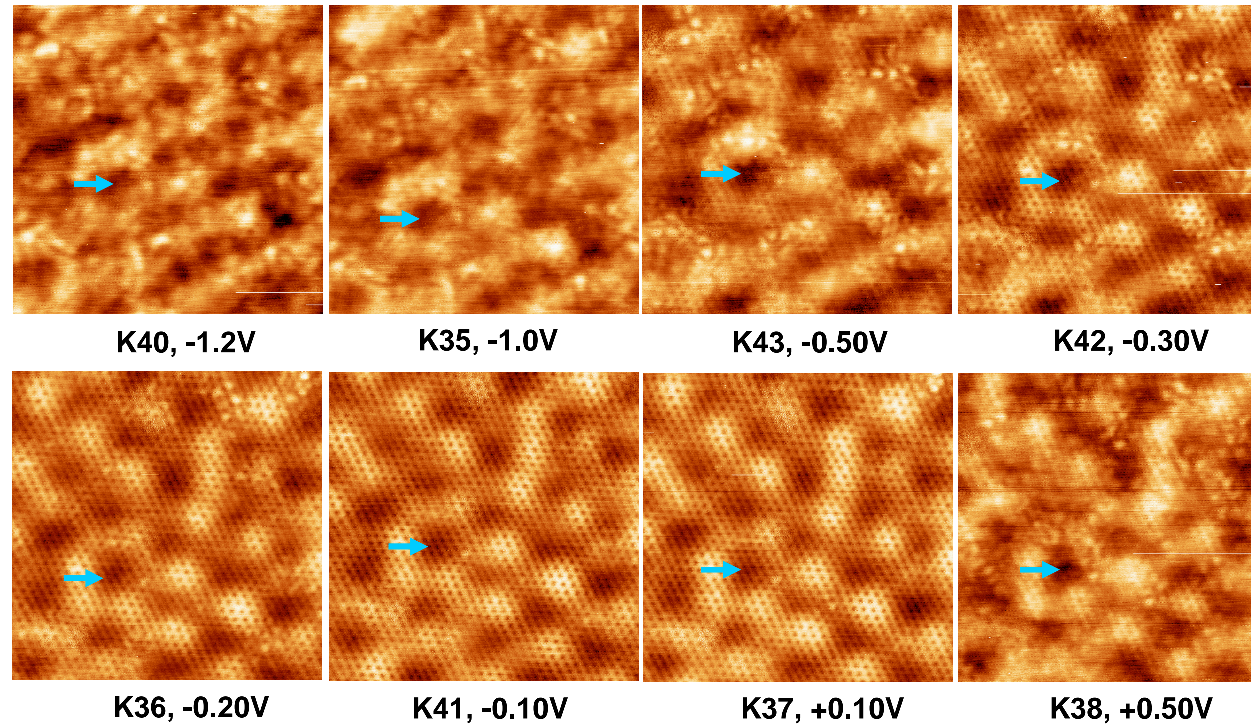

This transparency results from **High tunneling probabilities into the available interface states:**

- Large Interface LDOS at high bias (compared to graphene LDOS)

- Hindered tunneling into graphene states (due to their large k// component)

$$\left|\Psi_{\vec{k}}(x,y,z)\right|^2 \propto e^{-2\tilde{\kappa}z}$$

$$\tilde{\kappa} = \sqrt{\left|\overrightarrow{\Gamma K} + \vec{q}\right|^2 + \frac{2m\Phi}{\hbar^2}}$$

STM "Transparency" of ML graphene at high sample bias

Graphene on SiC – Si face

Iset=1.0nA, 8x8 nm².

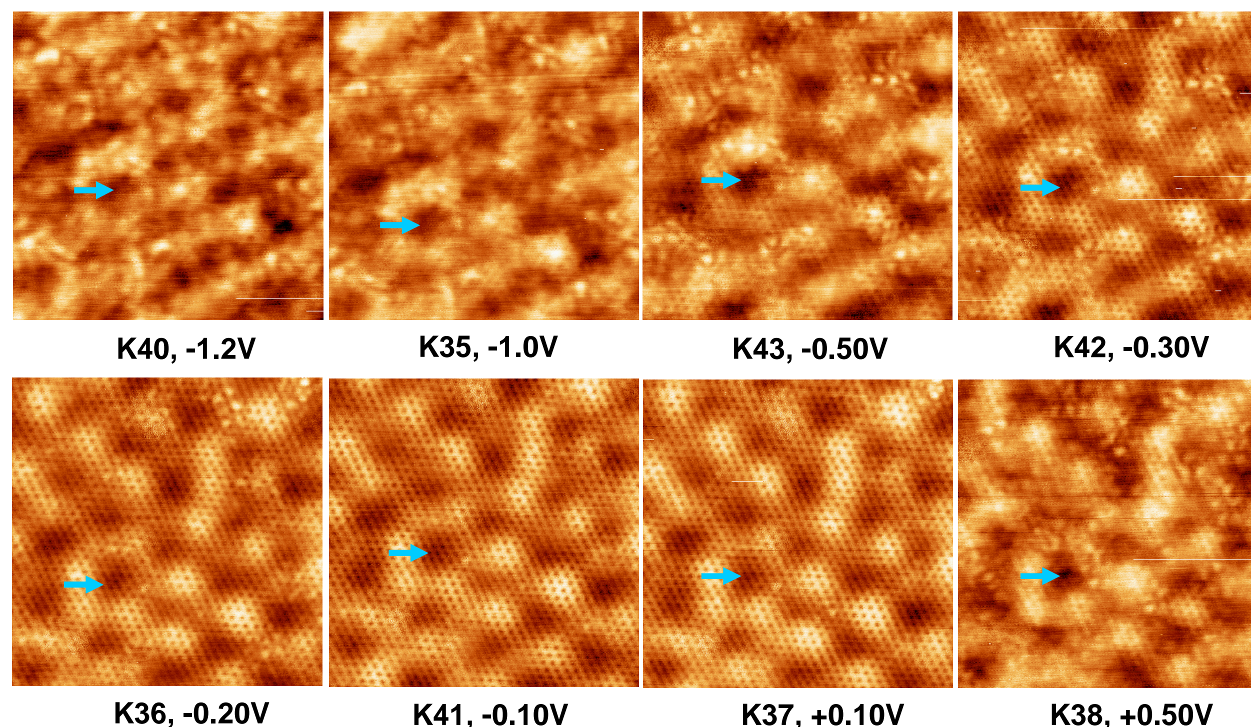

This transparency allows a direct study of the real interface structure (here the buffer layer), which is far from perfectly ordered !

More generally: allows for a study of the changes induced by Gr in the susbtrate atomic or electronic structure:

Gr on Me: Ir(111): S. J. Altenburg et al., PRL 108, 206805 (2012), Cu(111): H. Gonzalez Herrero et al. , ACS Nano 10, 5131 (2016)
Gr on SiC-C face: F. Hiebel et al., PRB 86, 205421 (2012)

www.neel.cnrs.fr

PHYSICAL REVIEW B 76, 235416 (2007)

Imaging the interface of epitaxial graphene with silicon carbide via scanning tunneling microscopy

G. M. Rutter,[1] N. P. Guisinger,[2] J. N. Crain,[2] E. A. A. Jarvis,[2] M. D. Stiles,[2] T. Li,[1] P. N. First,[1,*] and J. A. Stroscio[2,*]
[1]School of Physics, Georgia Institute of Technology, Atlanta, Georgia 30332, USA
[2]Center for Nanoscale Science and Technology, NIST, Gaithersburg, Maryland 20899, USA

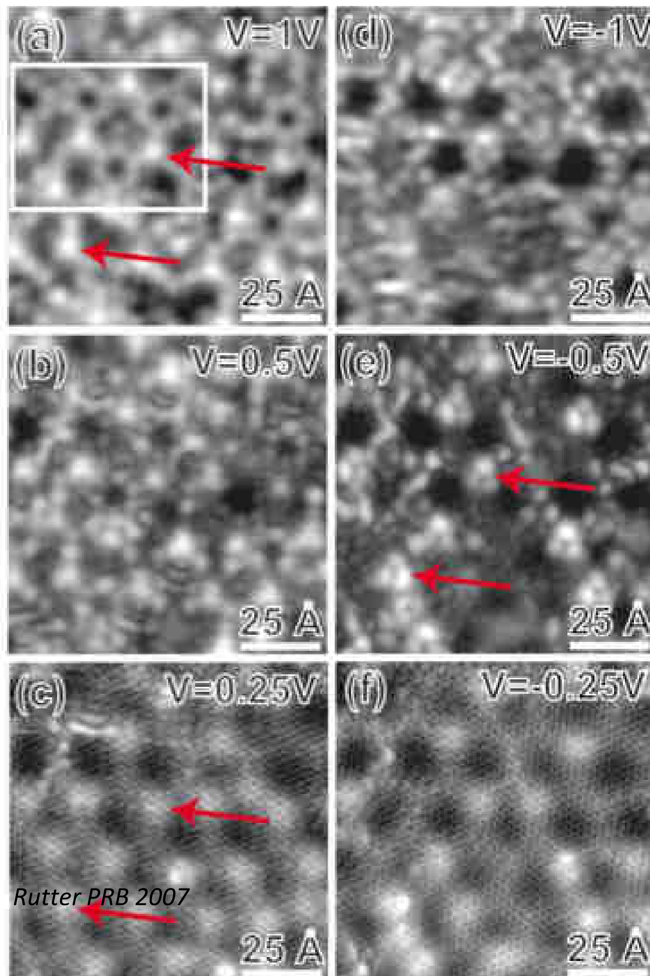

From empty-state images, STM revelas two predominant adatom structures: pyramidal clusters and hexagonal rings.

1. Si adatoms arrange in pyramidal clusters tetramers (red arrow). The top atom is transparent in filled states.
2. Hexagonal rings of Si adatoms

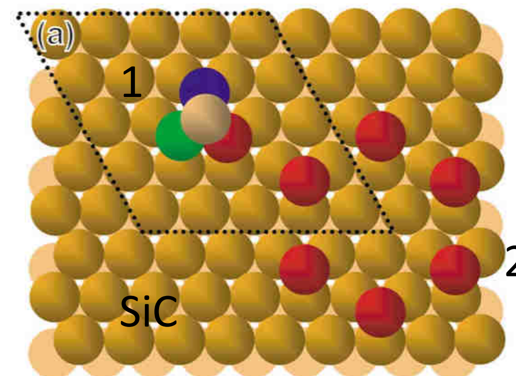

Part III.
Local spectroscopy, Dirac point mapping

$$dI/dV(V) \sim -\int_{-\infty}^{\infty} dE \frac{df(E-eV,T)}{dE} \rho_S(\mathbf{r},E)$$

→ Thermal broadening ~ 1meV à 4,2K

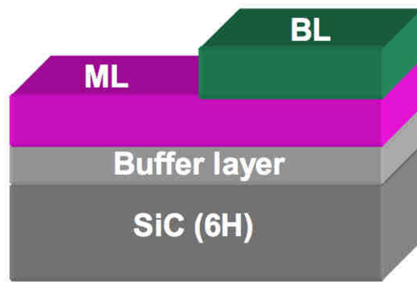

Graphene on SiC – Si face

STM in UHV @ 5K (except in Lauffer @ 77K)

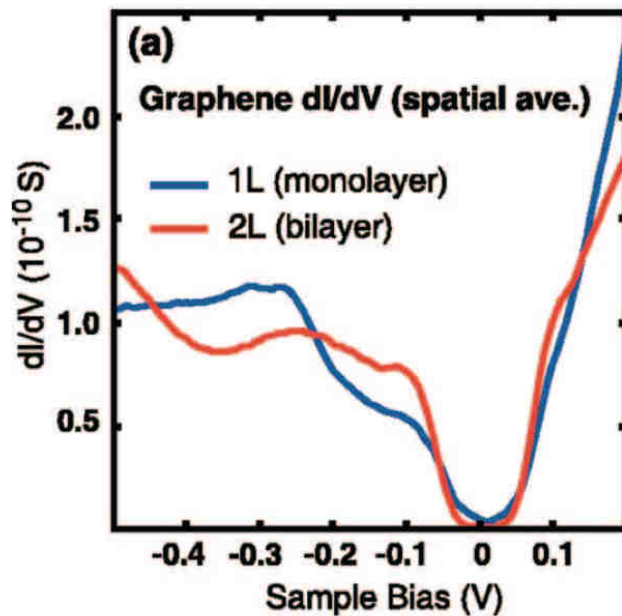

Brar APL 2007

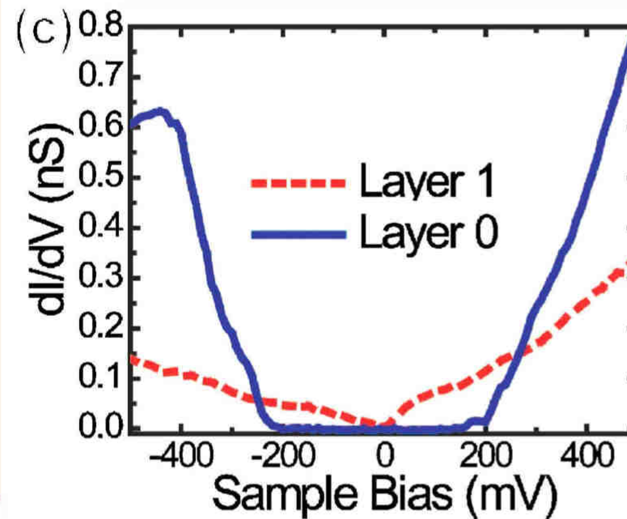

Rutter PRB 2007

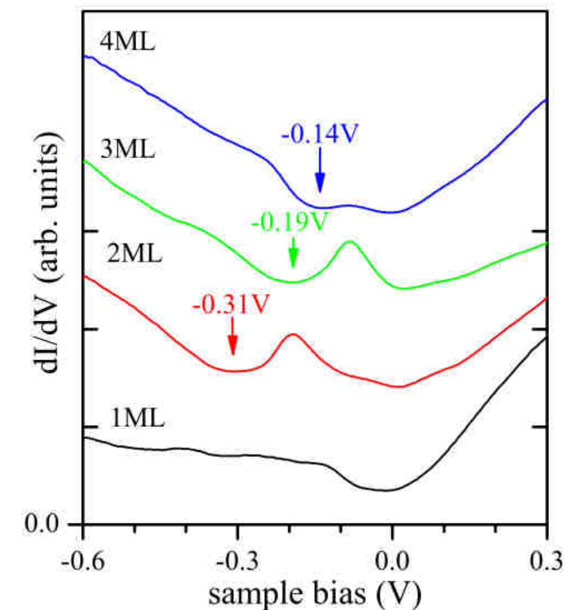

Lauffer PRB 2007

- Gap-like structure around E_F , **but not systematic** (Rutter PRB), width 100 – 130 meV
- Clear dip in occupied states (-0.3 ; -0.35 eV) for BL
- For ML ???

ARPES measurements on ML and BL on SiC(0001)

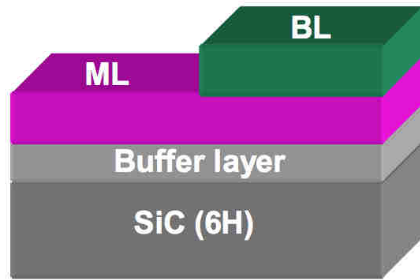

(E. Rottenberg's group, Berkeley)

T. Ohta et al., PRL'07

also Zhou et al., Nature Materials'07

ML

K

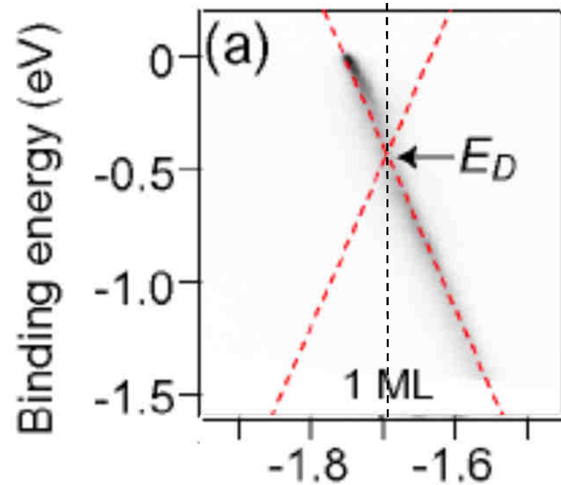

BL

K

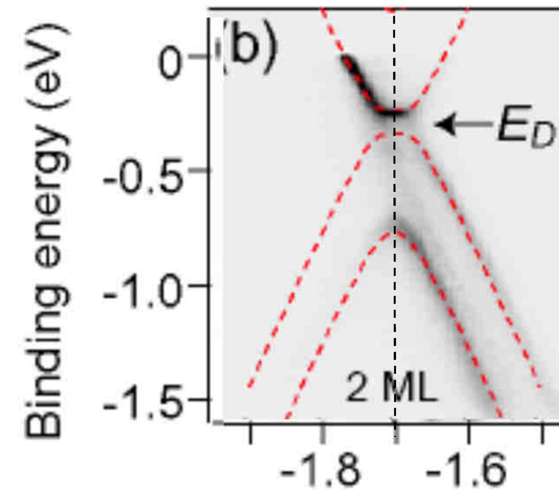

ML:	**Dirac cone at K point**	$E_D \approx E_F - 0.45$ **eV**
BL:	**Parabolic-like bands**	$E_D \approx E_F - 0.30$ **eV**

Both ML and BL graphene are n-doped due to charge transfer from the interface

- Thus for ML graphene on SiC(0001), a dip at – 0.45 V is expected in dI/dV(V)
- However, it is hardly detectable by STS, due to the large contribution of the interface states

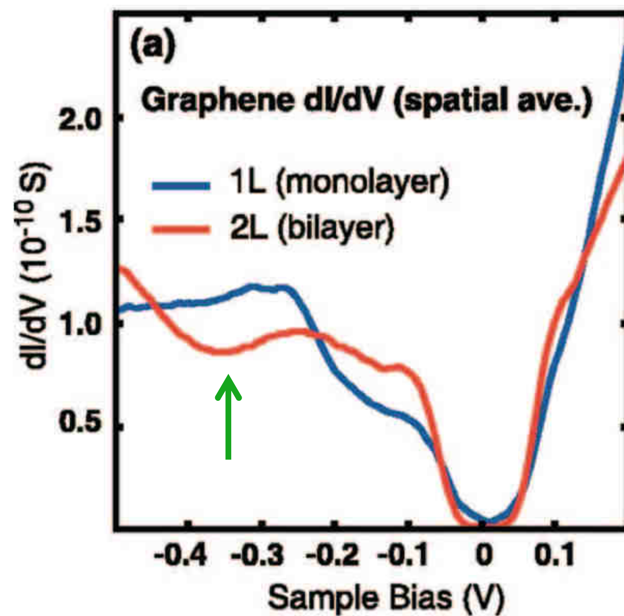

Brar APL 2007

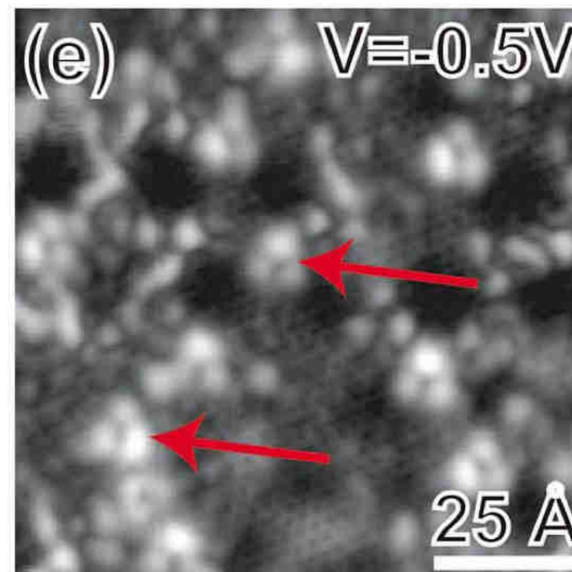

Rutter PRB 2007

- For BL graphene on SiC(0001), the dip @ -0.35 eV is indeed the Dirac point (No spurious contribution of interface states)

Possible origin for the zero bias gap

Giant phonon-induced conductance in scanning tunnelling spectroscopy of gate-tunable graphene

YUANBO ZHANG[1]*, VICTOR W. BRAR[1,2], FENG WANG[1], CAGLAR GIRIT[1,2], YOSSI YAYON[1], MELISSA PANLASIGUI[1], ALEX ZETTL[1,2] AND MICHAEL F. CROMMIE[1,2]*

[1]Department of Physics, University of California at Berkeley, Berkeley, California 94720, USA
[2]Materials Sciences Division, Lawrence Berkeley Laboratory, Berkeley, California 94720, USA
*e-mail: zhyb@berkeley.edu; crommie@berkeley.edu

Nature Physics 4, 627 (2008)

GATED Graphene on SiO2/Si++

Au electrodes contact the Graphene flakes

STM in UHV @ 5K

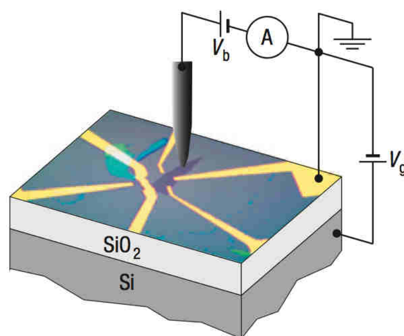

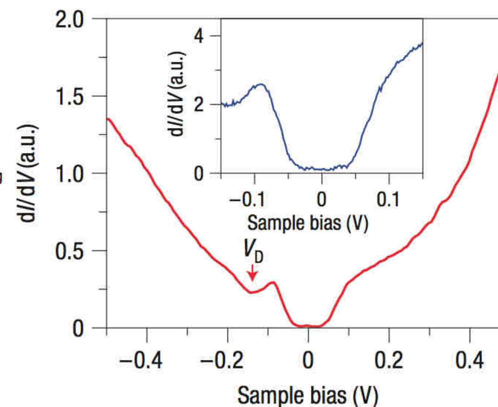

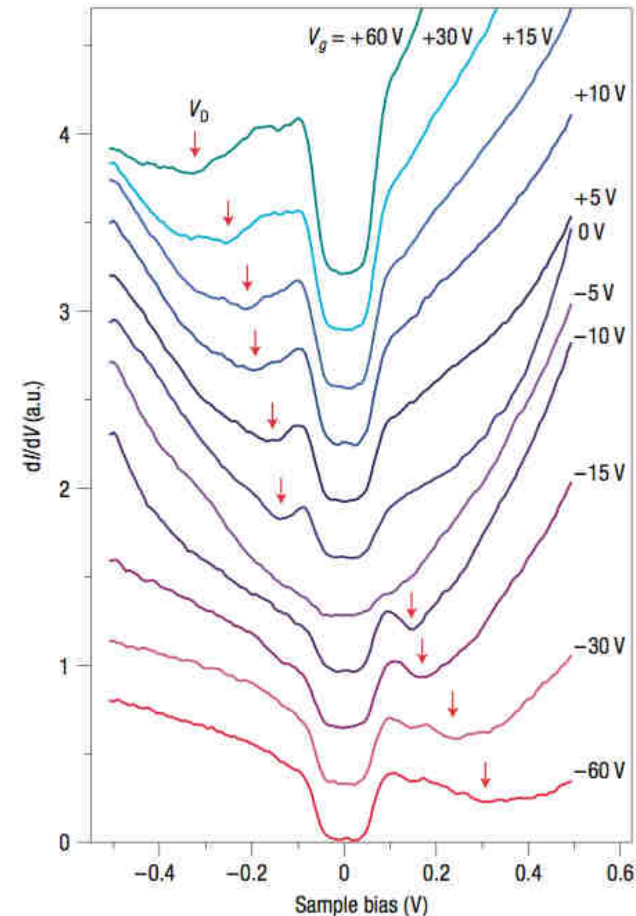

V_D is gate voltage dependant, not the zero bias gap (width 130mV)
Origin of the zero bias gap?

A mechanism based on Inelastic Tunneling

Above the energy threshold at 65 meV:
an inelastic tunneling chanel is activated,
giving rise **to a strong conductance increase.**

Possible coupling with the **67 meV out-of plane acoustic phonon modes located near the K/K' points**.

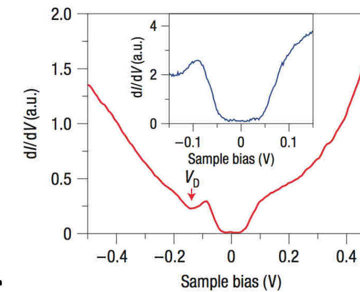

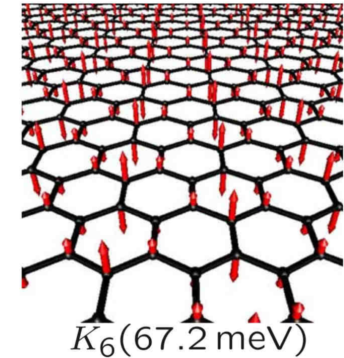

Mohr et al., PRB 76, 035439 (2007)

Zhang et al., Nature Physics 4, 627 (2008)
Wehling e tal., PRL 101, 216803 (2008)

A mechanism based on Inelastic Tunneling

Above the energy threshold at 65 meV:
an inelastic tunneling chanel is activated,
giving rise **to a strong conductance increase.**

Possible coupling with the **67 meV out-of plane acoustic phonon modes located near the K/K' points**.

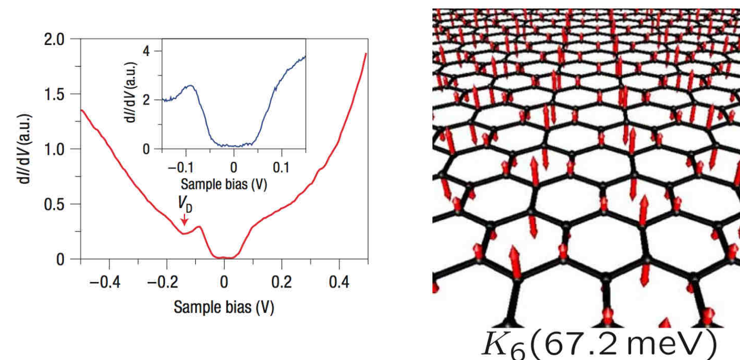

Mohr et al., PRB 76, 035439 (2007)

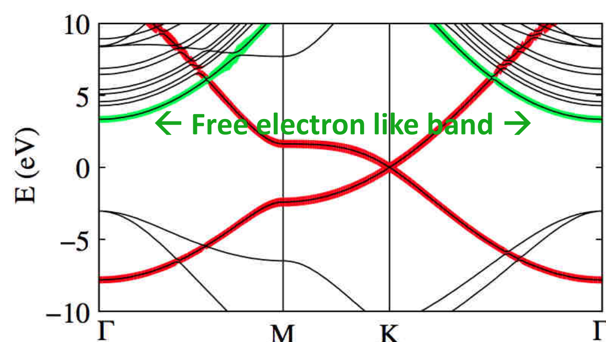

Such phonon modes **mix** the nearly free-electron bands at Γ with the Dirac-like π bands at K (virtual transitions between 2D electronic bands)

The strong conductance enhancement results from the much slower decay of states at Γ into the vacuum.

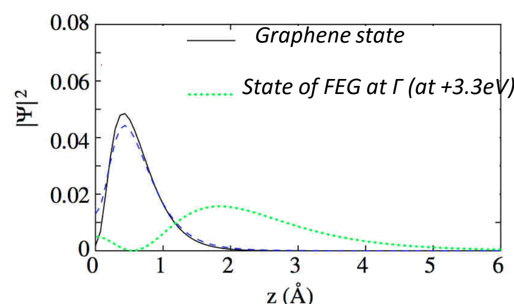

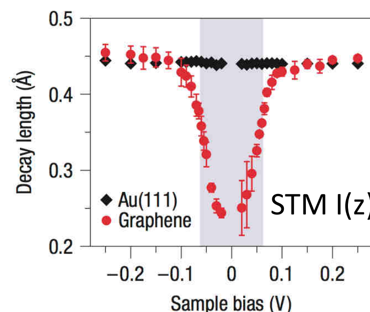

$$\mathrm{LDOS}(z, k_{\parallel}) \propto e^{-z/\lambda}, \qquad \lambda^{-1} = 2\sqrt{2m\phi/\hbar^2 + k_{\parallel}^2}$$

Zhang et al., Nature Physics 4, 627 (2008)
Wehling et al., PRL 101, 216803 (2008)

NB: no such « gap-like » feature on point defects (Nsub) due to local symmetry breaking (J. Lagoute et al., PRB 91, 125442 (2015))

Charge puddles

Origin of spatial charge inhomogeneity in graphene

Yuanbo Zhang[1*†], Victor W. Brar[1,2*], Caglar Girit[1,2], Alex Zettl[1,2] and Michael F. Crommie[1,2†]

Nature Physics 5, 722 (2009)

Graphene on SiO2/Si++

STM in UHV @ 5K

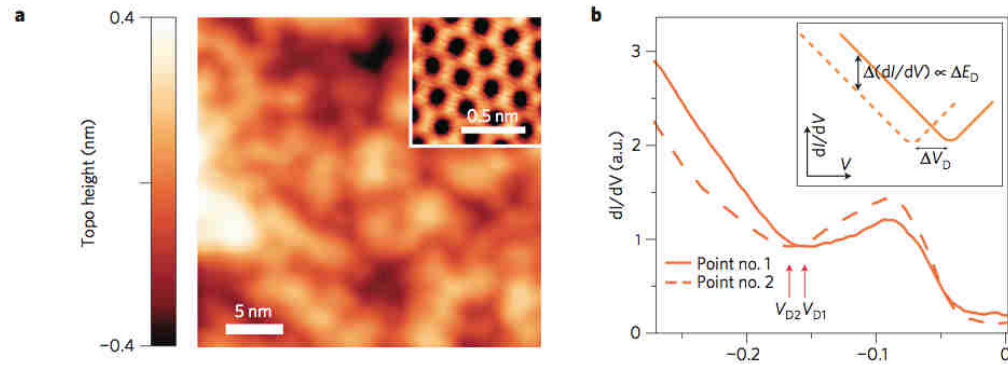

Origin of spatial charge inhomogeneity in graphene

Yuanbo Zhang[1*†], Victor W. Brar[1,2*], Caglar Girit[1,2], Alex Zettl[1,2] and Michael F. Crommie[1,2†]

Nature Physics 5, 722 (2009)

Graphene on SiO2/Si++

STM in UHV @ 5K

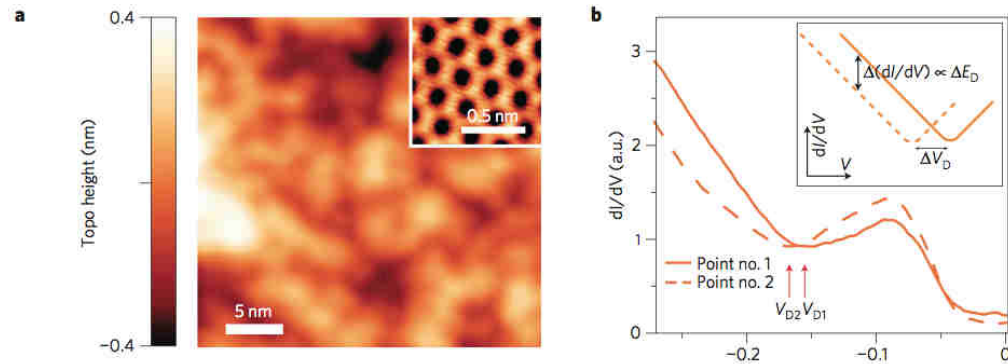

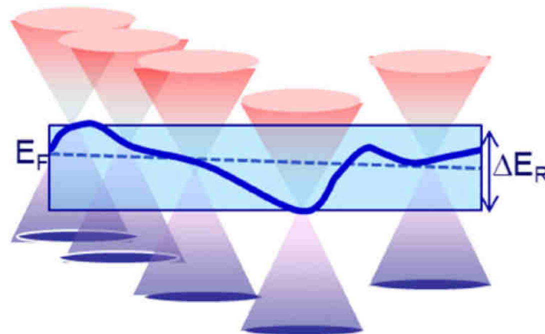

$$n(x,y) = E_D^2(x,y)/\pi(\hbar v_F)^2$$

→ **Charge puddles**

Origin of spatial charge inhomogeneity in graphene

Yuanbo Zhang[1*†], Victor W. Brar[1,2*], Caglar Girit[1,2], Alex Zettl[1,2] and Michael F. Crommie[1,2†]

Nature Physics 5, 722 (2009)

Graphene on SiO2/Si++

STM in UHV @ 5K (Backgate voltage: +15V)

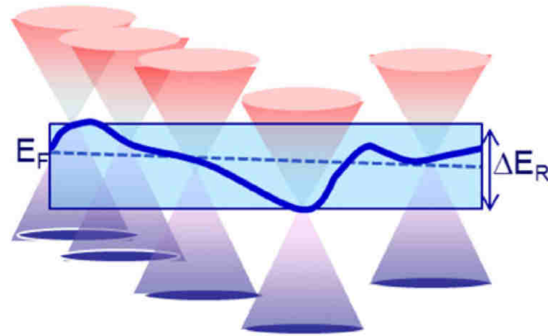

$$n(x,y) = E_D^2(x,y)/\pi(\hbar v_F)^2$$

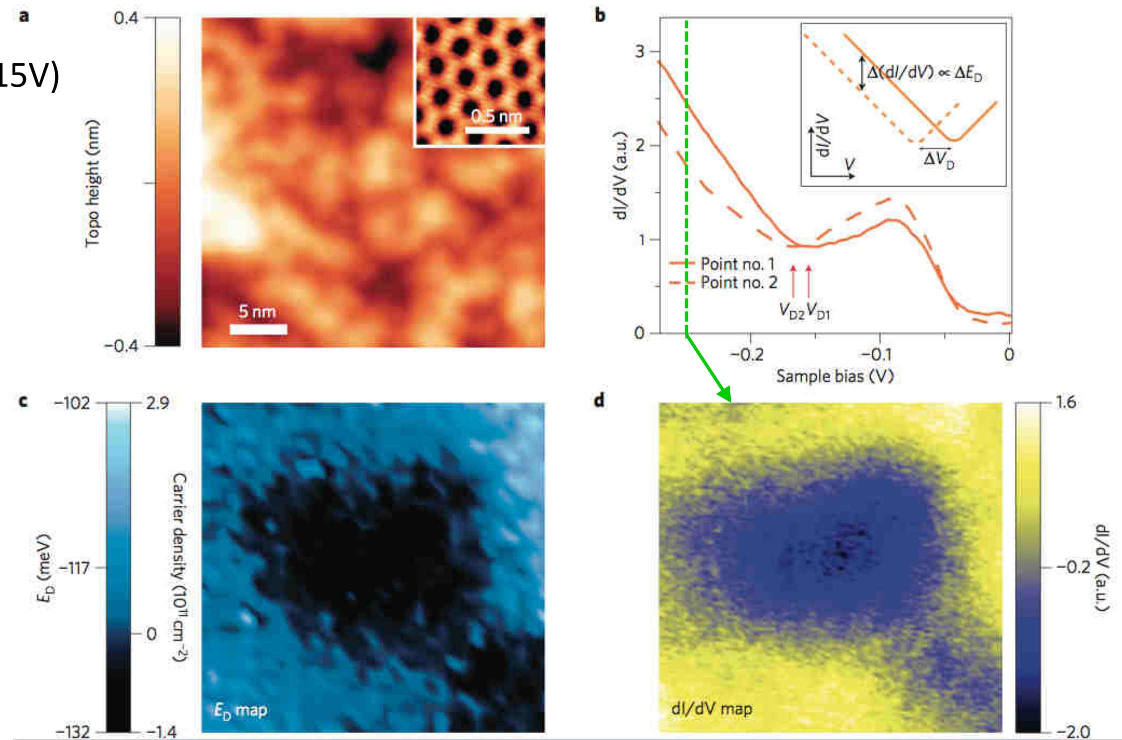

Spatial variation of E_D, revealing **charge puddles** an order of magnitude larger than the size of topographic corrugations
Origin: individual charge impurities located beneath the graphene sheet (from high bias dI/dV maps)

See also Deshpande et al., PRB 2009

Origin of spatial charge inhomogeneity in graphene

Yuanbo Zhang[1*†], Victor W. Brar[1,2*], Caglar Girit[1,2], Alex Zettl[1,2] and Michael F. Crommie[1,2†]

Same region 60x60nm² for all images.

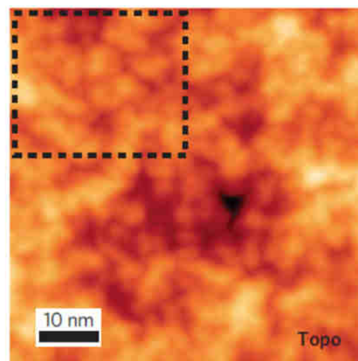

Topo

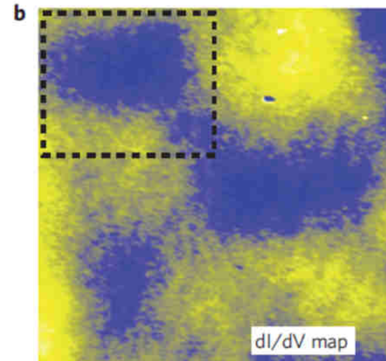

dI/dV just below DP
For puddles

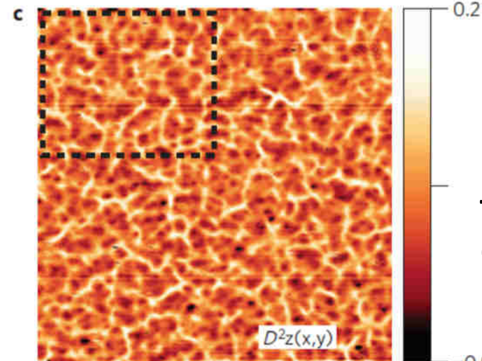

Curvature

No relationship between topo or curvature and puddles
(<puddle size>: 20 nm)

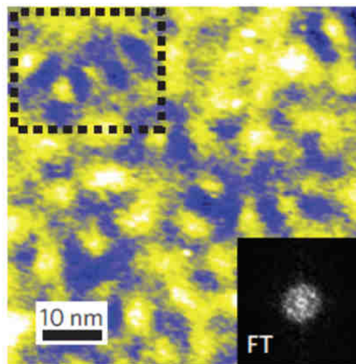

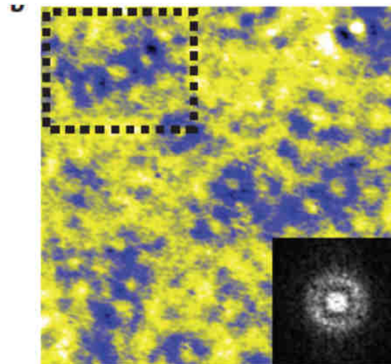

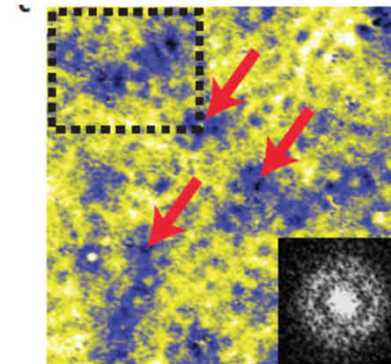

Scattering centers (dots in dI/dV maps).

dI/dV well above (>0.45eV) the DP identifying the **charged impurities** **as scattering centers**

Dependence of the puddles on the carrier density.

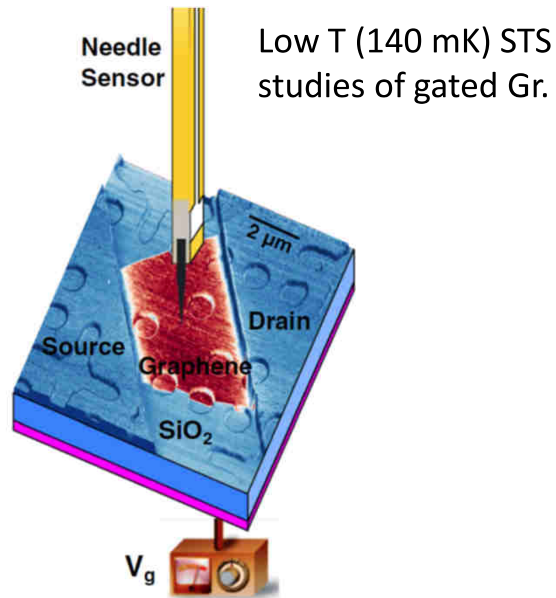

Low T (140 mK) STS studies of gated Gr.

S. Samaddar et al., PRL 116, 126804 (2016)

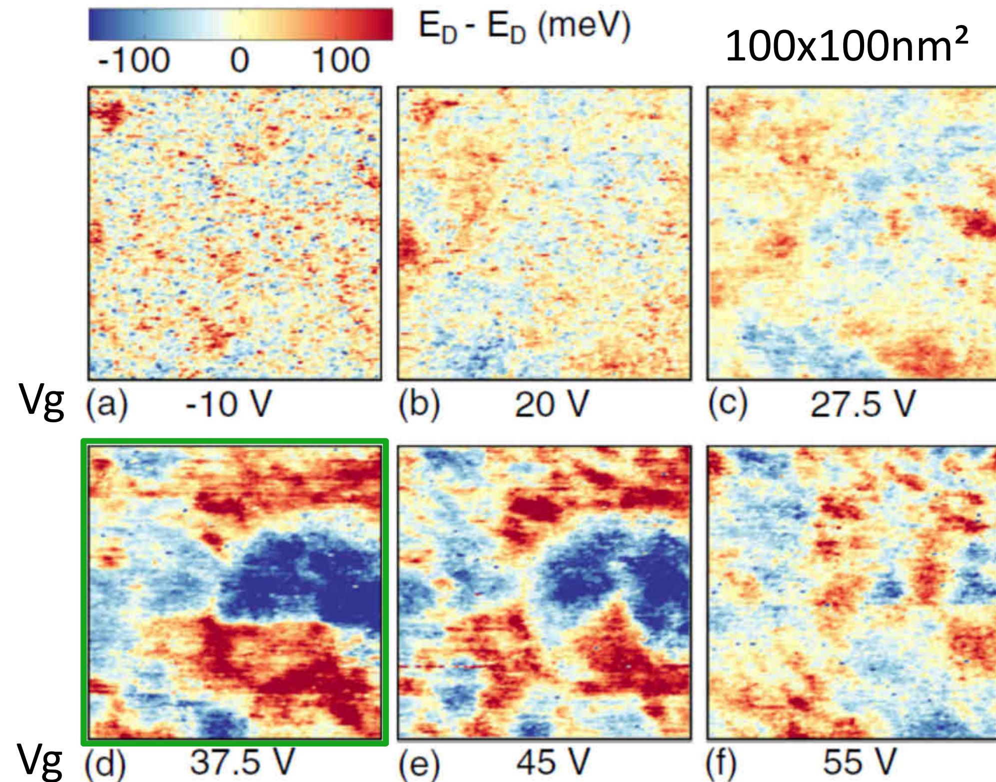

Spatial fluctuations of the Dirac point (% average value) for increasing gate voltages. <Neutral point> is for **Vg≈38 V**.

- Amplitude and size of the fluctuations (puddles) increases as the DP approaches E_F.
- Due to **increased** (decreased) **screening** by the Gr carriers as their density **n** increases (decreases): q_{TF} α q_F α √n for Gr *(q_{TF}: Thomas Fermi sreening vector).*
- Experimental: <Puddle size> α 1/q_{TF} α 1/√n
- *Well described by self consistent theory based on RPA.*

Scanning tunnelling microscopy and spectroscopy of ultra-flat graphene on hexagonal boron nitride

Jiamin Xue[1], Javier Sanchez-Yamagishi[2], Danny Bulmash[2], Philippe Jacquod[1,3], Aparna Deshpande[1†], K. Watanabe[4], T. Taniguchi[4], Pablo Jarillo-Herrero[2] and Brian J. LeRoy[1]*

Nature Materials 10, 282 (2011)

G/h-BN versus G/SiO2

STM in UHV @ 5K (at fixed gate voltage)

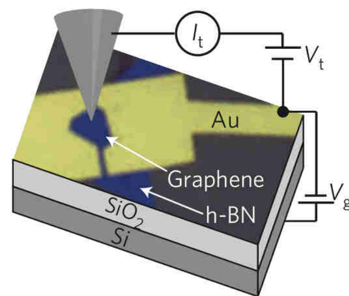

Scale bar 10nm

Topo G/h-BN

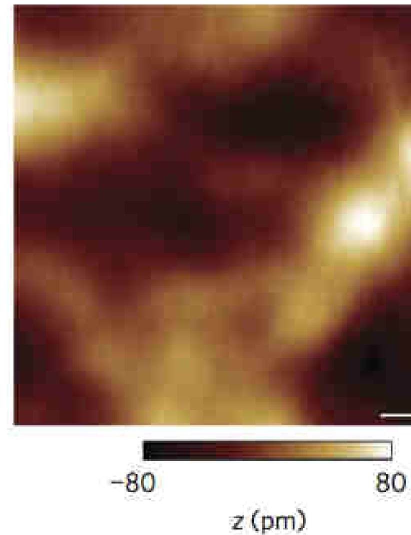

Dirac point map, G/h-BN

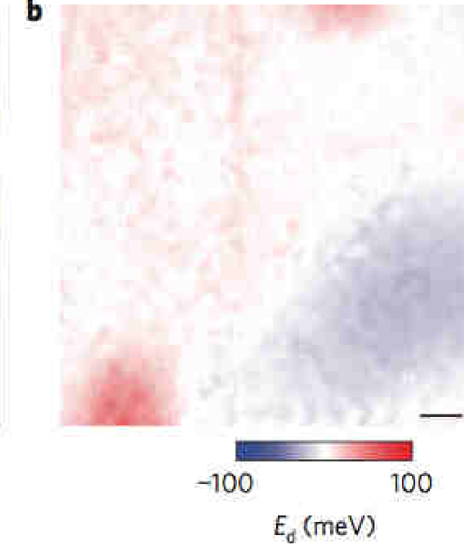

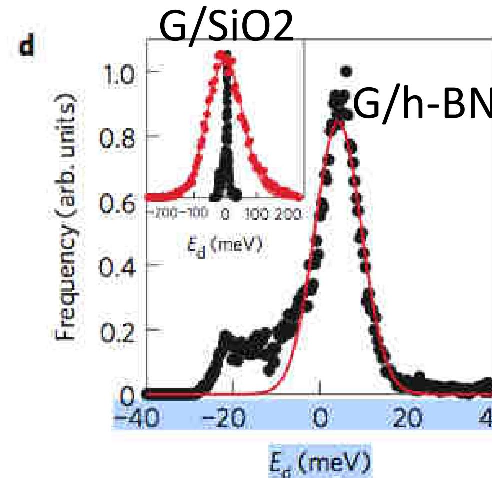

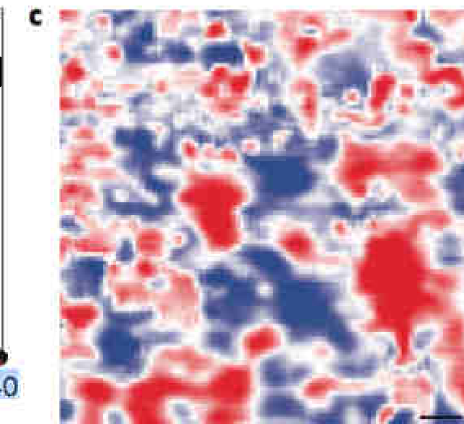

Dirac point map, G/SiO2
(**same** color scale as for G/h-BN)

G/h-BN versus G/SiO2:
Electron–hole charge puddles are reduced by two orders of magnitude (for charge).

Local Electronic Properties of Graphene on a BN Substrate via Scanning Tunneling Microscopy

Régis Decker,[*,†,‡,§] Yang Wang,[†,§] Victor W. Brar,[†,‡] William Regan,[†] Hsin-Zon Tsai,[†] Qiong Wu,[†] William Gannett,[†,‡] Alex Zettl,[†,‡] and Michael F. Crommie[†,‡]

[†]Department of Physics, University of California Berkeley, Berkeley, California 94720, United States
[‡]Materials Science Division, Lawrence Berkeley National Laboratory, Berkeley, California 94720, United States

Nano. Lett. 11, 2291(2011)

G/h-BN versus G/SiO2

STM in UHV @ 5K, with backgate voltage V_G

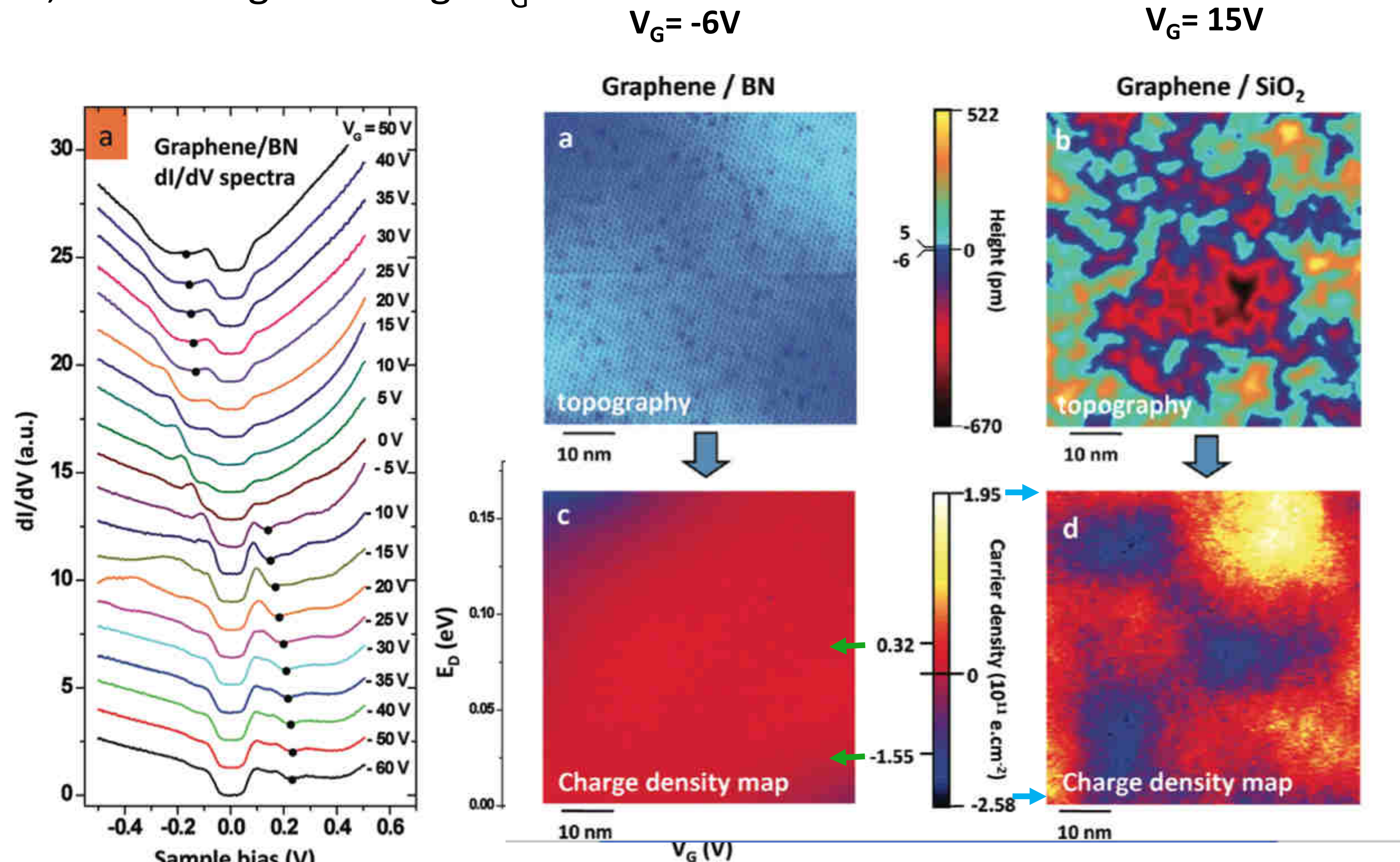

Part VI.
Point defects

Point defects on graphene

- Defects are supposed to degrade the transport properties of graphene, but can also be exploited for Gr functionnalization.

- A number of possible cases: adsorbates, substitutional, vacancies…. for various purposes: doping, creating local moments, inducing « topological » phases….

- A « classical » case: the C « vacancy » .
  Magnetism in graphitic systems.

- H on Graphene: local magnetic moments.

- Other defects: divacancies, substitutionnal N.

Early STM study: single vacancies on graphite

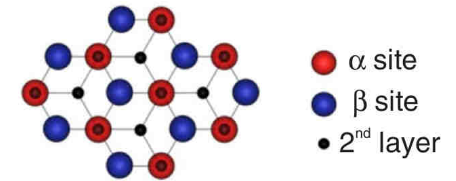

Vacancy on α site

Vacancy on β site

Tight binding
(unreconstructed vacancy)

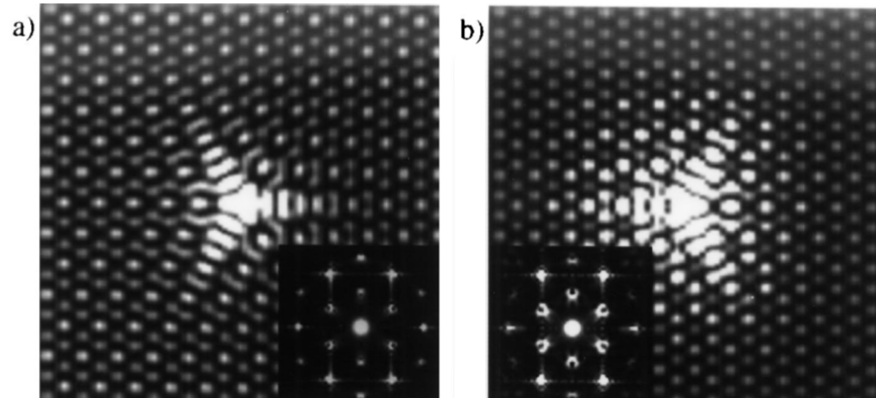

STM

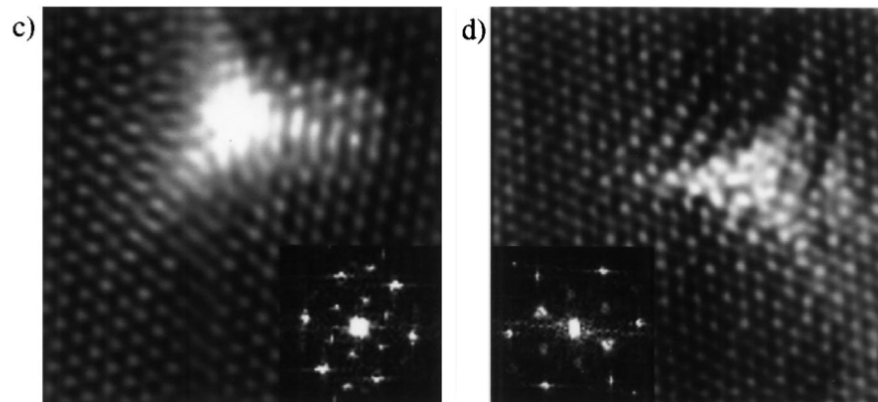

K.F. Kelly, N.J. Halas / Surface Science 416 (1998) L1085–L1089

H.A. Mizes, J.S. Foster, Science 244 (1989) 559

A very **localized defect** (atomic size) induces a **spatially extended** (a few nm) **perturbation**!

Plenty of calculation, cf DFT H. Amara, S. Latil, V. Meunier, P. Lambin, and J. C. Charlier Phys. Rev. B76 115423 (2007).

C « vacancy » in graphene

***A simple model*:**

- Graphene as a « honeycomb » lattice of p_z orbitals with only NN TB coupling.
- A « vacancy » is just a missing p_z orbital on one sublattice (A or B).

The « vacancy » in sublattice A generates a « zero energy mode » at the Dirac point, which exits only on sublattice B and which is « semilocalized » (WF decays as 1/r).

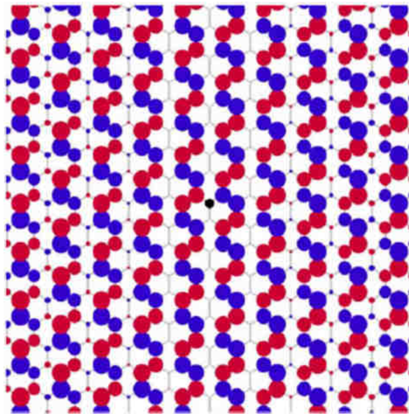

First non zero energy state: delocalized

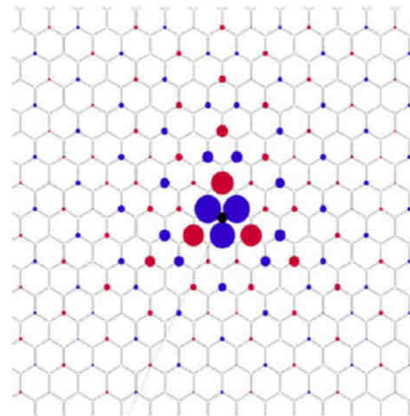

Zero energy state: (semi) localized

LDOS at the site closet to the vacancy

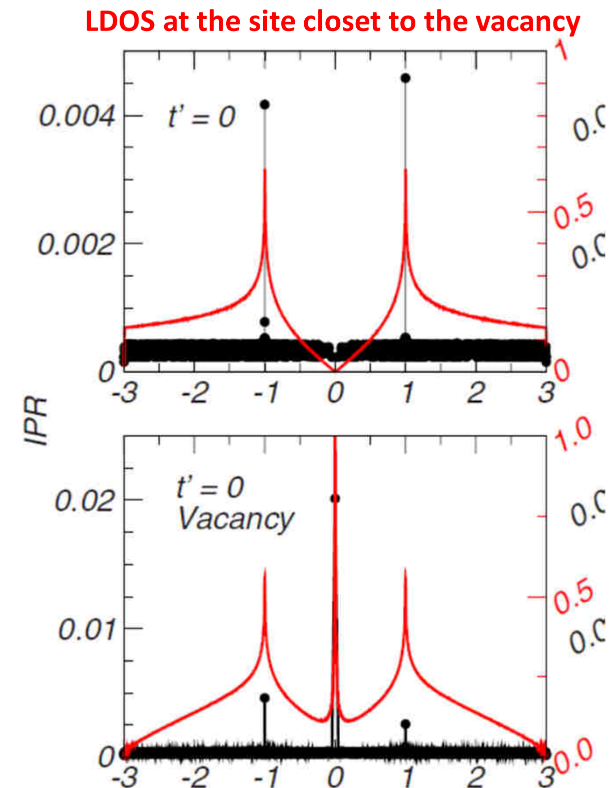

V. M. Peirera et al., PRB 77, 115109 (2008),
see also:
B. R. K. Nanda et al., NJP 14, 083004 (20012), M. Inui et al., PRB 49, 3190 (1994)

C « vacancy » in graphene

A simple model (continued):

- As a result of electron-electron interaction (exchange energy gain), this « zero energy mode » should undergo spin polarization.

  O. V. Yazyev, Rep. Prog. Phys. 73, 056501 (2010) for a **review.**

- Emergence of a local magnetic moment with spin S=1/2 (m=1 μ_B).

  In agreement with Lieb's theorem (E. H. Lieb, PRL 62, 1201 (1989))

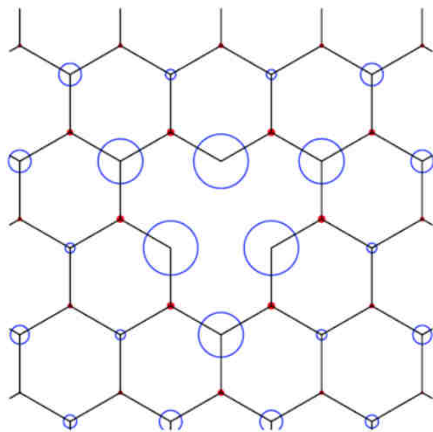

Spin density around a « vacancy »
Spins up and down
H. Kumazaki et al., JPSJ 76, 064713 (2007)

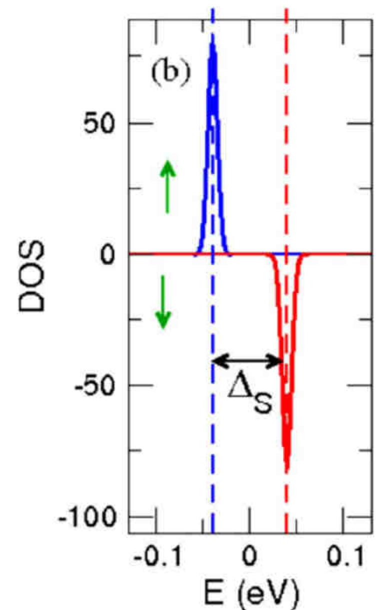

Spin splitting of the « zero energy mode » from a model Hubbard model (local **e-e interaction**).
J. J. Palacios et al., PRB 77, 195428 (2008)

The « magnetic » state should show up in STS measurements
(2 peaks straddling the Dirac point even in non SP measurements).

Experimental realization?

Possible realizations of a C « vacancy » in graphene

True vacancy: not that good (complex)

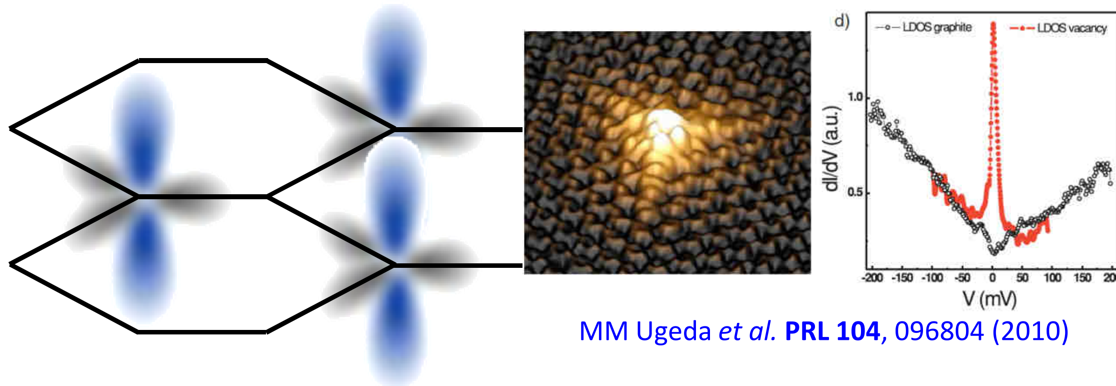

MM Ugeda *et al.* **PRL 104**, 096804 (2010)

$m_T \approx 1\mu_B + 0.5\mu_B$

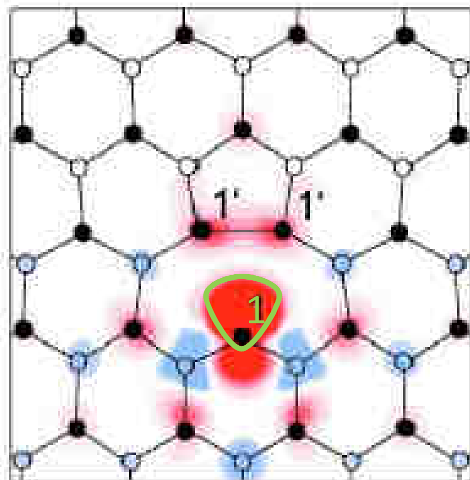

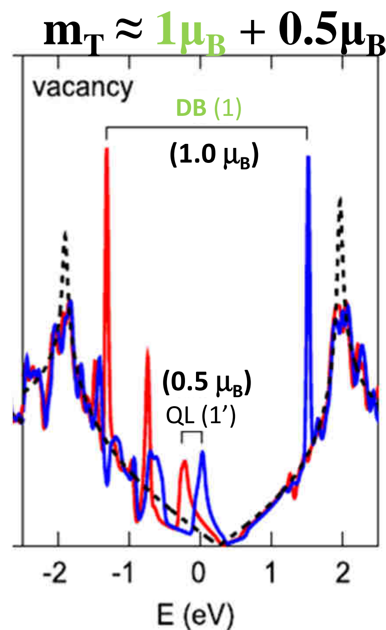

O. Yazyev et al, Phys. Rev. B. 75, 125408 (2007)

Atomic Hydrogen: better

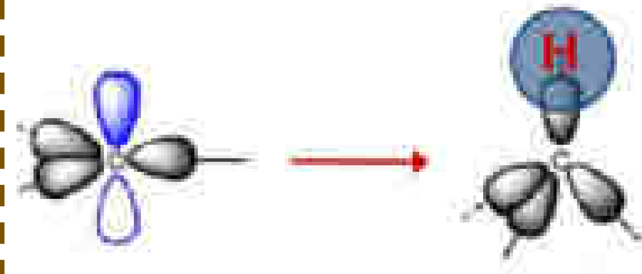

$m_T = m_\pi = 1\mu_B$

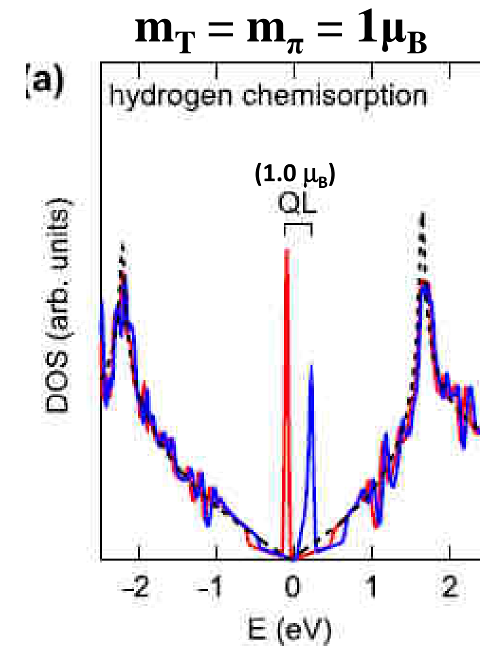

Existence of magnetic moments in graphene from **non local** measurements: K. M. McCreary et al., PRL 109, 186604 (2012) (H_G, transport); X. Hong et al., PRL 108, 226602 (2012) (F_G, transport); R. R. Nair et al., Nat. Phys. 8, 199 (2012) and Nat. Commun. 4, 2010 (2013) (Vacancies and adsorbates, SQUID magnetometry+doping).

H adsorbate on Gr from DFT calculations

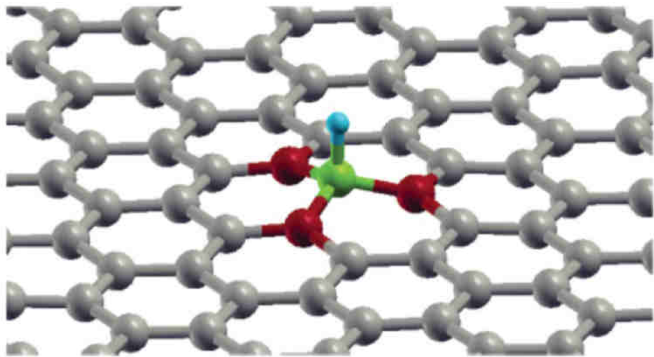

Structure of an H adsorbate from DFT
J. O. Sofo, PRB 85, 115405 (2012)
D. W. Boukhvalov et al., PRB 77, 035427 (2008)

« sp3-like » configuration fo the C atom bonded with H.

Adsorbtion energy for the H atom ≈ 1 eV from DFT.

Magnetic moment: 1 μ_B/unit cell.

M. Moaied et al., PRB 90, 115441 (2014)
and references therein.

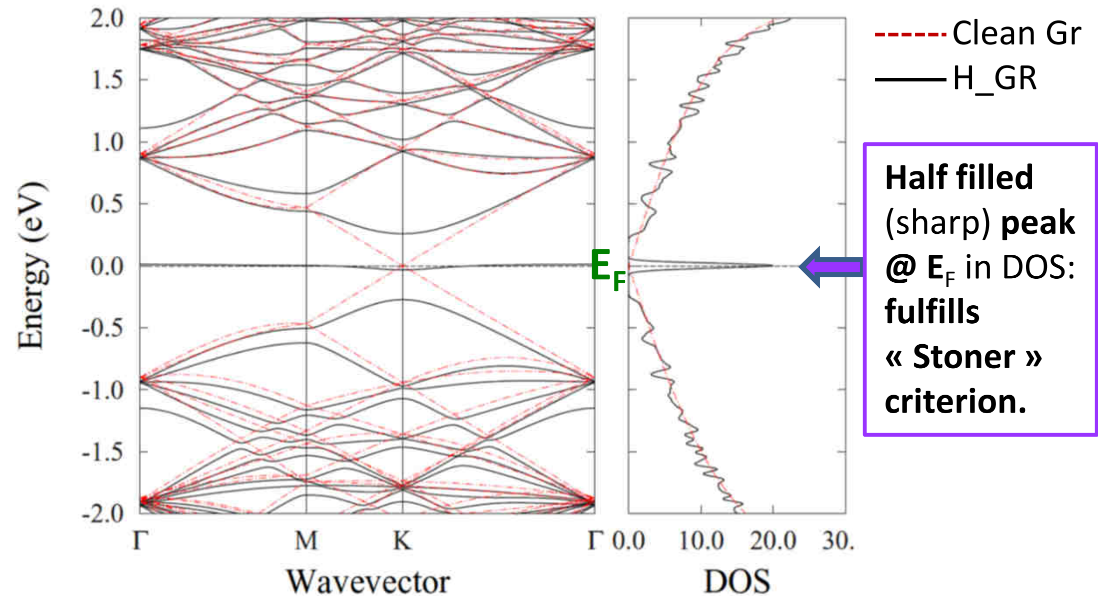

Band structure and DOS for an H adsorbate on graphene: **non SP** DFT calculation. F. Yndurain, PRB 90, 245420 (2014)

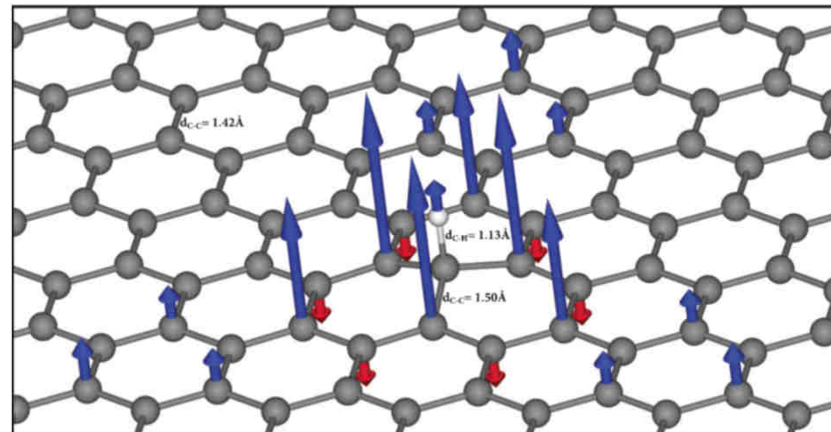

Structure and spin density of an H adsorbate on ML Gr from **SP DFT**. M. Moaied et al., PRB 90, 115441 (2014)

H adsorbate on Gr: monomers

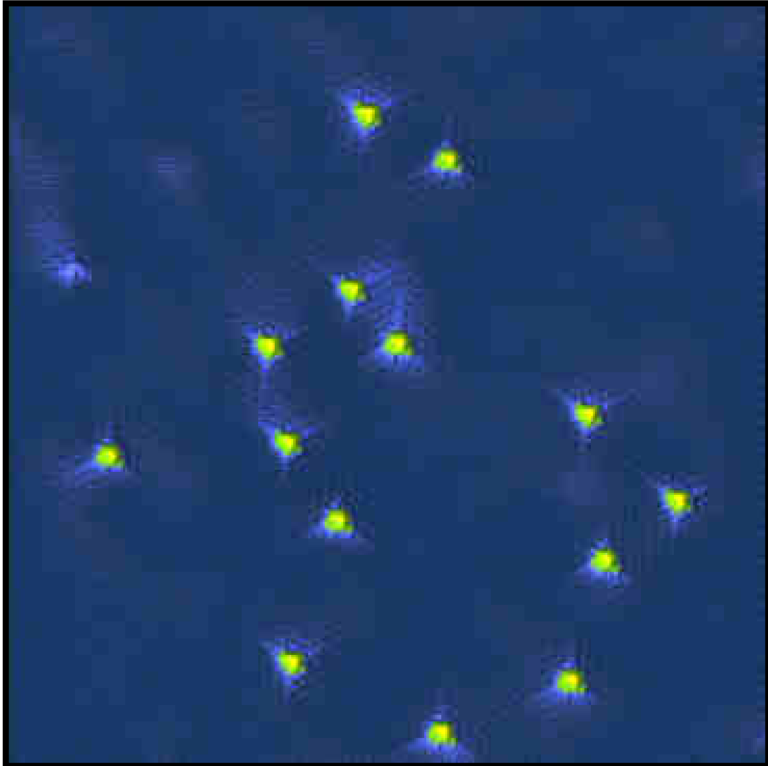

Overview: 0.4V, 30pA, 28 × 28 nm²

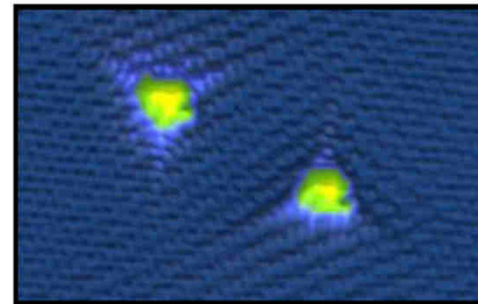

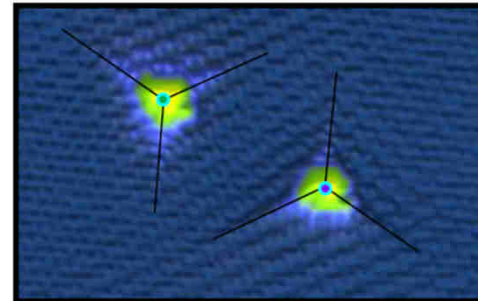

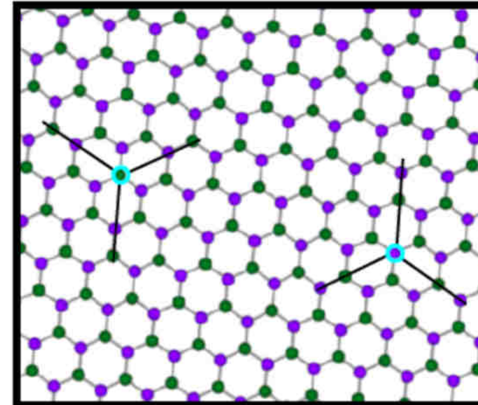

H atoms on different sublattices

0.4V, 30pA
8.8x5.5 nm²

H monomers obtained through atomic manipulation with the STM tip!

H. González-Herrero et al. Science 352, 437 (2016)

H adsorbate on Gr: monomers

Simulated STM image (Tersoff-Hamann)

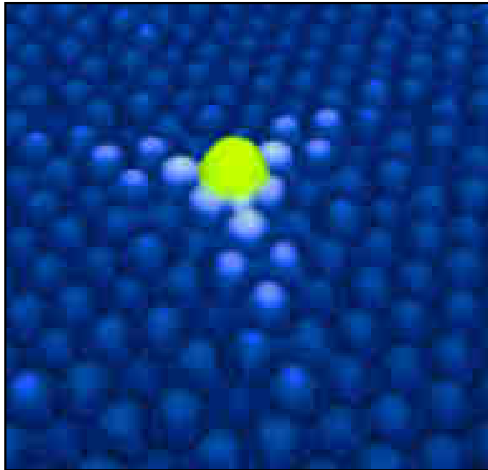

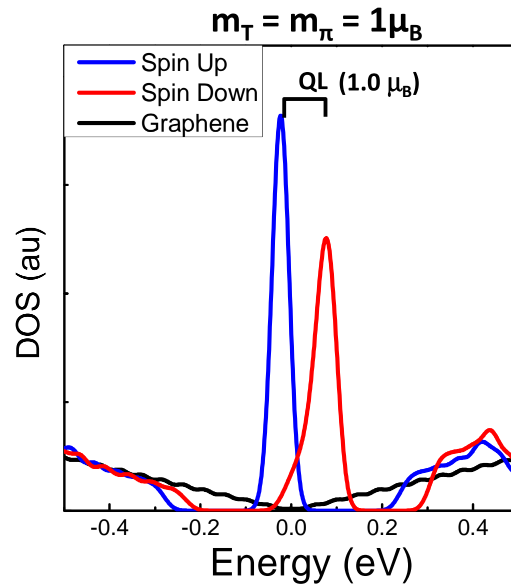

DFT calculations

On **neutral** (intrinsic) **graphene**.

H. González-Herrero et al.
Science 352, 437 (2016)

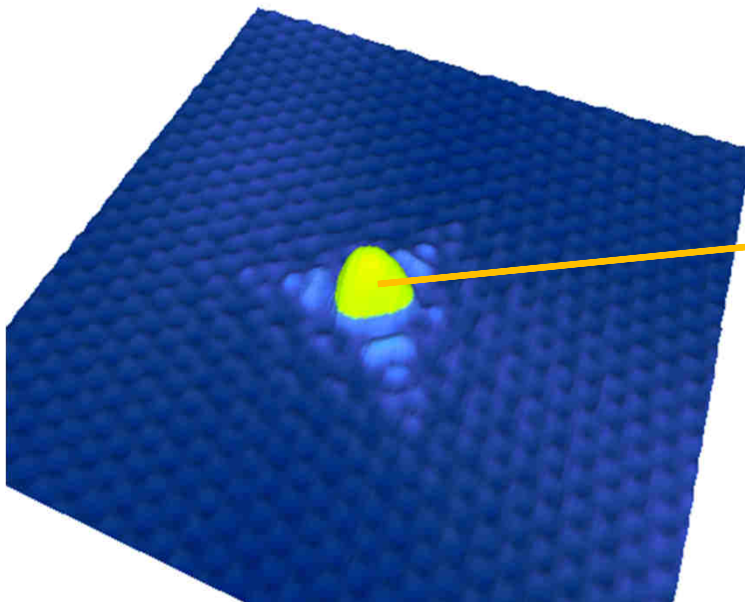

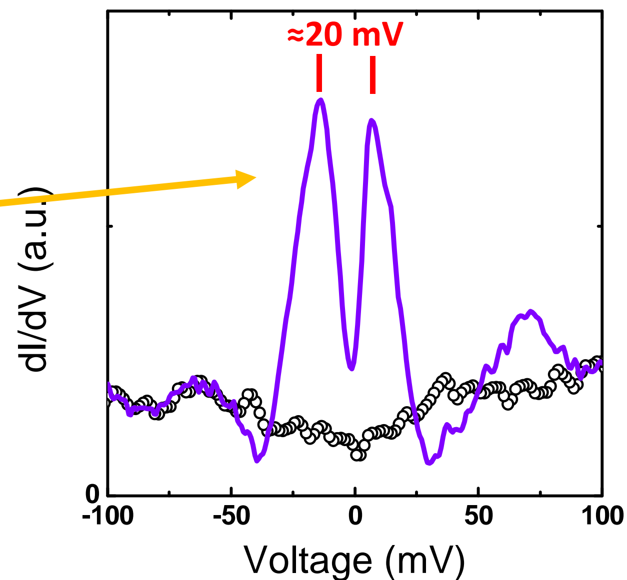

H adsorbate
○○○ Clean graphene

STS experiment:
Spin splitting by ≈20 meV!

Complete **spin polarisation** of the state.

H adsorbate on Gr: monomers

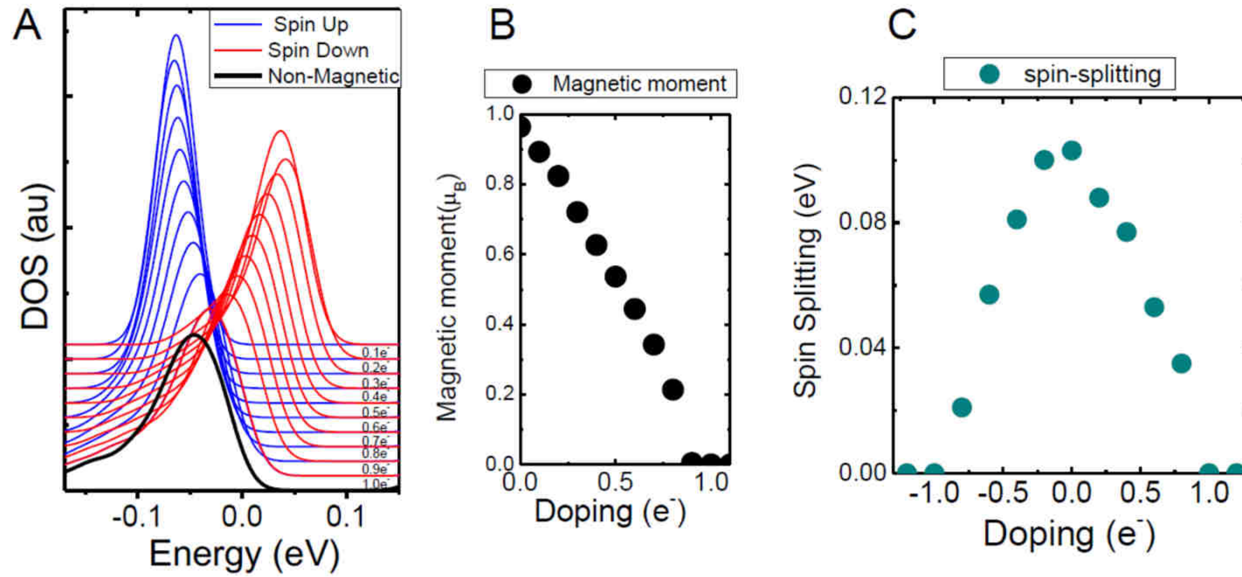

DFT calculations:

Doping (e/h) reduces and eventually **supress** the **spin splitting**/magnetic monent (analogous to the standard Anderson model)

On **doped graphene**.

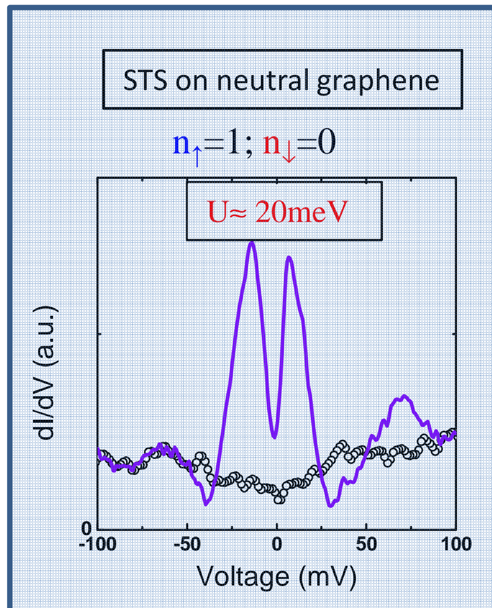

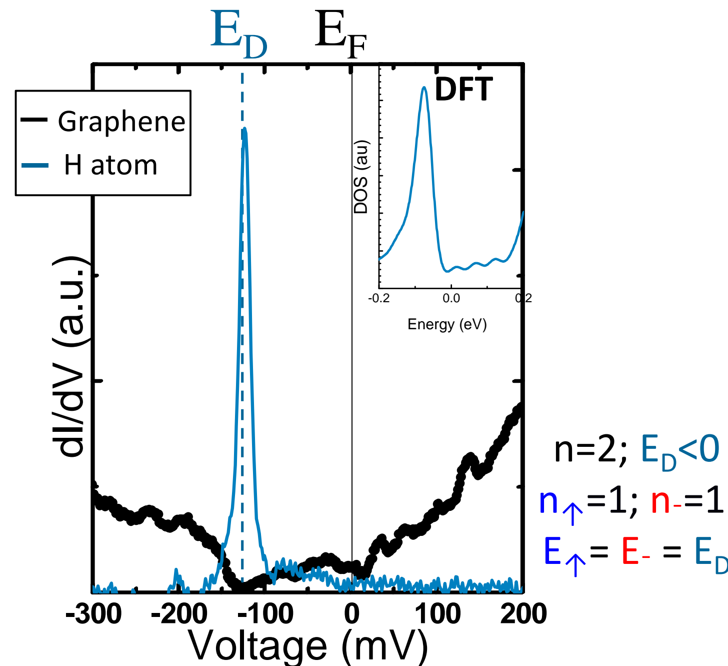

n=2; E_D<0

$n_\uparrow=1$; $n_-=1$

$E_\uparrow = E_- = E_D$

STS on n-doped graphene

Single peak at ≈ E_D on doped graphene confirms the magnetic nature of the splitting

H. González-Herrero et al. Science 352, 437 (2016)

H adsorbate on Gr: monomers

Spatial extension of the spin-polarized electronic state induced by H atoms in undoped graphene.

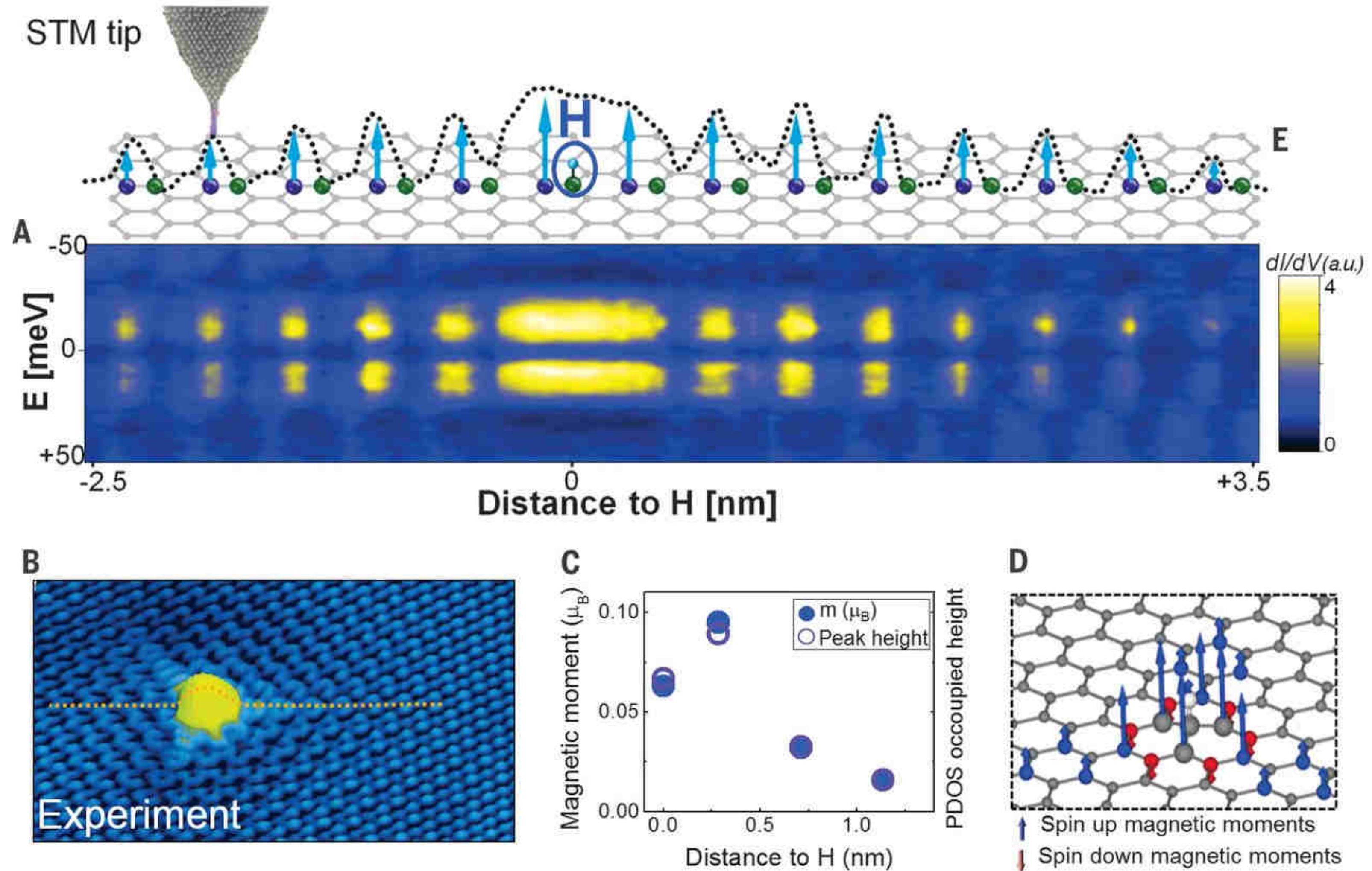

H. González-Herrero et al. Science 352, 437 (2016)

On **neutral** (intrinsic) **graphene**.

H adsorbate on Gr: dimers

Experiment

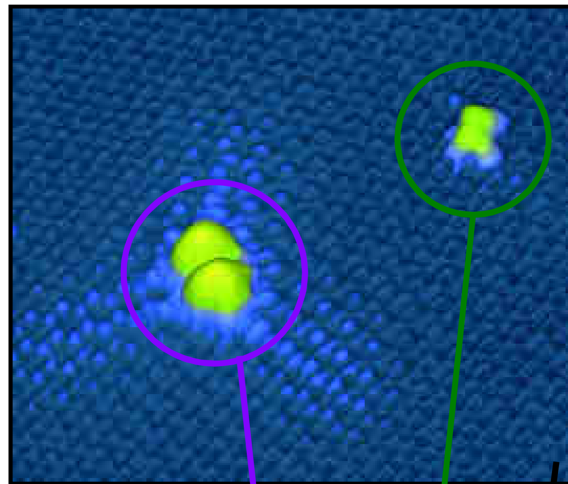

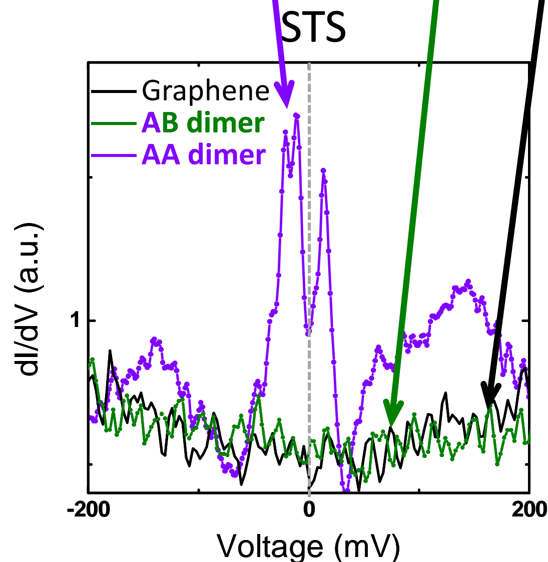

Theory (DFT)

H-H distance=0.28nm

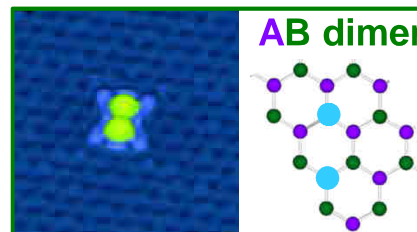

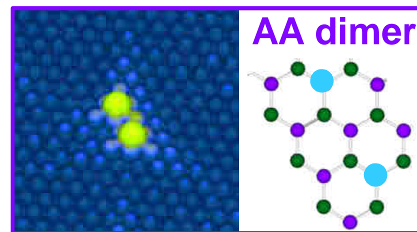

H-H distance=0.49nm

H. González-Herrero et al.
Science 352, 437 (2016)

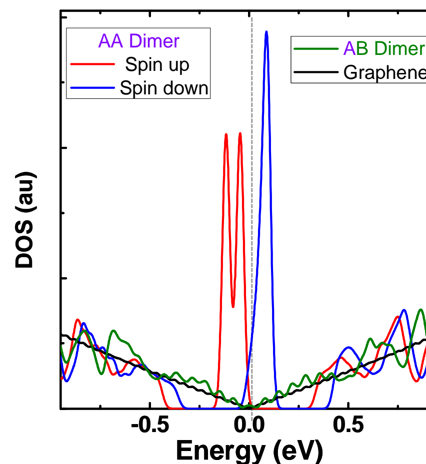

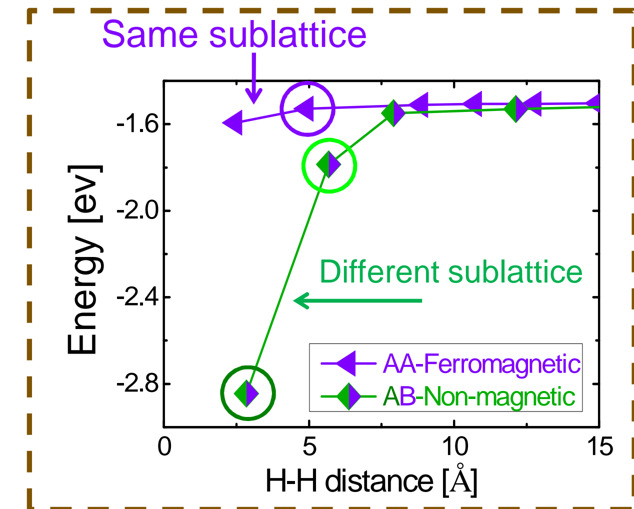

Energetics: AB pairs prefered!

Sublattice dependence of the magnetic coupling between neighboring H atoms.

Same sublattice => peak is polarized
Different sublattices => no peaks

As expected from Lieb's theorem for AA dimers and from the coupling of "vacancy" states for AB dimers (J. J. Palacios et al., PRB 77, 195428 (2008))

Substitutionnal N atoms in Gr: doping and defect state.

- Substitutional N expected to be an n-type dopant (e donor) to graphene with minimal structural perturbations.
- N incorporation: direct growth (e. g. CVD with NH_3) or post-treatment of pristine Gr (N radicals here).

Results: identification of N induced species (STM), **e-doping** (shift of the Dirac point in STS), **localized resonance** (donor state) induced by **N subst**.

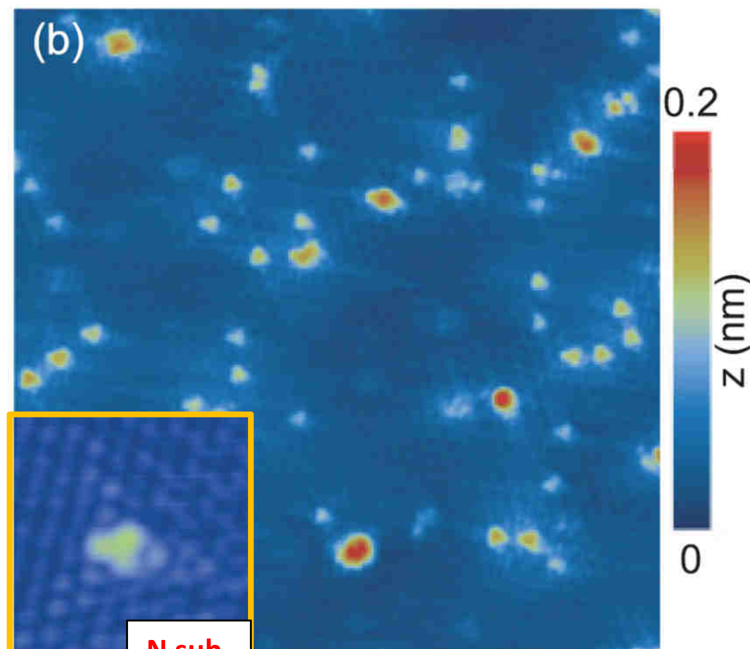

Doping:
0.55-0.8 e/N atom.

After N dosing (atomic N)
15x15 nm², -0.5V.
Defect density: 0.6%
75% substitutionnal N

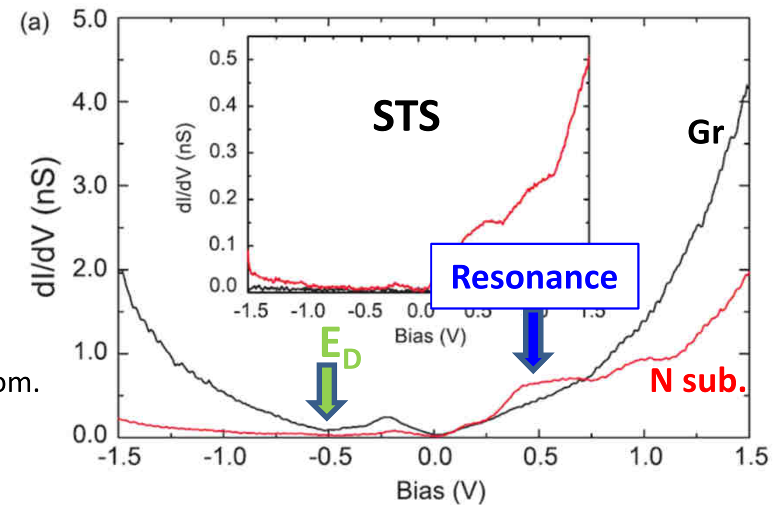

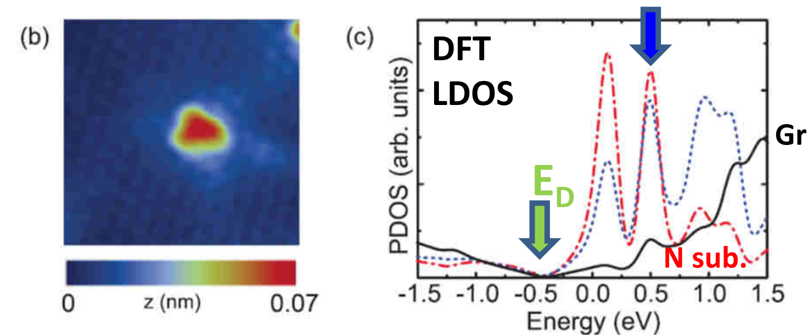

F. Joucken et al., PRB 85, 161408(R) (2012)
Also: L. Zhao et al., Science 333, 999 (2011).

DFT: peak splitting is a supercell artefact.

Divacancies on Gr

- « True » divacancies produced by mild ion bombardment (Ar^+, 140eV) and annealing (650°C).
- Observed on different realizations of « graphitic » samples (HOPG, ML and BL on SiC-Si, FLG on SiC-C).

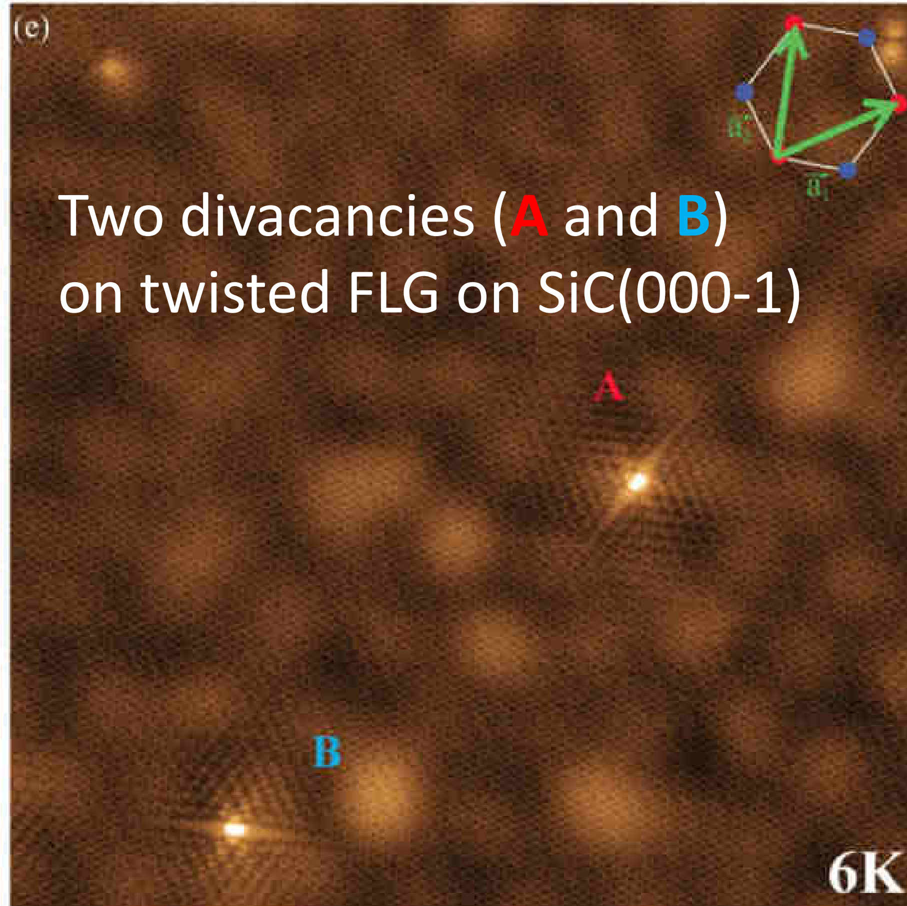

26x26 nm², +0.28V

M. M. Ugeda et al., PRB 85, 121402(R) (2012)

- Twofold symmetric features « A » and « B » (not single vacancies: 3 fold).

- Divacancies are much more stable than 2 isolated ones (by ≈8 eV) from DFT.

Gun-Do Lee eet al., PRL 95, 205501 (2005)

Divacancies on Gr

- « True » divacancies produced by mild ion bombardment (Ar^+, 140eV) and annealing (650°C).
- Observed on different realizations of « graphitic » samples (HOPG, ML and BL on SiC-Si, FLG on SiC-C).

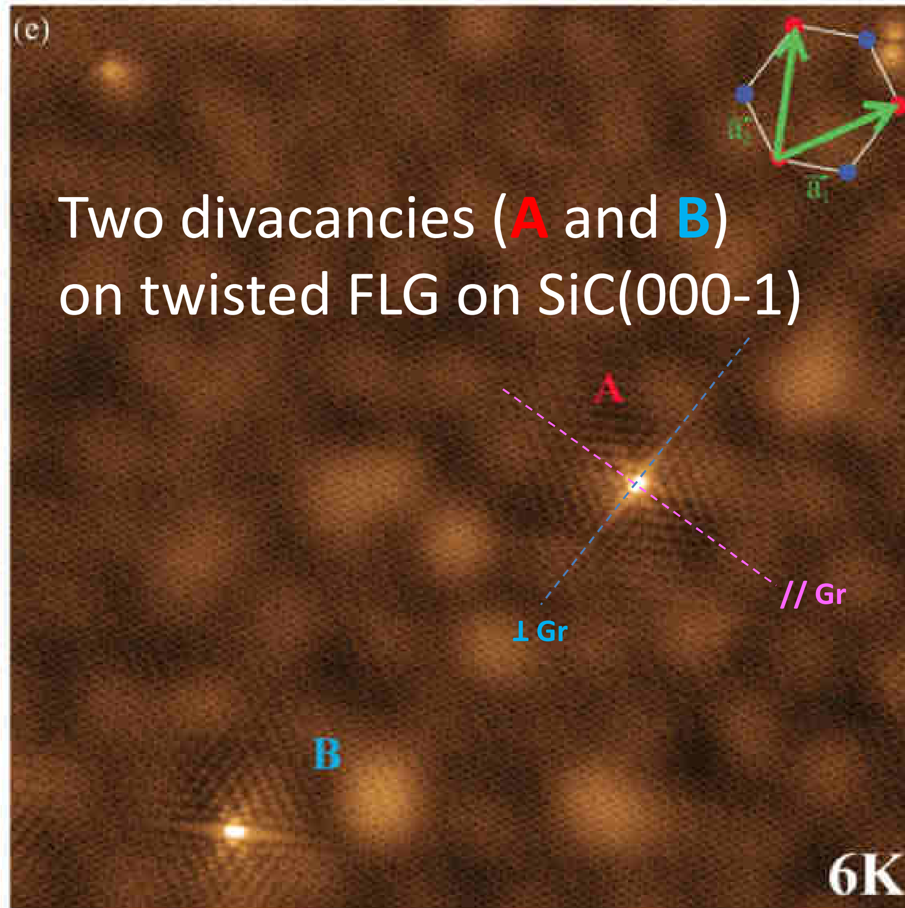

26x26 nm², +0.28V

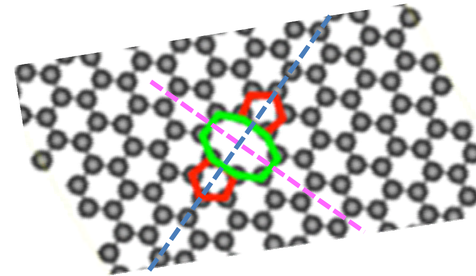

- Reconstructed « 585 » divacancies from the symmetry: 2 **pentagons**, 1 **octogon**.
- Also from DFT simulated images (next slide).
- The reconstruction suppresses the σ (sp2) DB in plane.

M. M. Ugeda et al., PRB 85, 121402(R) (2012)

STM/STS on divacancies in twisted FLG on SiC(000-1)

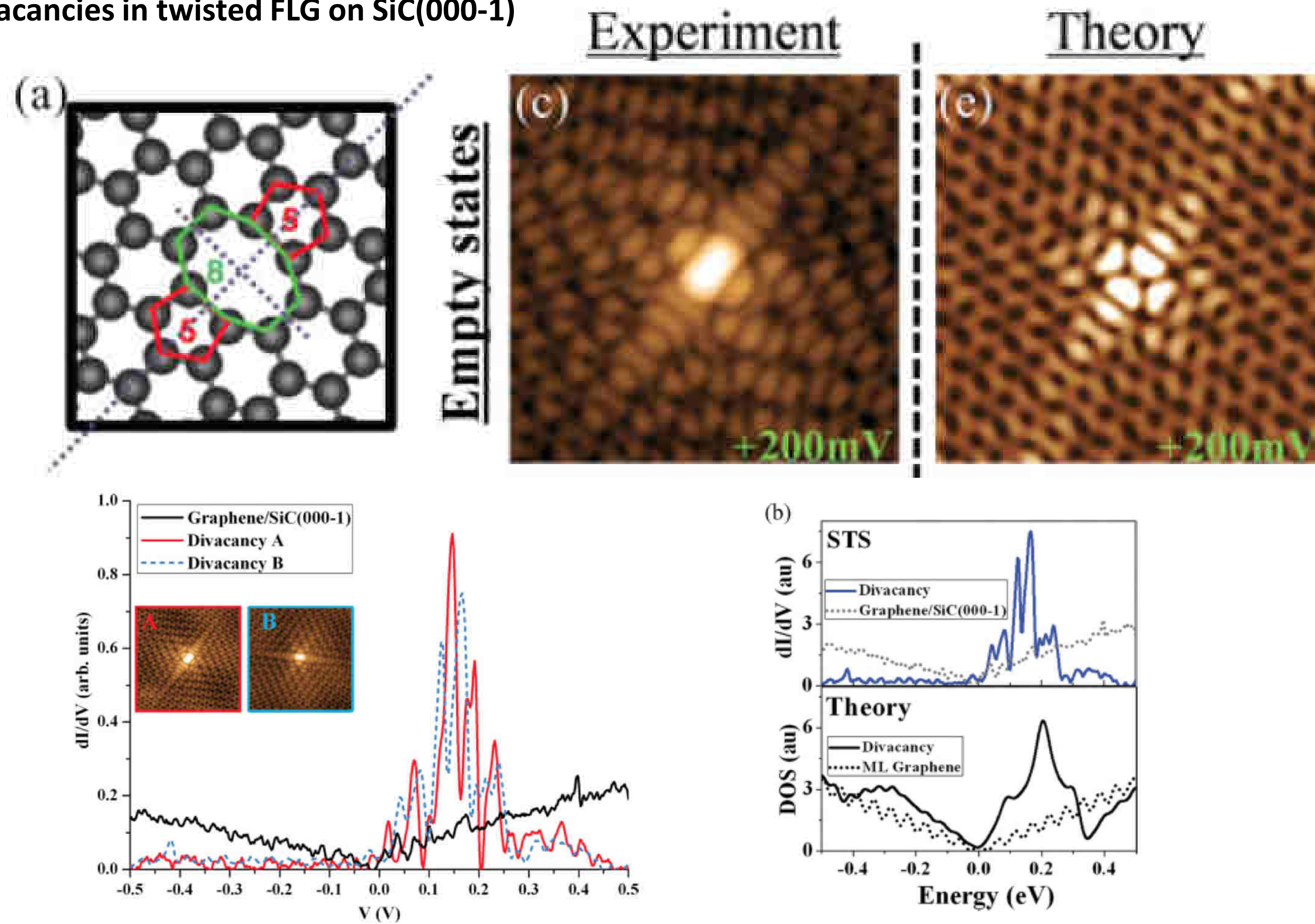

- Spectra recorded on A and B divacancies show a broad resonance centered at +150 mV, which present a rich internal structure.
- Resonance is reproduced by DFT calculations, but not the fine internal structure
- Spin polarized DFT: non magnetic

M. M. Ugeda et al., PRB 85, 121402(R) (2012)

STM/STS on TMDs

Outline:

- Introduction to TMDs (mono or few layers).
- STM/STS on TMDs,
- Influence of the substrate,
- QPI measurements: role of the spin texture,
- Electronic structure of defects (point defects, twin boudaries, edges);
- In-plane heterojunctions.

STM/STS on TMDs

Transition Metal Dichalcogénides (TMDs) : MX_2

A large (≈40) familly of 2D (lamellar) materials:

- Insulators
- **Semi-conductors**
- Métals (SC, CDW)

M – TM

X – chalcogene

H																	He
Li	Be											B	C	N	O	F	Ne
Na	Mg	3	4	5	6	7	8	9	10	11	12	Al	Si	P	**S**	Cl	Ar
K	Ca	Sc	**Ti**	**V**	Cr	Mn	Fe	**Co**	**Ni**	Cu	Zn	Ga	Ge	As	**Se**	Br	Kr
Rb	Sr	Y	**Zr**	**Nb**	**Mo**	**Tc**	Ru	**Rh**	**Pd**	Ag	Cd	In	Sn	Sb	**Te**	I	Xe
Cs	Ba	La-Lu	**Hf**	**Ta**	**W**	**Re**	Os	**Ir**	**Pt**	Au	Hg	Tl	Pb	Bi	Po	At	Rn
Fr	Ra	Ac-Lr	Rf	Db	Sg	Bh	Hs	Mt	Ds	Rg							

2H crystal structure of bulk materials.

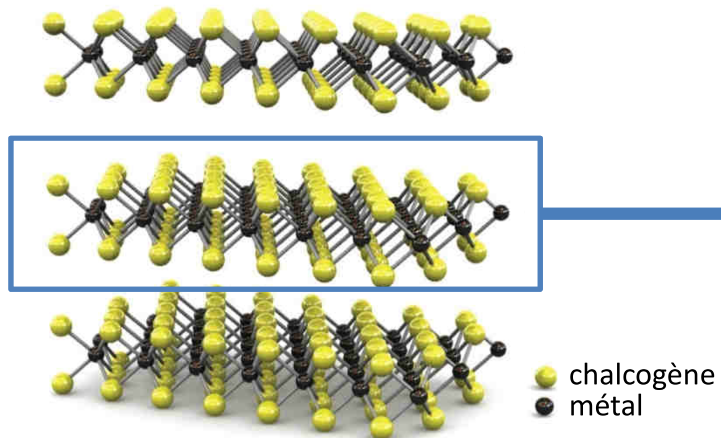

Radisavljevic Nature Nano 11

2D TMD

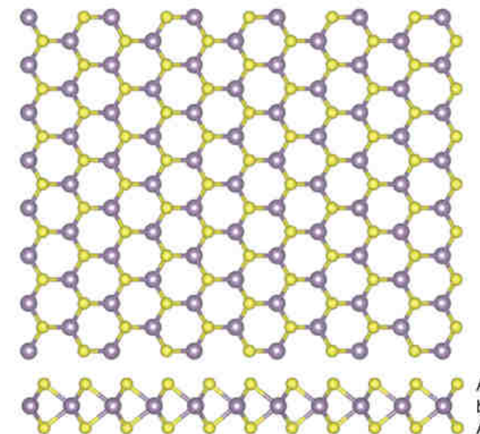

Chhowalla Nature Chem. 13

STM/STS on TMDs

Change of the band structure with the number of layers

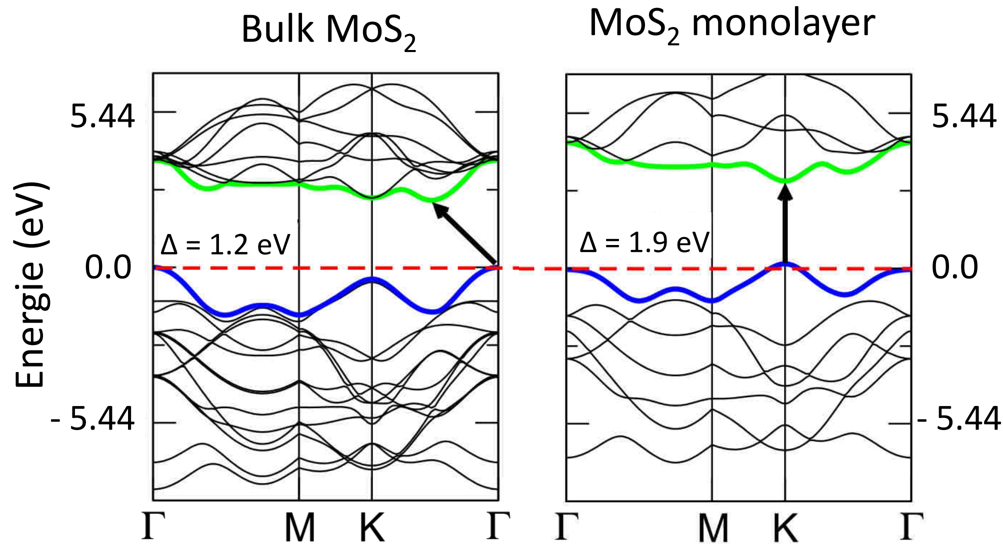

Kuc PRB 11

×10[4] amplification of photoluminescence signal for MoS_2 ML

Mak PRL 10

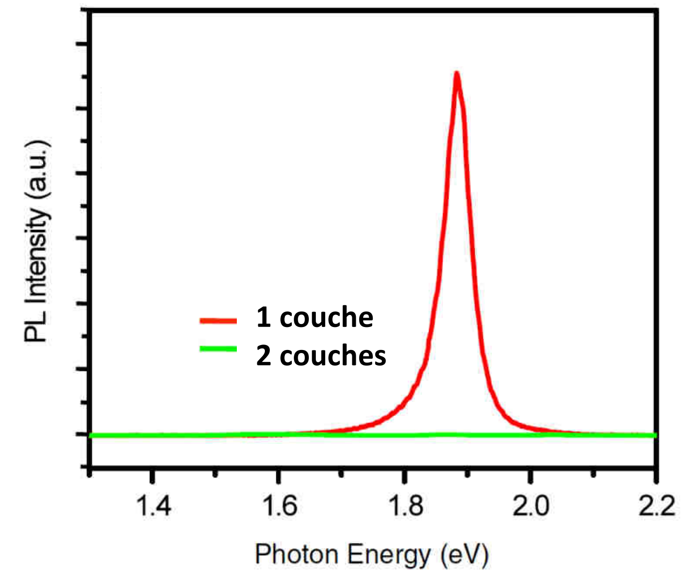

« Effective » band structure (MoS_2 ML)

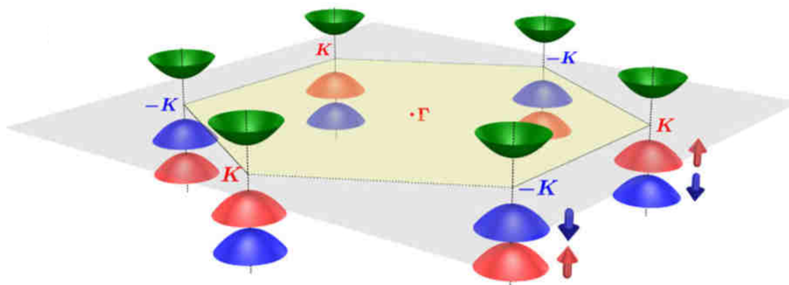

Strong spin-orbit coupling at VBM (150-450 meV),
Small so coupling at CBM (±10 meV)

Semiconducting 2D TMDs :

- Specific electronic structure (direct gap @±K)
- Optical control of valley polarisation
- Spin-valley coupling
- Valley Hall effect (K. F. Mak et al. Science'14)

STM/STS on TMDs

2D TMD 2D: some devices…

- electrostatic doping using backgate
- transparent, flexible layers

Transistor built on ML MoS_2

$\mu > 200\ cm^2 V^{-1} s^{-1}$ et $I_{ON}/I_{OFF} = 10^8$

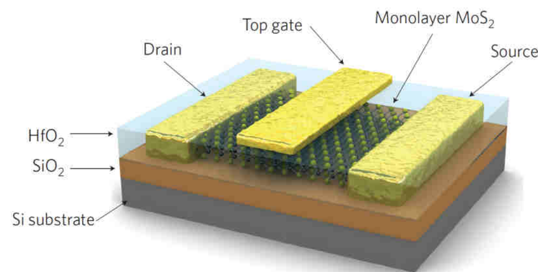

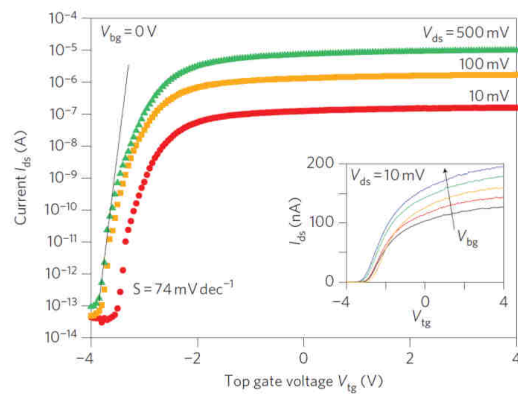

Radisavljevic Nature Nano 11

Ultrasensitive photodétector using ML MoS_2

R = 800 A W^{-1} et NEP = 1.8 10^{-15} W $Hz^{-1/2}$

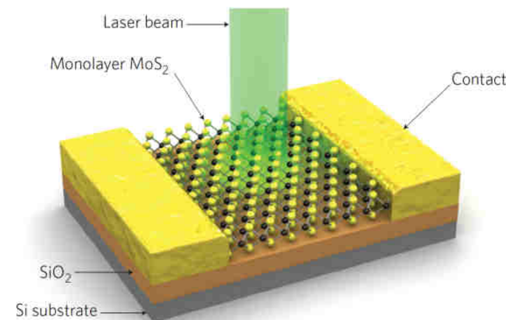

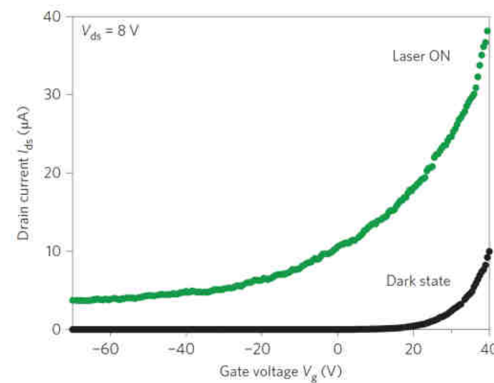

Lopez-Sanchez Nature Nano 13

2D Heterostructures : LED with a hBN/Gr/WS_2 stack

EQE up to 10%

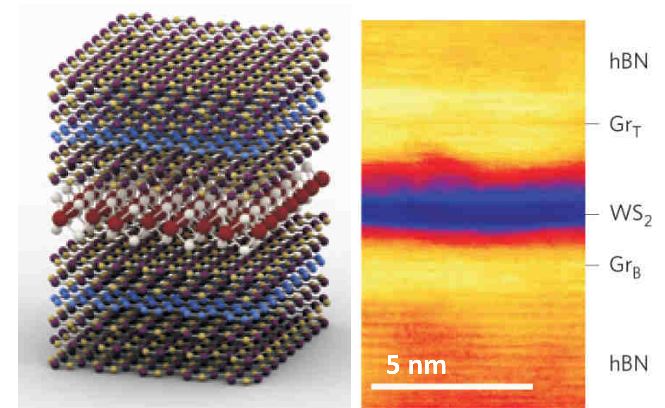

device **electroluminescence**

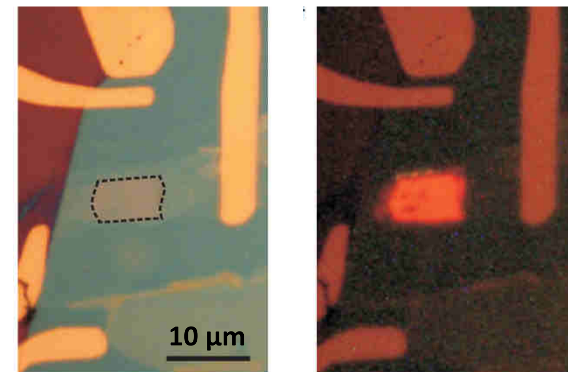

Withers Nature Mater. 15

STM/STS on TMDs

TMDs as 2D semiconductors…

- (Quasiparticle) Electronic bandgap measurement, exciton binding energy,
- Scattering on defects: band structure and spin effects,
- Defects in TMDs: edges, twin boudaries, X vacancies…
- Heterojunctions: band alignment (out of plane and in plane).

Materials: WX_2 and MoX_2.

1L: STS du gap

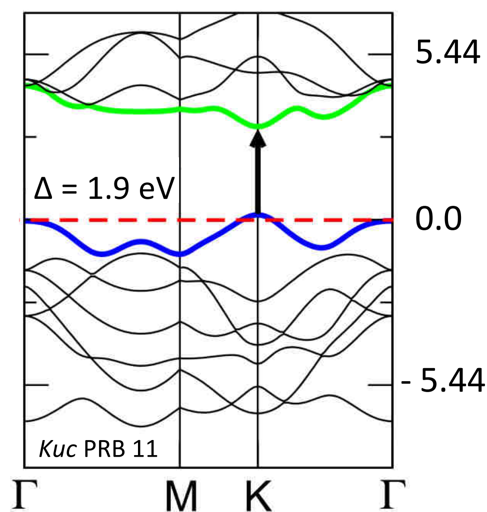

CVD grown in-plane (1L) Heterojunction

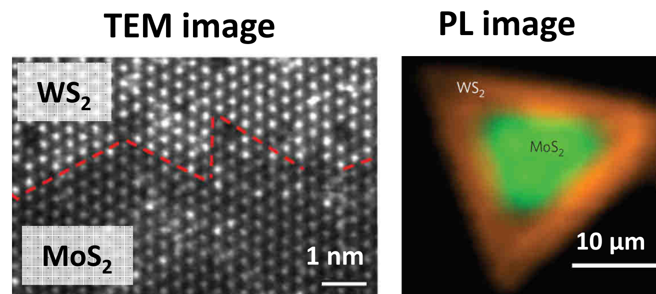

Gong Nature Mat. 14 et *Huang* Nature Mat. 14

1L: diffusion des quasiparticules

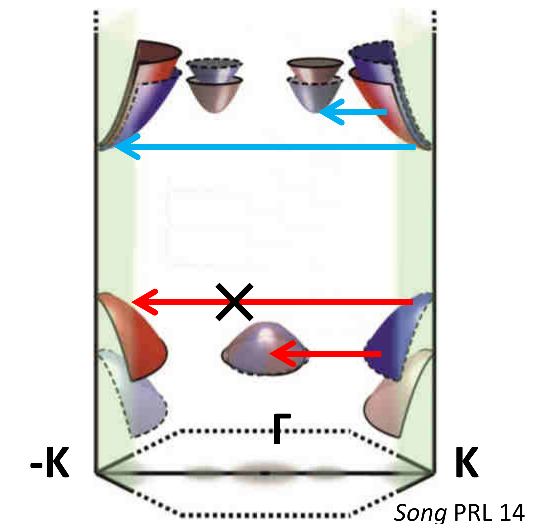

STM/STS on TMDs

- Determination of the VBM and CBM energies, consistency with ARPES for VB, Tip Induced Band Bending?
- Exciton BE,
- Role of the substrate,
- Evolution with number of layers

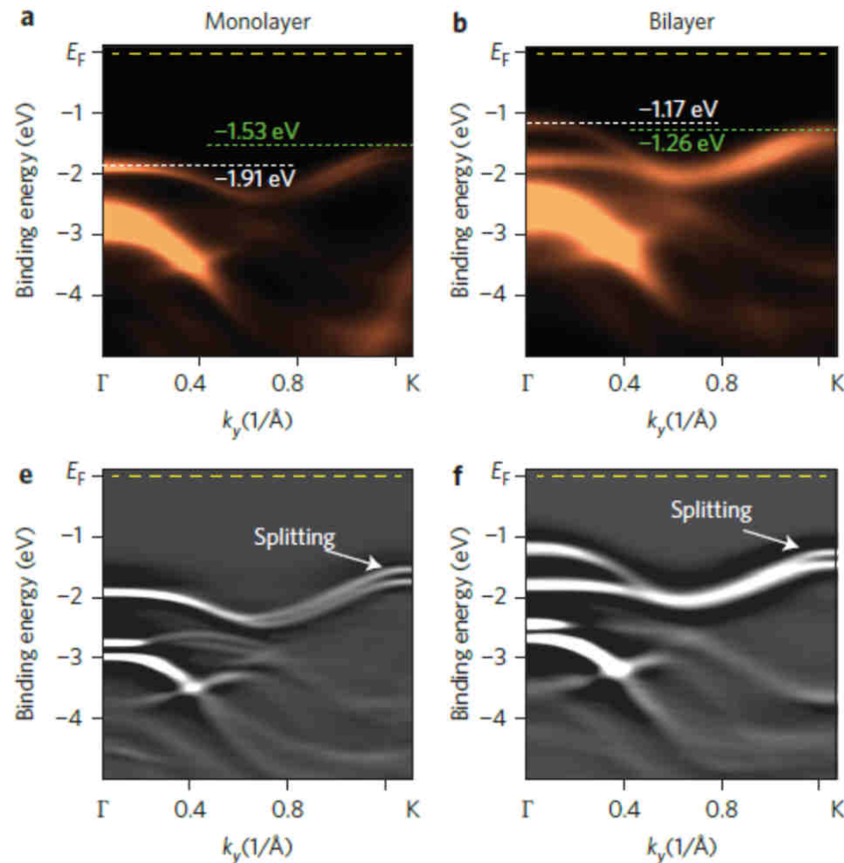

MBE grown $MoSe_2$ on BL Gr/SiC(0001): **ARPES**

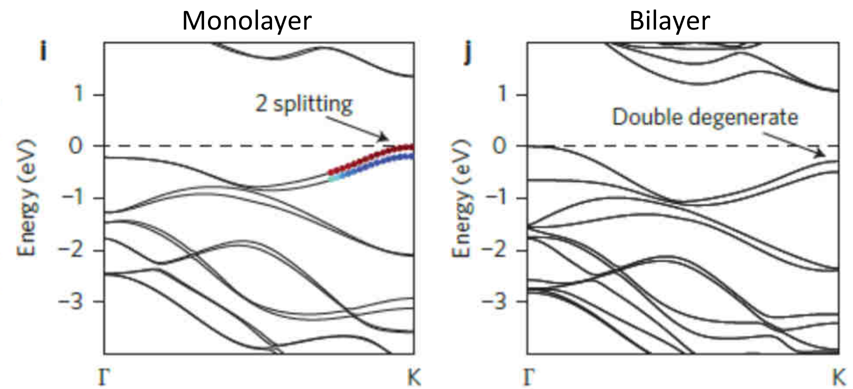

Computed band structure for ML et BL $MoSe_2$ (**DFT**)

Yi Zhang et al., Nat. Nano 9, 111 (2014)

- VBM at K point, spin-orbit split (180 meV),
- VBM shifts to Γ point from 2 L,
- Fair overall description of the band structure by DFT calculations.
- **CB??**

STM/STS on TMDs

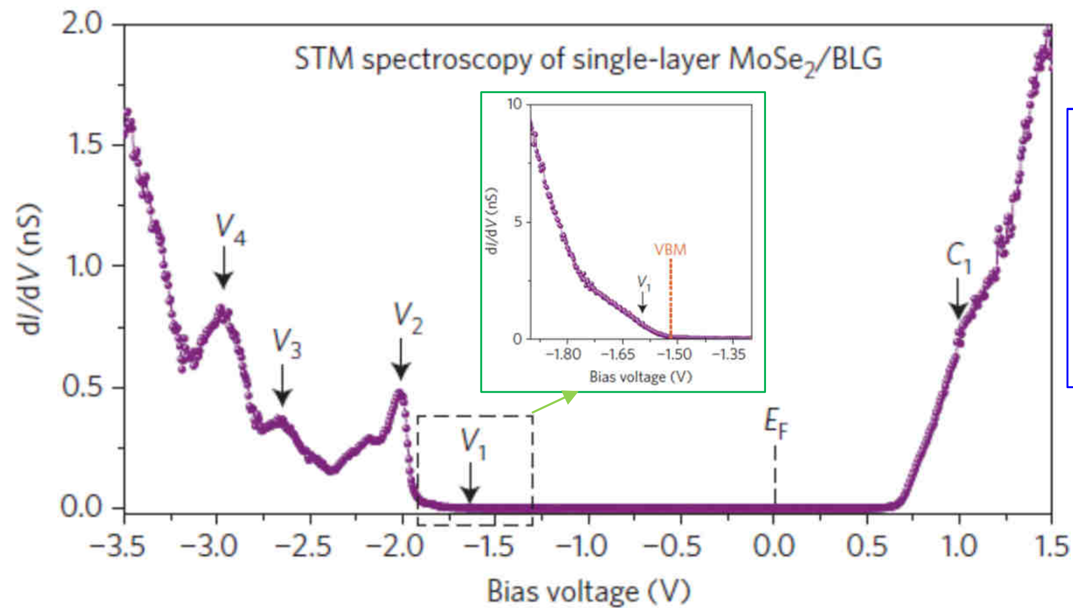

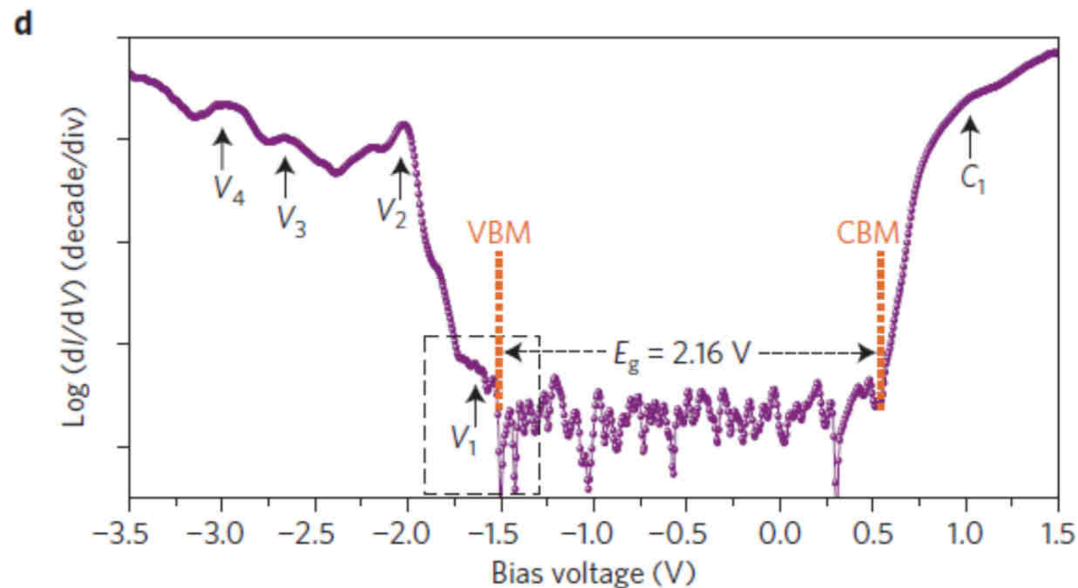

M. M. Ugeda, Nat. Mat. 13, 1091 (2014)

Experiment: T=5 K, Stab. +1.5V, 5nA

- Highly structured VB (origin : next slide),
- Small amplitude at the VBM : needs good S/N ratio and log scale!
- **Single-particle electronic bandgap: 2.18±0.04 eV**

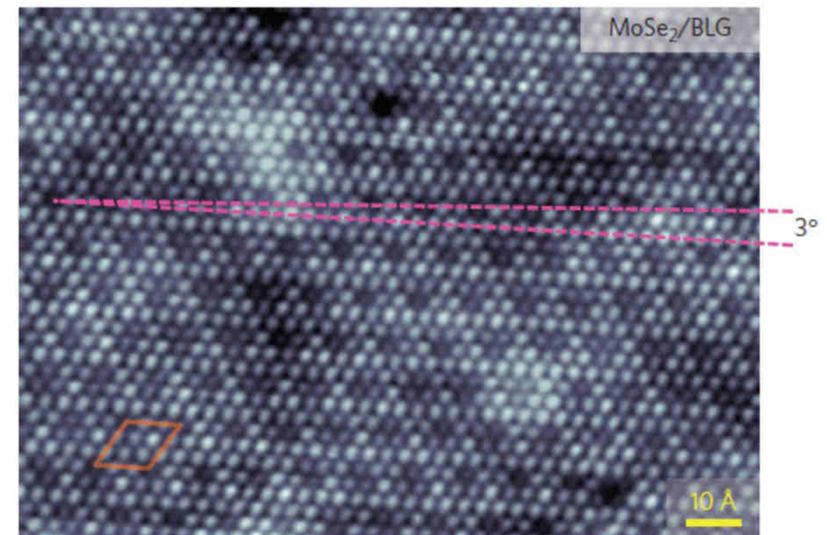

« Typical » atomic resolution image of the ML MoSe2 MBE grown on BL Gr/SiC.
a=0.33 nm, **MP**: 0.97 nm (rotated)
V=-0.9 V, I=20 pA.

STM/STS on TMDs

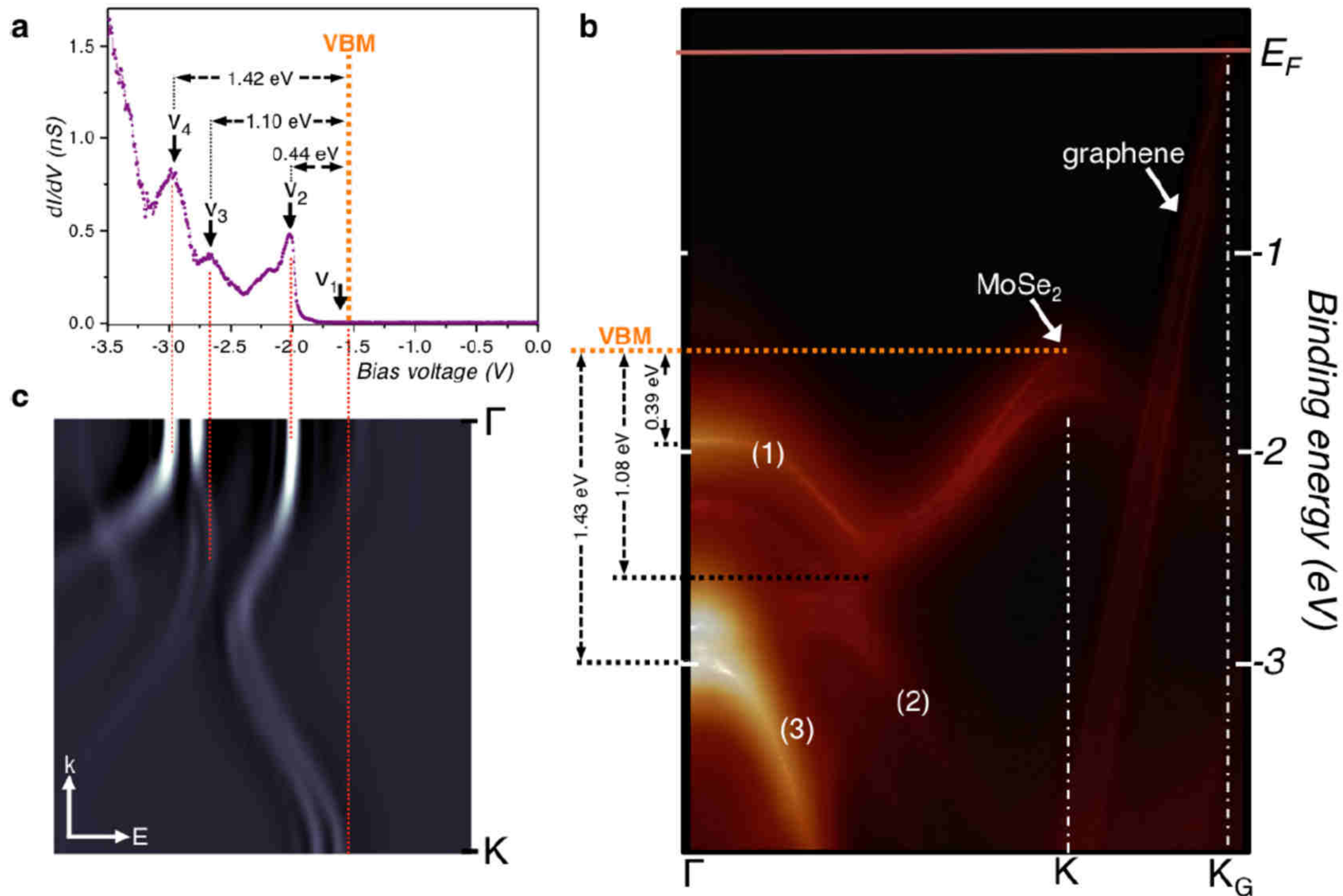

Assignment of the VB features from ARPES spectra on similar samples:

- Strong Γ point features V2 and V3 (« long » decay lengths and no dispersion at Γ)
- Weak V1 feature (« small » decay length in vacuum, more dispersive).

M. M. Ugeda, Nat. Mat. 13, 1091 (2014)

STM/STS on TMDs

M. M. Ugeda, Nat. Mat. 13, 1091 (2014)

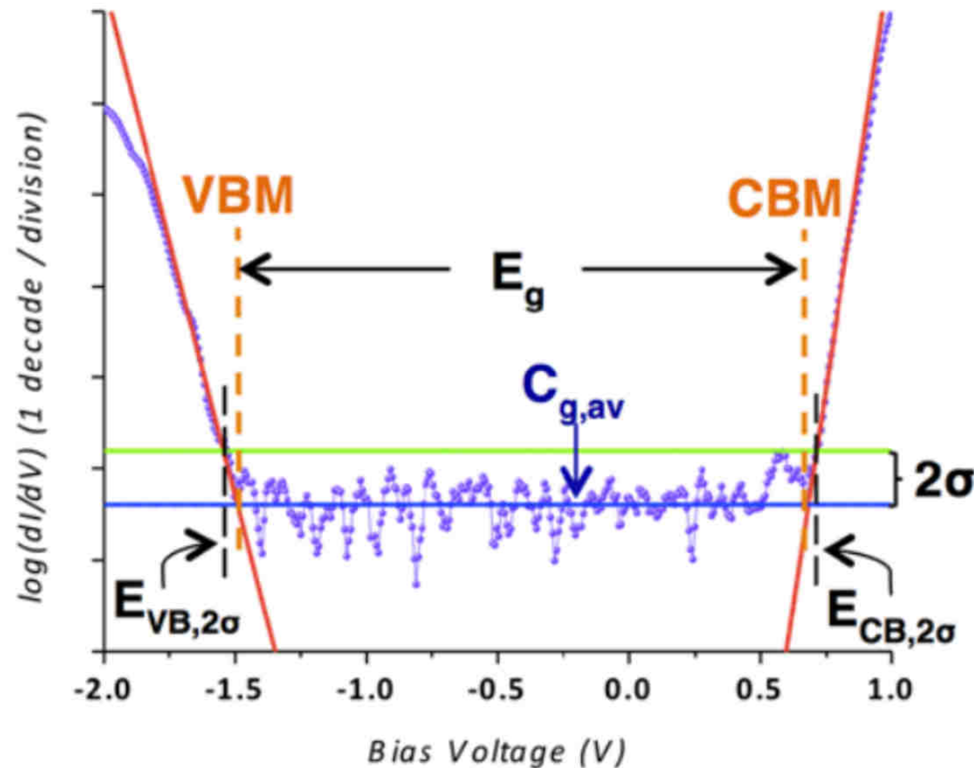

« Sophisticated » procedure for band edges determination. A linear fit is used between $E_{CB, 2\sigma}$ and $E_{CB, 2\sigma}+\Delta E$, with $\Delta E \approx 0.15$ V. Idem for VB.

Good S/N ratio and low T needed.

Figure S5. Bandgap determination. The bandgap of monolayer $MoSe_2$ was determined from the logarithm of 57 individual STS curves. One such curve is shown in purple. The logarithm of the mean of the signal within the bandgap is depicted in blue as $C_{g,av}$. The green line is two standard deviations above $C_{g,av}$. The red lines on either side of the curve are linear fit lines to the band edges. The gap edges are defined as the energies at which the linear fit lines cross $C_{g,av}$.

STM/STS on TMDs

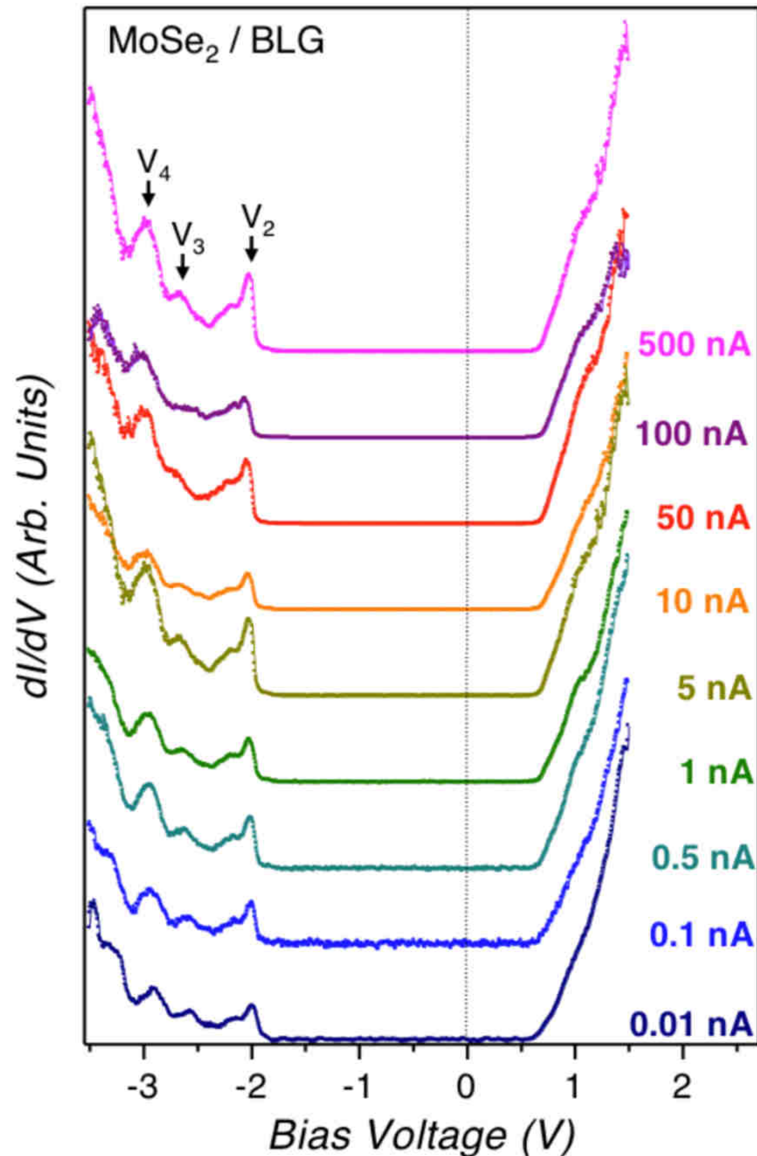

M. M. Ugeda, Nat. Mat. 13, 1091 (2014)

Tip Induced Band Bending (**TIBB**) results from poor screening of the electric field of the STS junction near the semiconductor surface.

- Well known for 3D systems (GaAs…),
  R. M. Feenstra PRB 50, 4561 (1994)
- Depends on tip sample-distance, doping, surface states…
- **Increases the gap** (lowers the effective tip-surface bias relative to the nominal one).

Variable current spectroscopy:

- Set-point bias: +1.5V,
- Set-point current range 10 pA to 500 nA: variation of the tip-sample distance by 0.5 nm!
  (can be measured through I(z) spectra).
- Shift of the V2 structure < 25 mV,
- Shift of the CB onset ≈ 0 mV.

→ **No « TIBB »**

Additionnal info: VBM structure V1 desappears at large tip-sample separation, as expected for a band located at K/-K

STM/STS on TMDs

STS: electronic gap, single (quasi) particle gap
Creation of independent electron and hole.

Optical gap: creation of a bound electron-hole pair (Coulombic interaction).
PL measurements give the exciton energy

Exciton BE: STS gap- Optical gap.

For this system: **Exciton BE: 0.55±0.04 eV**
Much larger than in 3D semiconductors (≈10 meV)
M. Dvorak et al., PRL 110, 016402 (2013)

Evolution of band gap and exciton BE with alloying in MoxWi-xS2: A. F. Rigosi et al., PRB **94**, 075440 (2016)

M. M. Ugeda, Nat. Mat. 13, 1091 (2014)

On the **same** **ML $MoSe_2$ /BLG sample**:
Optical gap: 1.63±0.01eV

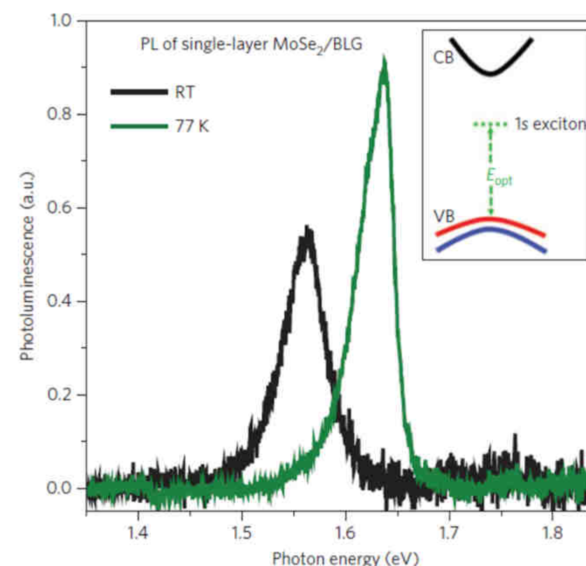

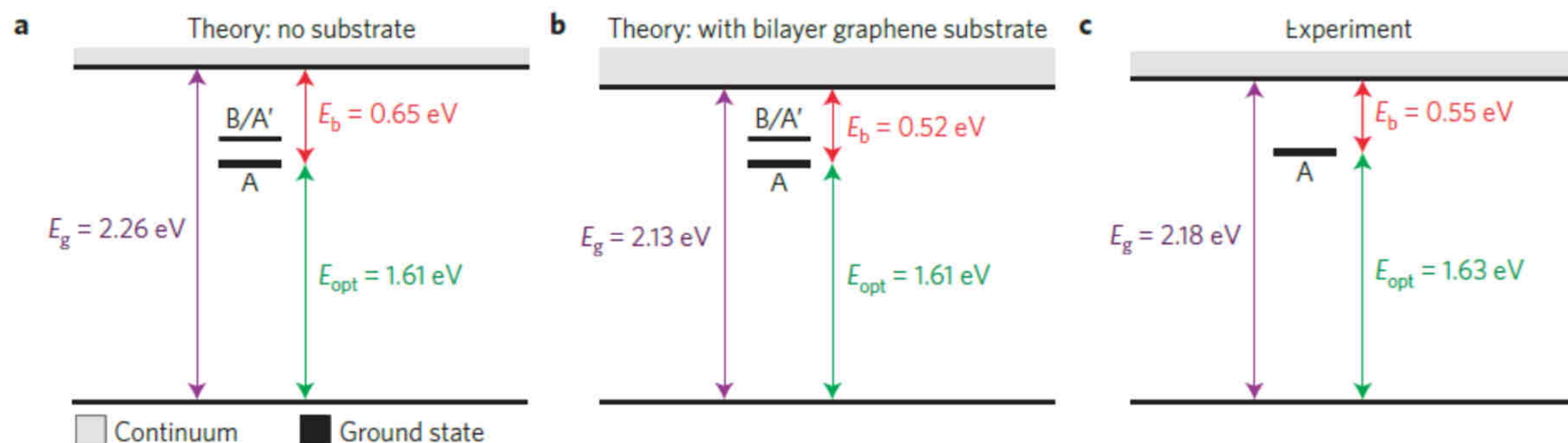

Theory: GW. Role of the screening by the susbtrate (BL G)

STM/STS on TMDs

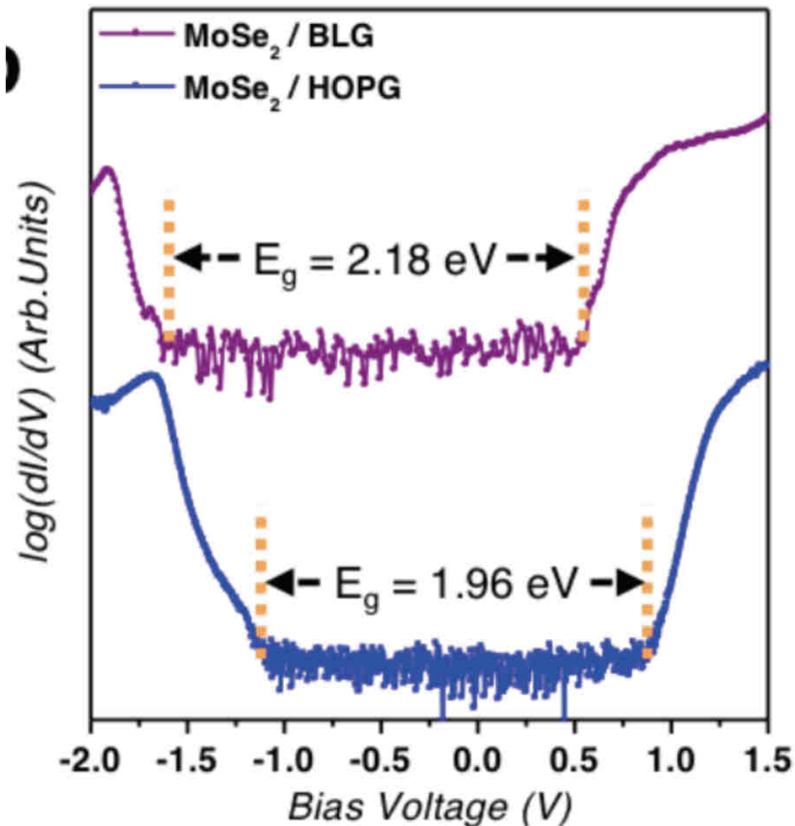

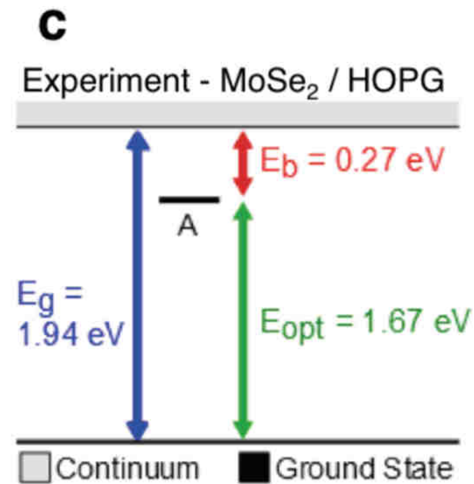

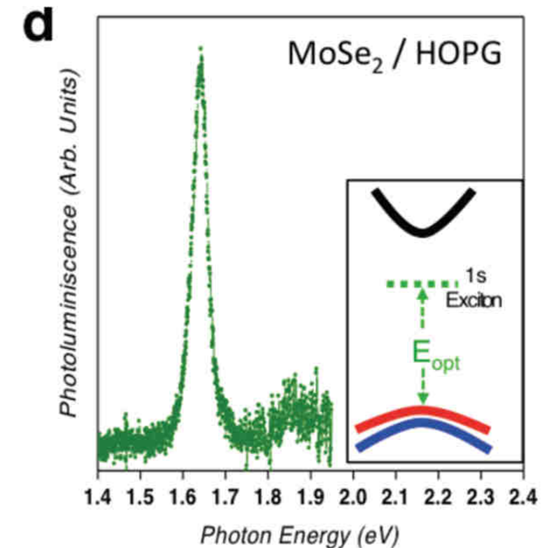

M. M. Ugeda, Nat. Mat. 13, 1091 (2014)

Stronger substrate screening: $MoSe_2$/HOPG

Same growth technique, HOPG: multilayer Gr…

- Shift of the FL relative to the band edges (discussed later).
- Electronic gap is reduced by 11% on HOPG!
- Exciton BE is reduced by 50%.
- Consistent with better screening of the Coulomb interaction by HOPG.
- (Same in Qiang Zhang et al., 7:13843 (2016) for $MoSe_2$/hBN/Ru)

Theory: The band gap and exciton binding energy decrease…. when a monolayer is surrounded by a high dielectric constant material *(such as graphene, and BN to a smaller extent)*. H-P. Komsa et al. PRB 86, 241201(R) (2012)

STM/STS on TMDs

Adsoption of benzene/Graphite (weakly coupled system)
J. B. Neaton et al., PRL 97, 216405 (2006)

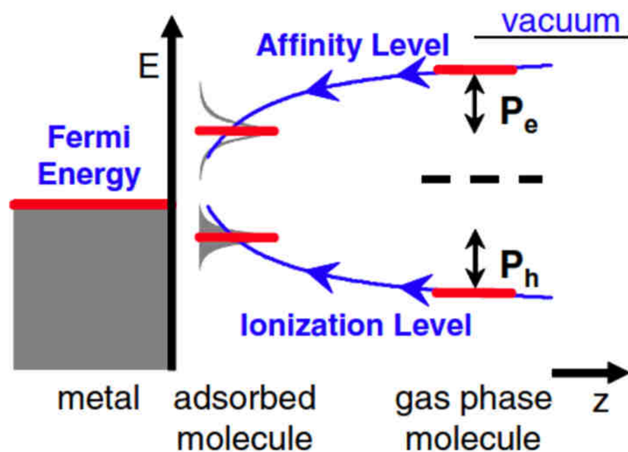

Finally, the Coulomb interaction between the added hole or electron associated with the ionization or affinity level will result in a polarization of the metal substrate. This additional correlation energy further stabilizes the added hole or electron, reducing the gap between affinity and ionization levels as illustrated (in Fig. 1) *above*.

A classical image potential model ($1/4|z-z_0|$) **gives a good estimate of the amplitude of the effect** (obtained from GW calculations).

Semiconducting CNT on Au substrate (homogeneous ϕ≈1.4nm)
H. Lin et al., Nat. Mat. 9, 235 (2010)

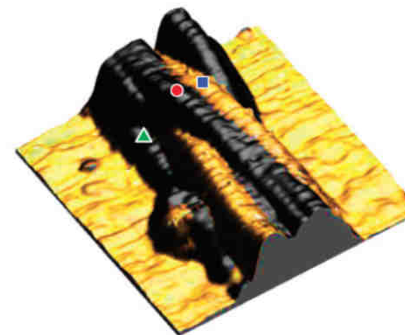

Tube 1: contact with Au
Tube 2: ≈2 nm higher.

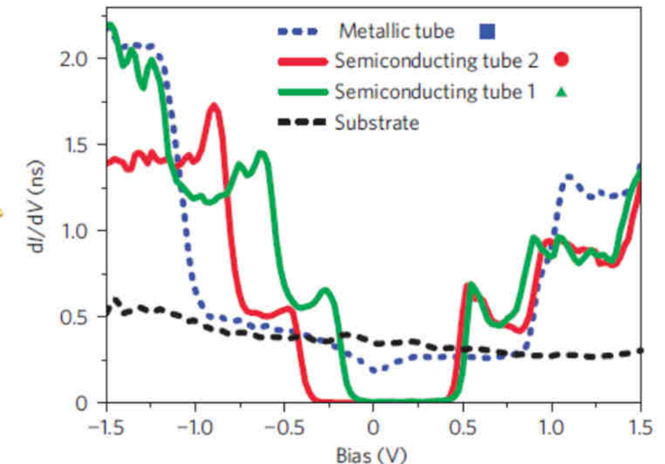

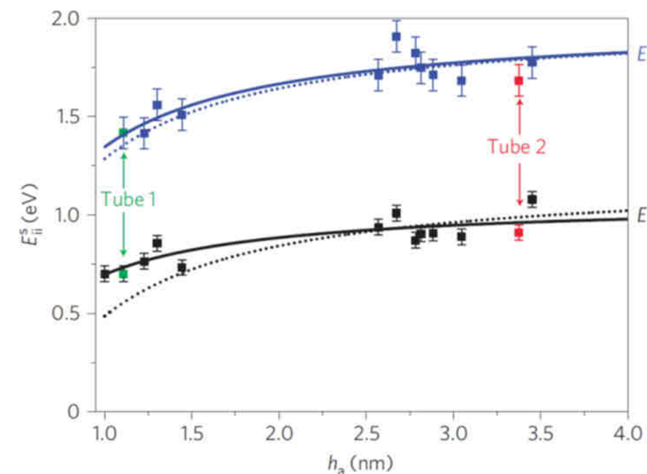

1st and 2nd vHs splitting vs. apparent height.

…….: image potential model.

- **Gap changes as a function of CNT/substrate distance,**
- **Correctly described by a classical image potential.**

STM/STS on TMDs

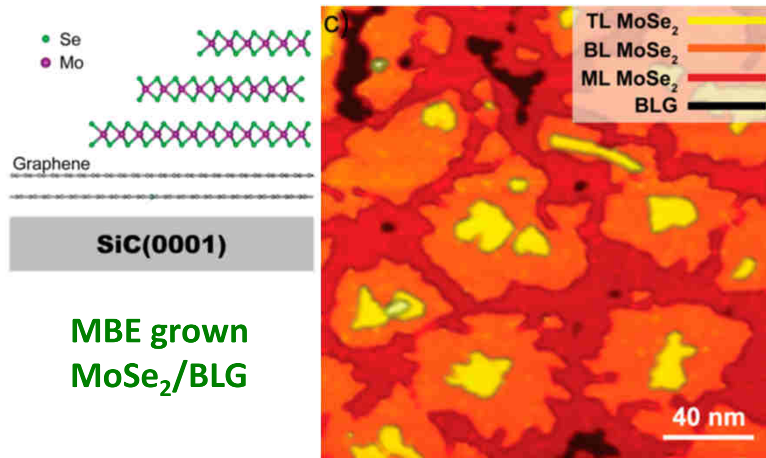

MBE grown $MoSe_2$/BLG

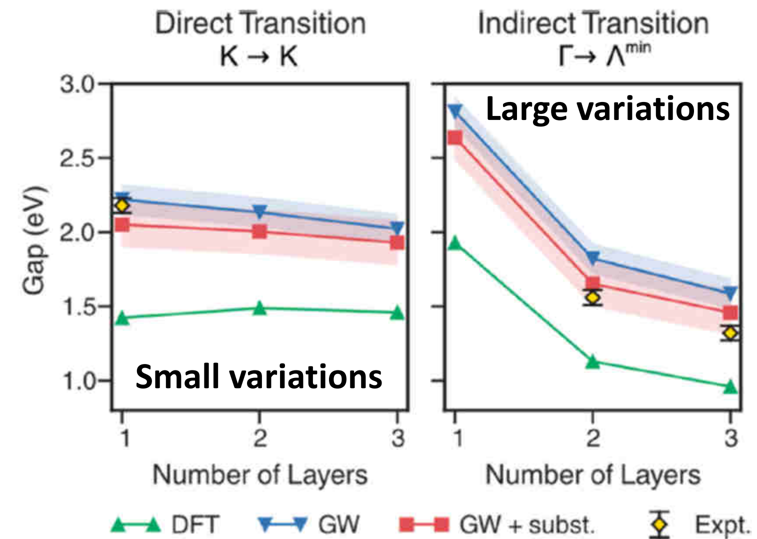

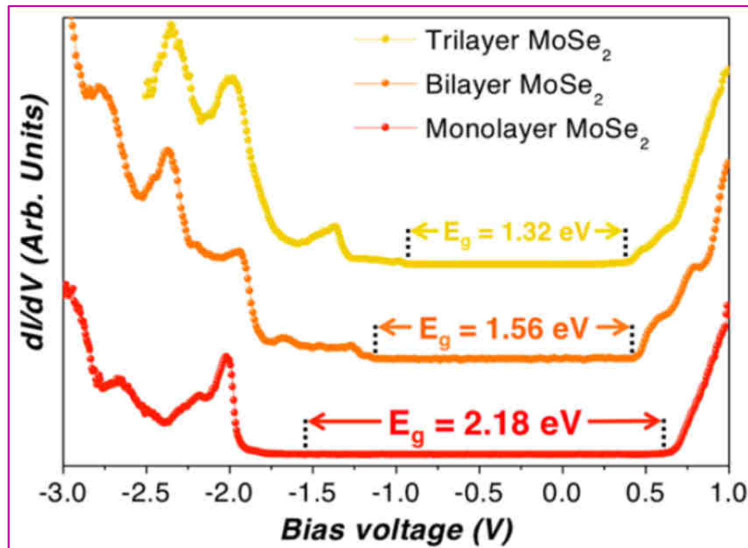

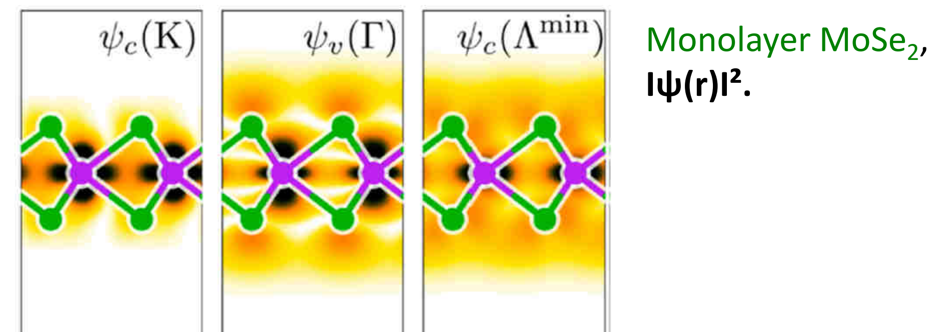

Monolayer $MoSe_2$, **$|\psi(r)|^2$.**

Band gap variation as a function of thickness. *The strong (relative) increase of the VB edge signal for >1 L indicates the shift of the VBM from K to Γ.*

- Measured gap consistent with GW calculations,
- Direct (at K)/indirect gap transition from 2 L, due to changes at Γ/Λ.
- Related to the spatial distribution of the states (at K, Γ, Λ).

A. J. Bradley et al., Nanolett. 15, 2594 (2015)

STM/STS on TMDs

Charged defects in hBN. Dillon Wong et al., Nat. Nano. 10, 949 (2015)

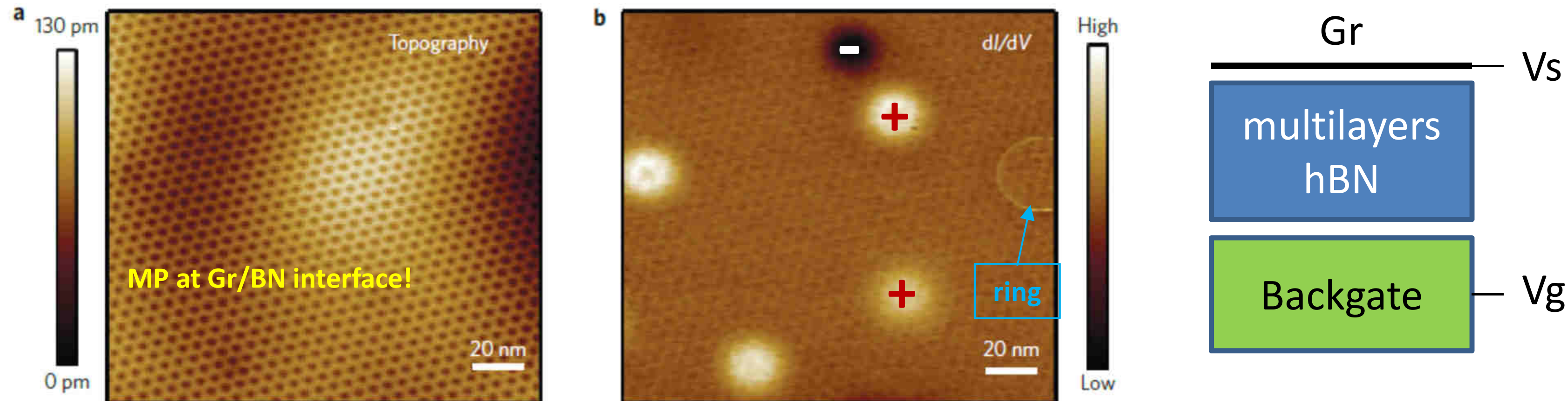

Topo and **conductance** image à Vs=-0.4V (0.25nA)
Charge sign of defects determined from additional STS data
p-n junctions and electron confinement on these objects: J. Lee et al., Nat. Phys. 12, 1032 (2016).

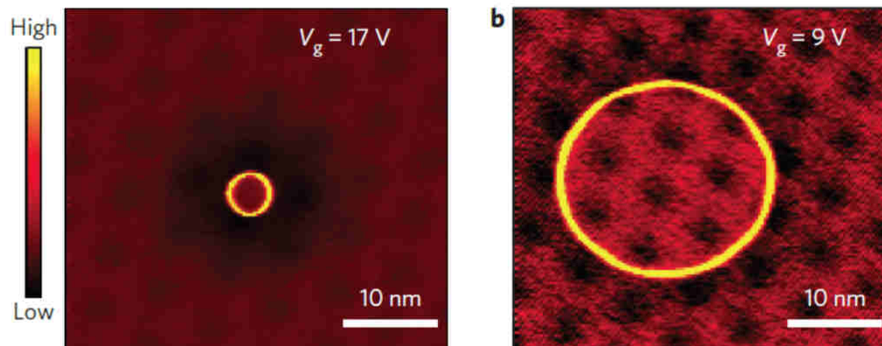

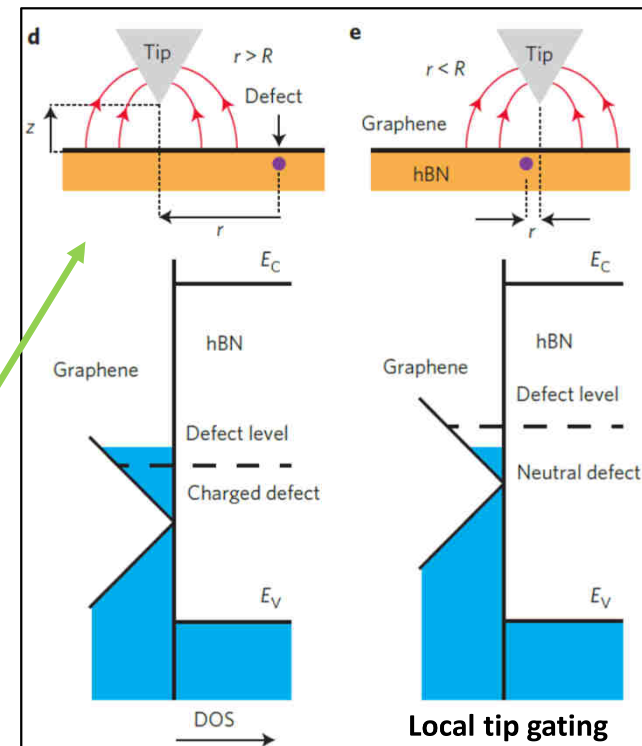

Conductance image à Vs=-0.3V, variable Vg
The ring radius varies with Vg!
Mechanism: tip induced ionisation of the defect (close to the surface).
On doped GaAs: K. Teichmann et al., PRL **101,** 076103 (2008)

STM/STS on TMDs

Twin boundary defects in MBE grown $MoSe_2$ (on BLG/SiC(0001) or on HOPG)

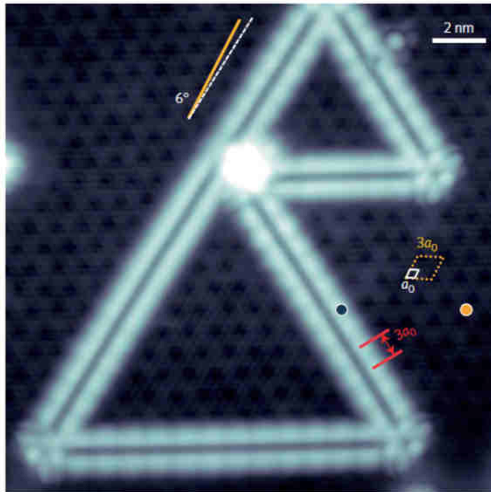

STM image: -1.3V , 20pA, 4.5K
MTB are the pairs of white lines.

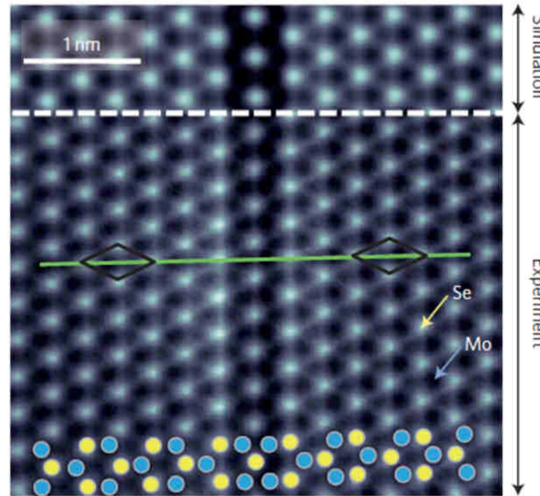

nc-AFM image: atomic structure of the MTB. Se and **Mo** atoms.

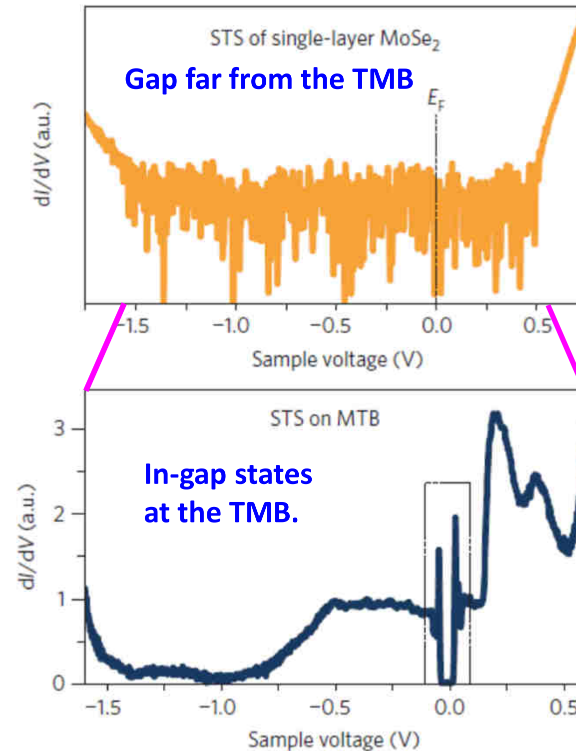

S. Barja et al., Nat. Phys. 12, 751 (2016)

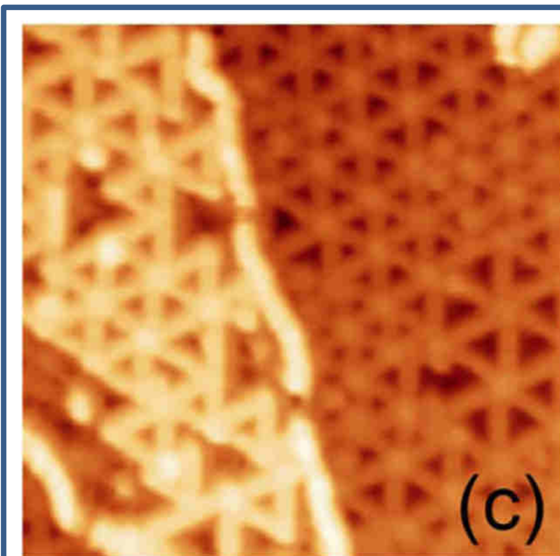

A **dense array** of such « **1D metallic** » features can be obtained….
STM image,
35x35 nm², -1.3V.

H. Liu et al.,
PRL 113, 066105 (2014)

Inversion or Mirror **Twin Domain boundaries** (MoSe2 grains rotated by 180°).

The grain boundary generates an (almost) **metallic 1D « band » in the TMD gap**.

*Possible **CDW** (x3a) distortion → gap @ E_F*

STM/STS on TMDs

Extended defects #2: **edges.**

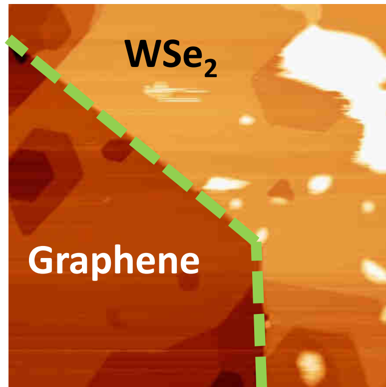

800x800nm², +1.0V

- **Edges** (outlined in green) on a TMD flake are created by **breaking strong covalent** (TM-X) **in plane bonds**.
- In analogy with (2D) surfaces of (3D) crystals, the **high energy ideal structure** will **relax** following different strategies: atomic displacements, rebonding (reconstruction), passivation (change in chemical composition).
- Some **« mid-gap »** (edge) **states** may remain within the TMD bandgap after relaxation which can impose (**pin**) **the Fermi level position at edges** (in analogy with 3D semiconductor surfaces).
- **Band bending at edges will** (most likely) **result!**

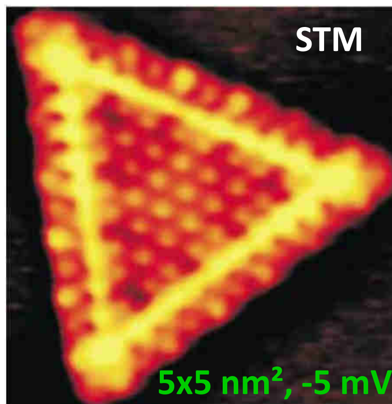

Model (DFT)

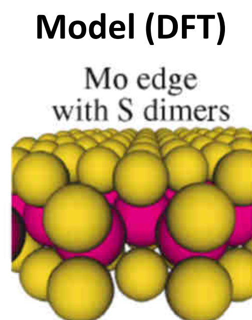

Theory (DFT)

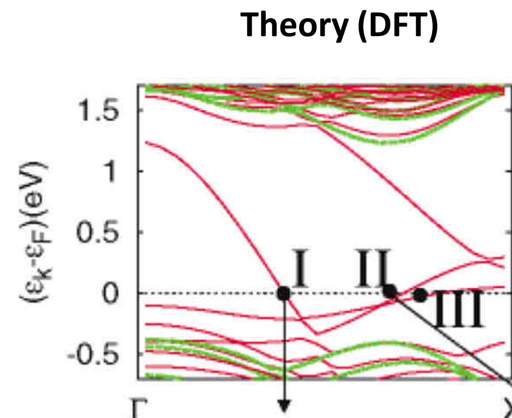

Computed band structure with or without edges.

First experimental evidence of edge states.

1D Metallic edge state in MoS_2 nanoclusters grown on Au(111).
M.V. Bollinger et al., PRL 87, 196803 (2001).

STM/STS on TMDs

Extended defects #2: **edges.**

More evidence for edge states and band bending.

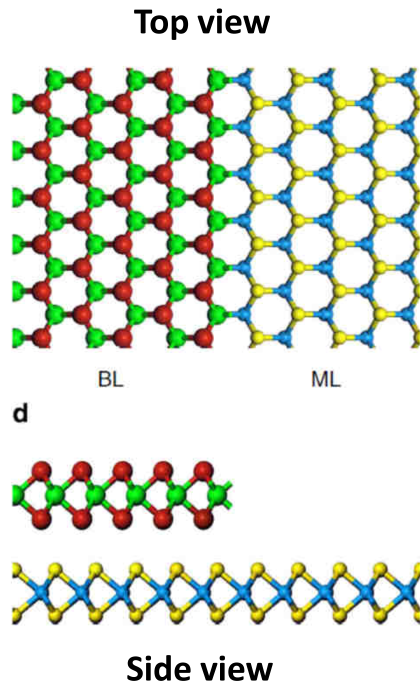

CVD grown WSe_2 on HOPG:

- **Band bending** at BL edge by **0.15 ev over 10 nm**,
- **Interface** (edge) **states** at the boundary.

Chendong Zhang et al., Nat. Comm. 7: 10349 (2016)

STM/STS on TMDs

In-plane Heterojunctions (MBE or CVD growth)

CVD grown in-plane (1L) Heterojunction on SiO2/Si

Optical image

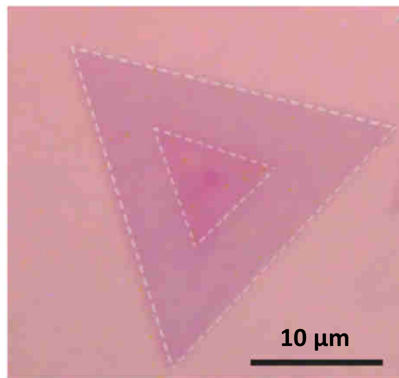

Composite PL image

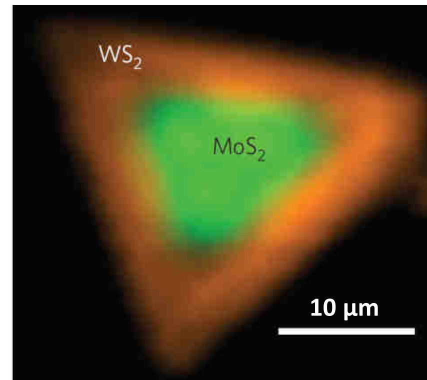

630 nm, 680 nm.

TEM image, Z contrast

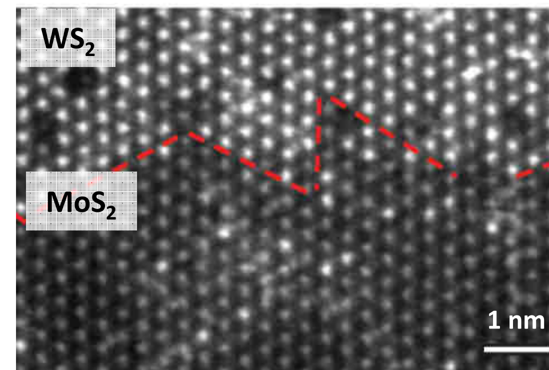

W atoms are brighter

Y. Gong et al., Nature Mat. 13, 1135 (2014). See also: C. Huang et al., Nature Mat. 13, 1096 (2014) for $MoSe_2$/WSe_2 in-plane junctions and M.-Y. Li et al. Science 349, 524 (2015) for WSe_2-MoS_2 lateral p-n junction.

- Heterojunctions are essential in 3D semiconductor electronics (HEMT, laser diodes…).
  New physics can emerge in 2D semiconductor heterojunctions…
- Similar atomic structure and lattice parameter allows for the growth of a coherent (seamless) interface between MoX_2 and WX_2 (X=S, Se) with limited interdiffusion.
- Enhanced PL intensity at the interface.
- Intrinsic p-n (rectifying) lateral junction.
- Band alignment at the interface?

STM/STS on TMDs

In-plane Heterojunctions (MBE or CVD growth)

STS study of an in-plane HJ : $WS_2/Mo_{1-x}W_xS_2$ (x=0.3) grown on graphite.

Type II heterojunction, as expected.

High electric field at the interface ($8\ 10^7$ V/m) for efficient e-h separation.

S. Yoshida et al., Sci. Rep. 5, 14808 (2015)

Topo@+1.6V | **Line spectroscopy** | **VBM position** on the image of (a) (2D map)

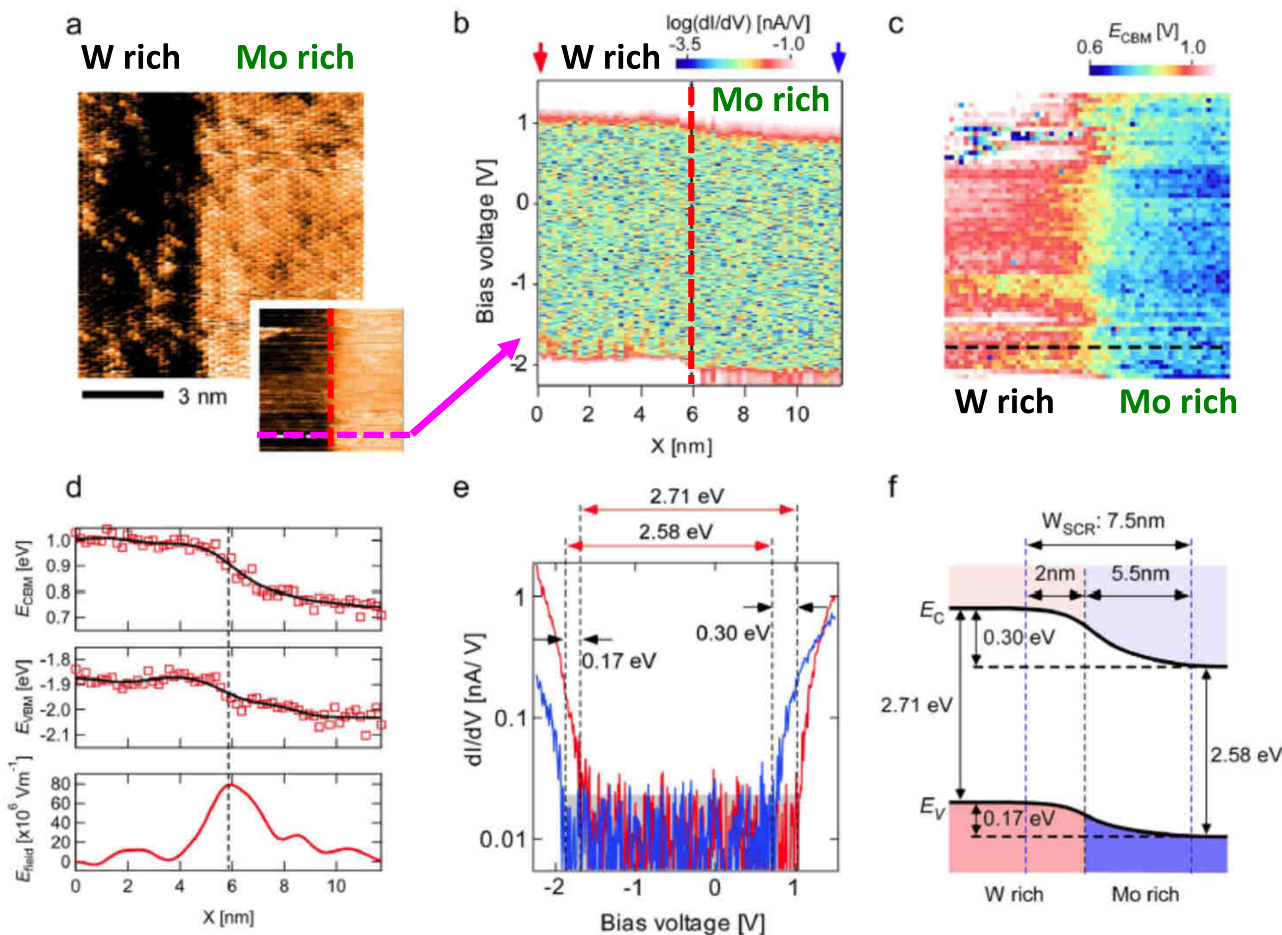

CB and VB offsets along the line + **« built-in » electric field** (dE_{CBM}/dx).

Spectra **far from the junction** (arrows in (b))

Schematics of the **staggered « type II » HJ**.